AD-A234 732 CUMENTATION PAGE

Form Approved
OMB No. 0704-0188

(2)

1. AGENCY USE ONLY (Leave blank)	2. REPORT DATE	3. REPORT TYPE AND DATES COVERED
	March 1990	Final Report 1 Mar 90-20 Nov 90

4. TITLE AND SUBTITLE

Workshop on 3-D Optical Memories

5. FUNDING NUMBERS

AFOSR-90-0178

6. AUTHOR(S)

Professor Esener

AFOSR-TR- 91 0271

7. PERFORMING ORGANIZATION NAME(S) AND ADDRESS(ES)

Dept of Electrical & Computer Engineering, 0407
Univ of California
LaJolla CA 92093-0407

8. PERFORMING ORGANIZATION REPORT NUMBER

9. SPONSORING / MONITORING AGENCY NAME(S) AND ADDRESS(ES)

AFOSR/NE
Bldg 410
Bolling AFB DC 20332-6448
Dr Alan E. Craig

10. SPONSORING / MONITORING AGENCY REPORT NUMBER

2305/B4

11. SUPPLEMENTARY NOTES

12a. DISTRIBUTION / AVAILABILITY STATEMENT

UNLIMITED

12b. DISTRIBUTION CODE

13. ABSTRACT *(Maximum 200 words)*

WORKSHOP WAS HELD

14. SUBJECT TERMS	15. NUMBER OF PAGES 126
	16. PRICE CODE

17. SECURITY CLASSIFICATION OF REPORT	18. SECURITY CLASSIFICATION OF THIS PAGE	19. SECURITY CLASSIFICATION OF ABSTRACT	20. LIMITATION OF ABSTRACT
UNCLASSIFIED	UNCLASSIFIED	UNCLASSIFIED	UL

NSN 7540-01-280-5500

Standard Form 298 (Rev. 2-89)

DISCLAIMER NOTICE

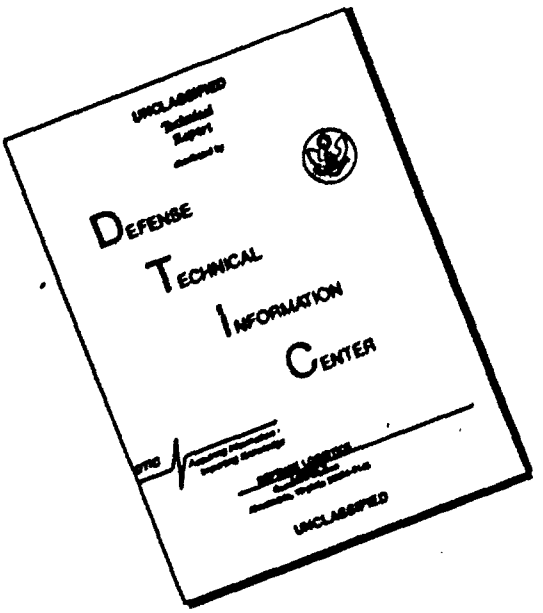

THIS DOCUMENT IS BEST QUALITY AVAILABLE. THE COPY FURNISHED TO DTIC CONTAINED A SIGNIFICANT NUMBER OF PAGES WHICH DO NOT REPRODUCE LEGIBLY.

Proceedings of
The 3-D Memory Workshop

Sponsored by: AFOSR and RADC

Organized by: Sadik Esener, UCSD
Alan Craig, AFOSR

Snowbird, Utah
March, 1990

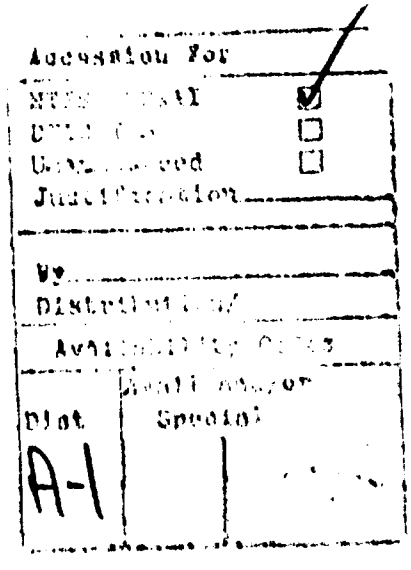

TABLE OF CONTENTS

SUMMARY OF THE WORKSHOP

The first workshop on 3-D memories was held March 12 -13, 1990, in Snowbird, Utah. The workshop was funded by AFOSR and RADC and organized by Prof. Sadik Esener from UCSD and Dr. Alan Craig from AFOSR.

The intent of the workshop was to bring together members of the optical storage and materials, computer architectures, and optoelectronic device communities to discuss issues associated with 3-D storage systems for various high-performance computers. The common concern among the diverse set of about 25 workshop participants was that storage is becoming a major limitation in terms of I/O bandwidth and capacity to achieving higher system performance, and will impede the future development of high performance computer systems. The question was if and how 3-D memories can provide better storage devices. The highlights of the technical program are given below.

Dr. Di Chen from Chen Associates opened the technical program by providing an overview of the existing optical disk technology and by providing his vision on the potential new developments in this technology. He described several schemes that will allow optical disks to be accessed in parallel.

During the presentations related to computer architectures and storage systems Dr.Mitkas from University of Syracuse and Prof. B. K. Jenkins from USC have discussed the importance and potential role of parallel-accessed optical storage devices in database machines and in optical computing. Later, Dr. M. Murdocca from Rutgers University pointed out that for optical computers based on symbolic substitution cache memory is essential and he described a method of constructing a free-space RAM compatible with his architectures. Finally, Dr. V. Heuring from University of Colorado discussed a guided-wave approach to dynamic memories where bits are stored as bundles of photons.

During the presentations related to photorefractive 3-D memory materials and devices Prof. C. Warde from MIT discussed how he can improve the storage characteristics of photorefractive materials. Later, he also proposed a rotating cylindrical photorefractive device and peripheral devices to realize a parallel-accessed 3-D memory. Prof. B. Hesselink presented his approach to photorefractive 3-D memories using SBN fiber bundles. He also discussed how the characteristics of these fibers can enhance the storage capacity. Finally, Prof. S. Fainman from University of Michigan summarized how system approaches can be used to correct some of the limitations of photorefractive materials for storage applications. Prof. S. H. Lee from UCSD also pointed-out the need for simulating 3-D photorefractive media for better optimization and utilization of the materials. He also discussed that by using a larger aperture that would be provided by the deposition of photorefractive films on large substrates one could greatly circumvent some of the present limitations.

Some of the emerging 3-D materials were discussed next. Prof. T. Mossberg from University of Oregon introduced the Time-Domain Frequency-Selective Optical memories which may

store data at a molecular level. He described the advantages of temporally addressing frequency selective optical data storage. Later. Dr. R. Kachru from SRI summarized his work on stimulated echo optical memory, encoding data by using its temporal profile. He further showed some of the signal processing capabilities of his approach. Prof. P. Rentzepis from UCI described a novel approach to volume 3-D memories using two-photon sensitive materials. In his approach the two-photon effect enables selective and efficient access to any location in the volume of the material. Dr. H. Haskal from Sparta presented a new organic material where diffraction gratings can be recorded and erased several times. He discussed the utilization of such a material for parallel-accessed memories. Also Dr. P. Henshaw from Sparta described the requirements for 3-D memories and suggested an approach that may offer possibilities for 4-D storage.

Finally, Dr M. Handschy from DisplayTech and Dr. C. Kuo discussed peripheral devices such as SLMs and methods of characterizing optical storage materials, respectively.

During the discussion periods on materials the committee drafted a table comparing various characteristics of the proposed materials. This table is shown below.

UNCORRECTED, UNEDITED DATA				
Criteria	**Photorefractives**	**2-photon**	**stim echo**	**polymers**
1. Sensitivity	.5-10 nJ/micron^2	1 nJ/0.5 mm^2	10^7 photons/bit	
2. Erasure mech	light			switch pol dir
3. W,R,E time const	nsec - sec	10^-13	10^11bits/sec	1 microsec
4. Power reqs	mw -microw/cm^2	Gwatt/cm^2	eta=20%	>20 mW sat
5. Mem persist time	days to months	20 min T=75F	weeks	2 weeks room T
6. Temp dep/req	< Tcrit		4-30K	>115C
7. Wavelength	UV - IR	300nm-1.8 micron	450-880 nm	500-530 nm
8. Res: pix/cm^2; pix/cm^3	10^13/cm^3	10^13 bits/cm^3	20x20 microns	
9. Read contrast	>30db	10 db		dep on pol
10. Coh req	y		none	none
11. Page or bit?	10^6 bits.pg	page	bit	bit
12. Reads per write	10^7 @30db		1000	?

However, it was also pointed out that some of the characteristics can be improved by orders of magnitude if a coherent research effort could be put together. Discussions on systems issues focussed on addressing formats, holographic vs bit oriented storage and peripheral devices. It was concluded that system experiments especially on photorefractive memories should be pursued before these issues could be clearly addressed. It was also pointed out that 3-D memory system components will leverage on the progress made on opto-electronic devices (e.g. SLMs). Discussions on architectural issues addressed the possible utilizations of 3-D memories. It was suggested that in addition to their usage as secondary storage, 3-D memories could also be used to control interconnections in an optical computer and could be applied advantageously for

associative recall. It was suggested that critical characteristics of various 3-D memory systems such as time constants, persistence, and required read and write energy per pixel should be made available such that the potential role of each approach could be defined in the memory hierarchy.

While there was no clear agreement on where the 3-D memory technology will go in the future, there was a consensus that this technology must evolve in some form to meet the performance requirements of future systems and much research work must be carried out until then. Feedback from the workshop participants indicated that most people believed that the field promises to be an exciting and fruitful one. Participants also indicated that they were pleased with the amount of interaction that took place in the workshop among participants with widely varying points of view and experiences with regard to memory technologies. Several participant suggested that they will try to organize sessions and symposiums on 3-D memories in different conferences.

3-D optical memories for high performance computing.

Sadik Esener

University of California, San Diego
Electrical and Computer Engineering Department, R-007
La Jolla, CA 92093

ABSTRACT

The design of high performance computers such as array processors has reached a critical stage. These machines are increasingly using parallel processing methods to achieve higher performance. They require low cost memory systems with much higher capacities and bandwidths than available today while retaining small volume, weight, and power consumption characteristics. Massively interconnected optical computers will require even higher performance memory systems. The paper reviews various 3-D memory concepts that are proposed to meet these demands.

1. INTRODUCTION

The advent of opto-electronic computers and highly parallel electronic processors has brought about a need for storage systems with enormous memory capacities and memory bandwidths. These demands cannot be met with current memory technologies without having the memory system completely dominate the processors themselves in terms of the overall cost, power consumption, volume, and weight. Existing high capacity storage devices rely on two-dimensional storage media such as optical[1,2] and magnetic disks[3]. These storage media exhibit large access times because of their two-dimensional nature and are not well suited for parallel access. However, to achieve high performance, computer architectures are relying increasingly on parallel processing methods which require higher capacity and bandwidth memory systems than those necessary for sequential computers.[4-6] High performance computers such as systolic arrays, supercomputers, and array processors have reached a critical design stage because of the increasing demand for large data storage and ultra fast access times and transfer rates. This increased memory requirement for parallel processing applications has reached the point where size, cost, and power requirement of the memory greatly exceeds that of the processor. Figure 1 demonstrates this point for the Hughes 3-D computer. This disparity in memory and processor characteristics is even worse for optical computing systems as shown in Figure 2. To improve on the present memory restrictions, alternate means for storage including three-dimensional optical memory devices[7-8] are being investigated.

This paper reviews bit-oriented 3-D optical memories that are proposed as a solution to meet the requirements imposed by high performance computers on memory systems. This need for 3-D memories is discussed and different approaches for achieving such memories are explored.

2. DEFINITION AND ADVANTAGES OF 3-D MEMORIES

Present storage devices store one-dimensional information in a two-dimensional space. On the other hand, a three dimensional memory device would allow the storage of two-dimensional information (bit planes) throughout the volume. A 3-D memory is, therefore, a single memory unit where three independent coordinates are used to specify the location of information. 3-D memories are generally classified as bit-plane oriented and holographic. This paper will focus only on bit-oriented memories. For 3-D holographic memories we refer the reader to the following paper in this issue or to Reference 9. Bit-oriented 3-D memories, where each bit occupies a specific location in 3-D space, differ significantly from 3-D holographic memories where the information associated with stored bits is distributed throughout the memory space. Bit oriented 3-D memories generally use amplitude recording media while holographic memories use phase recording media. In bit oriented 3-D memories, the coordinates that specify the location of the information can be spatial, spectral, or temporal giving rise to a variety of 3-D memory concepts that use different materials with various properties. For example, materials that exhibit 2-photon absorption will constitute a basis for the implementation of true volume memories while materials wherein spectral holes can be burnt, provide a storage medium for spectral/spatial storage. In addition, materials that exhibit the photon-echo effect could in principle lead to temporal/spatial storage.

In 3-D memory, information is partitioned in binary planes that are stacked in the third dimension. One memory operation is performed on the entire plane of bits, thus achieving a tremendous memory bandwidth increase over conventional 2-D bit-oriented memories. By storing information in volume media, optical 3-D memory can achieve very high density (10^{13}bits) in a very small space ($1cm^3$). In addition, high speed reading and writing of an entire plane of

memory may become feasible. These considerations make 3-D memory very compatible to the newly emerging highly integrated parallel array processors and opto-electronic multiprocessors such as the UCSD Programmable Opto-Electronic Multiprocessor System (POEMS).[10] In addition, the method of storing information in planes is very compatible with the SIMD synchrony used in array and vector processors, where every processor essentially references the same memory address, but in a different memory plane.

The list below summarizes the performance requirements desired from a 3-D memory system for a parallel electronic or opto-electronic computer: 1) High capacity - The memory capacity should generally be one or two orders of magnitude larger than the I/O bandwidth of the parallel computer; 2) High memory bandwidth - opto-electronic computers have much higher memory bandwidths than their electronic counterparts, due to their parallel optical data loading capability; 3) Random access - Any bit plane in the memory must be accessible; the SIMD nature of array processors ensures that the entire bit plane is used in the computations; 4) High bit accuracy; 5) Non-volatile; 6) Erasable; 7) Small volume/bit storage; 8) Low power consumption.

3. A BRIEF REVIEW OF SOME EXISTING 3-D MEMORY CONCEPTS

3.1. Spatial 3-D memories

In this section some of the bit-oriented 3-D memory concepts that have been put forward to meet the above requirements are reviewed, and their relative merits discussed. The free-space circulating optical 3-D memory, the 3-D magnetic bubble storage and optical retrieval system, [11] the two-photon 3-D memory [12] and the multi-frequency optical memory [13] are typical examples of bit-oriented volume 3-D memories. Such memories can be designed to operate at or near room temperature and benefit from the increased capacity provided by volume media.

The concept of circulating 3-D memory, as shown in Figure 4 relies strongly on the availability of ultra fast spatial light modulators (SLMs) with a large space-bandwidth product. Although such 3-D memories may find applications as cache-memories for optical computers, they would only provide relatively modest storage densities precluding their utilization for mass storage. Their storage densities will be limited by the switching energy density e_{sw} and the maximum allowed power dissipation density p_d of the spatial light modulators as described by:

$$m = p_d / c e_{sw}$$

where c is the speed of light. This storage density would be only about 1MBit/cm^3 if such a memory was built using todays state of the art multiple quantum well SLMs operating at their thermal limit, precluding its usage for mass storage.

On the other hand, the three dimensional magnetic bubble storage and retrieval system [11] shown in Figure 5 has the potential of providing, high density storage and is well suited for mass storage applications in supercomputing. In this approach, a transparent magnetic material is deposited on special transparent substrates that are stacked together. 2-D planar waveguides are also fabricated on the other side of each transparent substrate. Information is stored via electrical inputs by creating magnetic bubbles (domains) of 1μm diameter in the magnetic material. These bubbles are then read by a 1-D optical field using the Faraday rotation effect. A portion of this information is coupled into the waveguide and the associated polarization rotation is detected by a special detector array that can extract the stored information. Since moving parts can be avoided, such a memory can withstand harsh environments while being capable of providing tera-bytes of information using a few hundred layers. The present limitations of this approach is that the writing is performed electrically, and that the absorption within each layer may significantly limit the number of stacked layers and hence the overall capacity.

The two-photon 3-D memory [12] has the potential of providing high capacity, density and throughput because it allows true parallel access to the data in a volume. An important factor is that the two-photon material can be incorporated in a polymer matrix, which is relatively inexpensive and easily fabricated in large dimensions.

Two-photon absorption [14] refers to the excitation of a molecule to an electronic state of higher energy by the simultaneous absorption of two photons. The first photon excites the molecule to a virtual state, while the second photon further excites the molecule to a real excited state. Although neither of the beams is absorbed individually, the combination of the two wavelengths is in resonance with a molecular transition. Therefore both beams must temporally and spatially overlap in order for two-photon absorption to result. This allows 3-D optical storage since the beams can penetrate the material to record, read, or erase information without affecting it except at the region where they overlap. As a result, a memory unit based on two-photon processes has a precise addressing capability as shown in Figure 6. One optical beam is used to select a particular region, while the second beam is directed orthogonally and carries the information. In the region of overlap, molecules are excited first to a high energy state and later decay into a "written" form. In this form their absorption properties differ from that of the "non-written forms". Written forms persist for several minutes at room

temperature and for days in dry ice. The memory can be erased by shining a high energy optical beam on the storage material. It is important to note that because the changes occur on a molecular scale, the information in the plane can be made very dense with low crosstalk between neighboring bits. In addition since one is detecting molecular phenomena, nanosecond response speeds are obtainable. The "read" process is also based on the two-photon absorption of laser light. The "written" form of the molecule is excited with longer wavelength light resulting in two-photon absorption of the infrared photons and emission of fluorescence from the "written" form.

It is desirable for the 3-D memory systems to have the highest possible access speed. In the two-photon 3-D memory system, the speed is not limited by material considerations but rather by the response time of the peripheral devices that support it. As shown in the system diagram in Figure 7, these are the Input and Output SLMs, the optical power supplies and the Dynamic Focusing Lens. Therefore, the design of these components is critical for maximizing the performance of the two-photon 3D memories. However, the performance of opto-electronic computers is also limited by these technologies. It is therefore believed that two-photon memories will remain compatible with opto-electronic processing for many years to come, as these technologies progress.

Another approach to access data in a volume is to use the difference generated in the absorption characteristics of molecules that are written by different wavelength optical beams. This addressing mechanism is used in the multi-frequency optical volume memory[13] that is being developed in Japan. This memory consists of many layers of J-aggregate photochromic Langmuir Blodget films having different sharp absorption bands. By pre-exposing the films with appropriate UV radiation the required sharp difference in the absorption spectrum of each layer can be synthesized. Bits are written by exciting molecules with a UV beam while reading is performed by selecting the appropriate storage layer using a laser with tunable wavelength.

The capacity and density of such a memory is ultimately restricted by the sharpness of the synthesized absorption bands and how well their relative positions in the spectra are controlled. The success of this concept depends also on the availability of tunable laser sources with line widths compatible with the material requirements.

3.2 Spectral/spatial 3-D memories

In order to further increase the capacity of 2-D spatial memories researchers have sought methods of using the spectral dimension. A good example for this approach is the use of Persistent Spectral Hole Burning (PHB)[15] for data storage. PHB occurs in solid state materials that exhibit sharp inhomogeneously broadened absorption lines. Such lines result from the superposition of many narrower homogeneous lines whose center frequencies are shifted by strain induced by the host material. A narrow band laser tuned to a particular frequency within the inhomogeneous line can induce a permanent change in the absorption characteristics. Since interactions occur only with the molecules that are resonant with the laser, the laser beam effectively burns a hole in the inhomogeneous line profile. This phenomena can be used for spectral/spatial 3-D memories by associating the presence or absence of a hole to a true or false states. The capacity of such memories is limited by the ratio of the width of the homogeneous lines to that of the inhomogeneous line as well as by the line width and tunability of the laser source. A major drawback of this scheme is that it requires a very low operating temperature (4K). However, spectral/spatial memories concepts if combined with volume memories may lead to 4-D memories for reaching an even higher storage capacity.

3.3 Temporal/spatial 3-D memories

It is also possible to devise 3-D memories by using time as one of the coordinates. Indeed this principle has been demonstrated using photon echo effect.[16] Photon echo effect relies on the storage of information in the hyperfine states of a solid at very low temperatures (~2K). The required operation temperature and short retention time limit the applicability of this scheme.

4. CONCLUSIONS

In summary, 3-D memories can fill the gap in the memory hierarchy that has been created by the advent of parallel processing. Progress in VLSI based electronic processing and the advent of opto-electronic technology now utilize smaller, faster, and highly integrated computing devices for parallel processing. This translates into an enormous memory bandwidth requirement which cannot be matched by semiconductor or magnetic based technologies. Similarly, the size of the storage system with respect to the processing system has increased steadily and becomes unrealistic for highly integrated parallel processor arrays. 3-D memories store information in volume media and allow parallel access to planes of information, thereby increasing memory bandwidths by orders of magnitude over conventional methods and reducing the volume occupied by the memory systems. In addition, some 3-D memories such as the two-photon 3-D memory seem to have even more utility for newly emerging opto-electronic computers, since they can provide compatible parallel optical input and output to the opto-electronic computer.

6. REFERENCES:

1. M. L. Le[redacted]igh Data Rate, High-Capacity Optical Disk Buffer," *IEEE*, 17 (1985).

2. W. P. Al[redacted] M. Claffie, and M. L. Levene, "Optical Storage for High Performance Applications in the Late 1980s and Beyond," *RCA Engineer* (1986).

3. A. E. Bell, "Critical Issues in High-Density Magnetic and Optical Data Storage: Part 1," *Laser Focus* 19, 61 (1983).

4. K. R. Wallgren, "Optical Disks and Supercomputers," *SPIE* 529, 212 (1985).

5. L. M. Thorndyke, "Supercomputers and Mass Storage: The Challenges and Impacts," *IEEE*, 27 (1985).

6. R. H. Ewald and W. J. Worlton, "A Review of Supercomputer Installations' Mass Storage Requirements," *IEEE* 33 (1985).

7. D. Chen and J. D. Zook, "An Overview of Optical Data Storage Technology," *Proceedings of the IEEE*, 63, 1207 (1975).

8. L. d'Auria, J. P. Huignard, C. Slezak, and Spitz, "Experimental Holographic Read-Write Memory Using 3-D Storage," *Appl. Opt.*, 13, 808 (1974).

9. J. E. Weaver and T. K. Gaylord, "Evaluation Experiments on Holographic Storage of Binary Data in Electro-Optic Crystals," *Optical Engineering*, 20, 404 (1981).

10. F. Kiamilev, S. Esener, R. Paturi, Y. Fainman, P. Mercier, C. C. Guest, and S. H. Lee, "Programmable Optoelectronic Multiprocessors and Their Comparison With Symbolic Substitution for Digital Optical Computing," *Optical Engineering*, 28, 396 (1989).

11. F. Mehdipour, "Three Dimensional Magnetic Bubble Data Storage and Optical Retrieval System," U.S. Patent 4,660,173.

12. S. Hunter, F. Kiamilev, S. Esener, D. Parthenopoulos, and M. Rentzepis, "Potentials of Two-Photon Based 3-D Optical Memories for High Performance Computing," submitted to *Appl. Opt.* (1989).

13. E. Ando, J. Miyazaki, K. Morimoto, H. Nakahara, and K. Fukuda, "J-Aggregation of Photochromic Spiropyran in LB Films," International Symposium on Future Electron Devices-Bioelectronic and Molecular Electronic Devices, November 20, 1985, pp. 47-52.

14. *Multiphoton Processes*, P. Lambropoulos and S. J. Smith, Eds. (Springer-Verlag Berlin Heidelberg) (1984).

15. U. P. Wild, S. E. Bucher, and F. A. Burkhalter, "Hole Burning, Stark Effect and Data Storage," *Appl. Opt.* 24, 1526 (1985).

16. N. W. Carlson, L. J. Rothberg, and A. G.Yodh, "Storage and Time Reversal of Light Pulses Using Photon Echoes," *Optics Letters*, 8, 483 (1983).

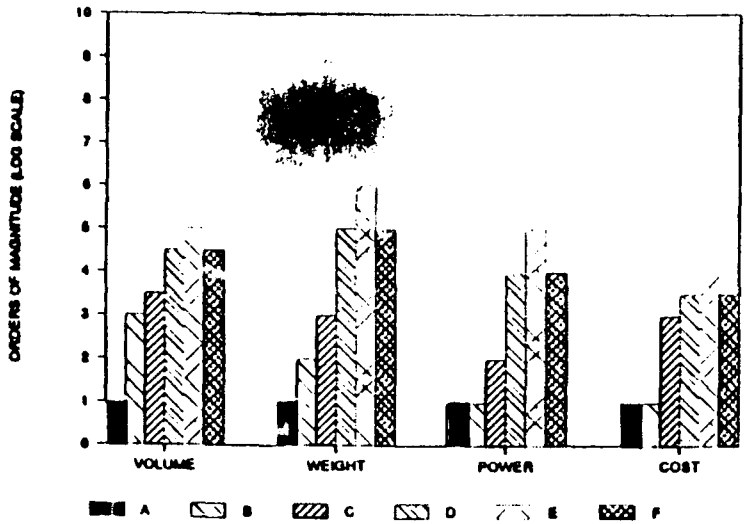

A. 512x512 Processor Array
B. 10Gbytes of 16Mbit CMOS DRAM (MAIN MEMORY)
C. 10Gbytes of 1Mbit CMOS DRAM (MAIN MEMORY)
D. 100Gbytes with 300Mb Magnetic Drives (SECONDARY STORAGE)
E. 100Gbytes with 2.5Gb Magnetic Drives (SECONDARY STORAGE)
F. 100Gbytes with 125Gb Optical Drives (SECONDARY STORAGE)

Figure 1. Comparison of storage devices for 3-D electronic array processors for a throughput of 6.2 GFlops (From Ref.12).

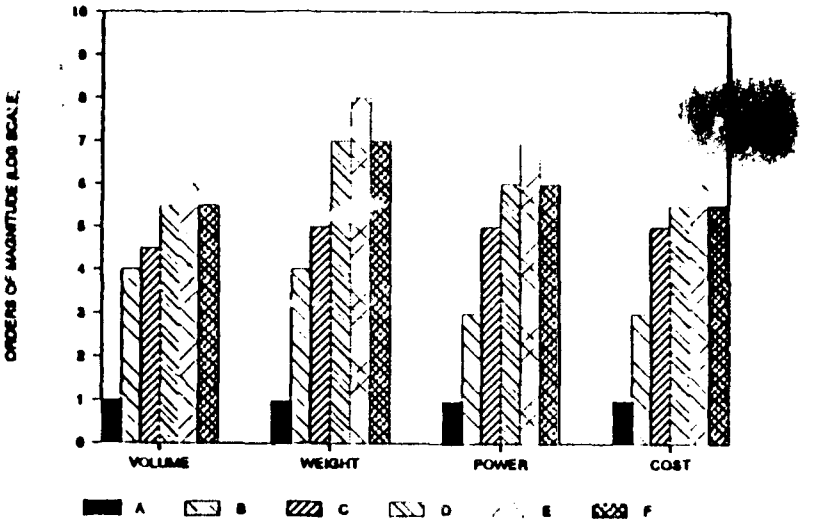

A. 512x512 Processor Array
B. 1Tbytes of 16Mbit CMOS DRAM (MAIN MEMORY)
C. 1Tbytes of 1Mbit CMOS DRAM (MAIN MEMORY)
D. 10Tbytes with 300Mb Magnetic Drives (SECONDARY STORAGE)
E. 10Tbytes with 2.5Gb Magnetic Drives (SECONDARY STORAGE)
F. 10Tbytes with 125Gb Optical Drives (SECONDARY STORAGE)

Figure 2. Comparison of storage devices for opto-electronic computers for a throughput of 6.2 GFlops (From Ref.12).

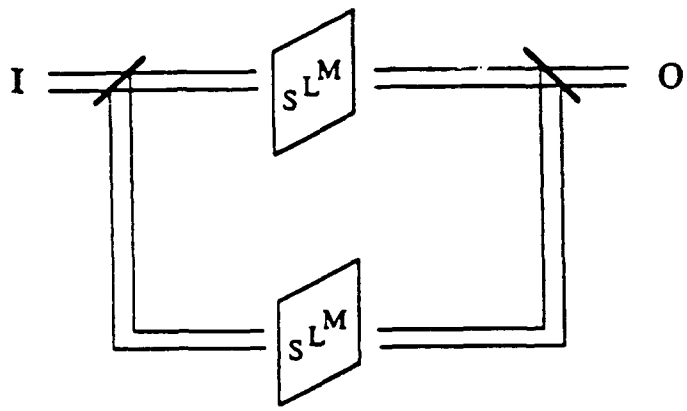

Figure 3. A circulating free-space 3-D memory based on Spatial Light Modulators

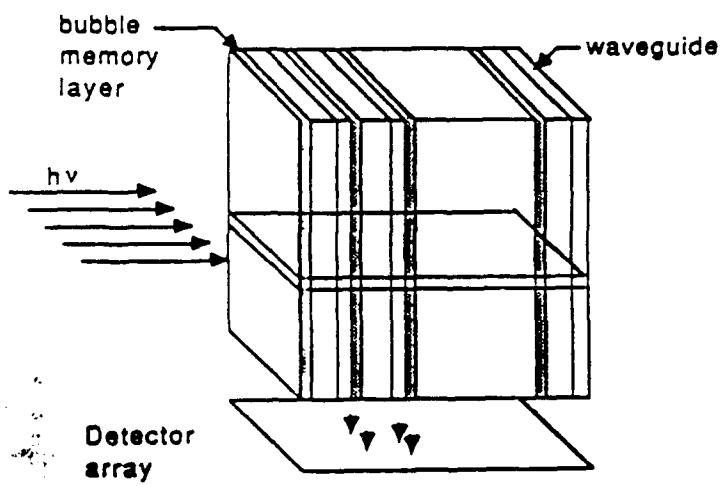

Figure 4. The 3-D magnetic bubble storage and optical retrieval system concept.

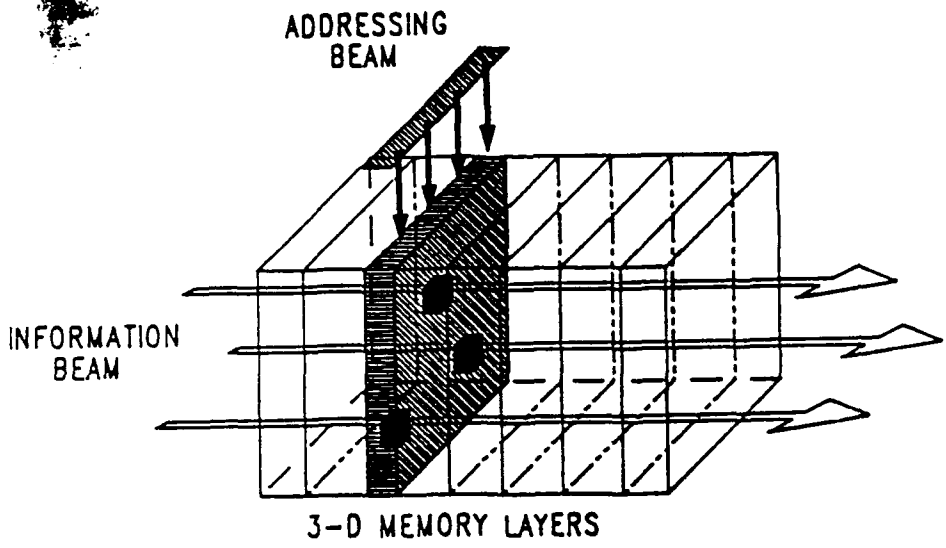

Figure 5. *Addressing a two-photon volume storage material. The dark regions indicate the "written" bits.*

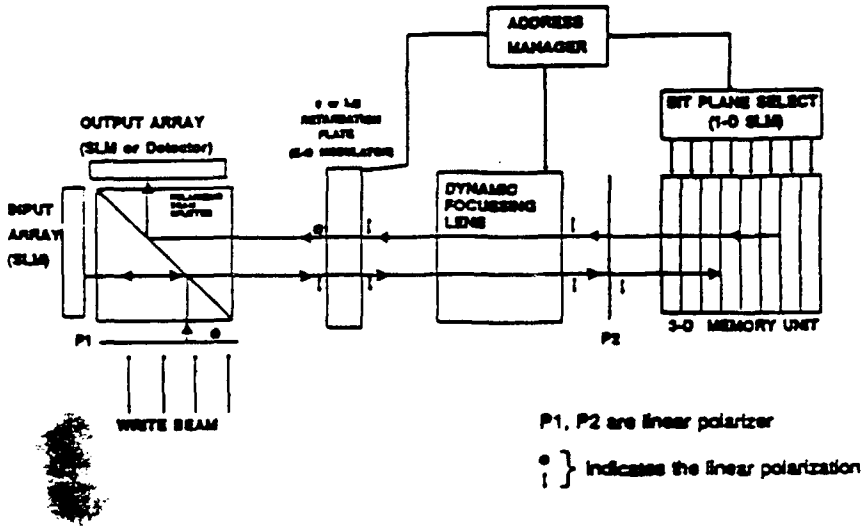

Figure 6. The two-photon 3-D memory system. The memory I/O is achieved via the Input and Output SLMs. The Address Manager controls the internal components to assure proper imaging between the data arrays and the correct memory layer (From Ref. 12).

3-D OPTICAL DISK RECORDING

Di Chen
Chen and Associates Consulting
302 Sunbird Cliffs Lane
Colorado Springs, CO 80919

Optical technique for data storage is rapidly maturing in recent years. Some of the unique features of this new recording technology are being realized in various forms of optical recording disks and drives, especially the large storage capacity, the removability, and the random access capability. However, one of the major advantage of the optical recording technology, the ability to store data in another dimension besides the areal storage, has not been fully exploited.

The added dimension of data storage can take the form of the third spatial dimension, the dimension in the wavelength of the light, or a combination of both. To apply the 3-D approach for the optical disks, one may consider the use of the thickness dimension of the disk. A stack of disks could be implemented much like the Winchester disk drives. However, the volume storage density improvement with this approach is very limited, owing to the large physical size of the current optical recording head. Furthermore, the removable feature offered by optical disk in cartridge can not be readily applied for a optical disk stack.

A more efficient method is to prepare the disks with multiple recording layers on the same disk. If the sensitive layers are separated by transparent separating layers each exceeding 10 um, the focused beam will be properly defocusing at the adjacent layers and the interference will be negligible. In this method, the sensitive layer material and its thickness must be chosen such that the absorption in each layer is controlled to allow sufficient beam penetration for interaction with each layer. Based on a simple analysis, up to four layers will be possible using currently available material. By proper design of the sensitive layer and separating layer materials, the data encoding scheme, and the disk geometry through an optimization analysis, it is possible that many more layers could be constructed on the same disk.

To address each of the sensitive layer, a wavelength sensitive objective lens such as a Fresnel lens may be employed in conjunction with a tunable laser diode. Each layer can be focused instantaneously by a wavelength change without additional lens motion. On the other hand, parallel processing of the information on all layers is made possible by using a number of laser diodes or a laser diode array with each laser operating at a different wavelength to address each of the sensitive layers on the disk simultaneously. Wavelength

selective optical elements are used to direct the incoming beam onto the disk and the return beams to the proper detectors.

In the rotating disk format, both the data rate and the capacity are linearly proportional to the number of multiple layers the disk contains. Furthermore, the performance of the optical disk drive is commonly given as the ratio of capacity to the access time. Since adding multiple layers to the disk does not affect the access time, the performance is also directly proportional to the number of layers in a disk. This multilayer approach could be one of the most beneficial technology development available to the optical disk industry, made possible because of the unique non-interacting nature of the optical beams.

To achieve the full benefit of this 3-D recording approach, four areas of research needs to be developed:

(1) Detailed computer modeling of the thermal and optical interaction of the multilayer disk structure to direct the selection and research of the sensitive layer and the separating layer material

(2) Techniques for the preparation of the selected sensitive layer and separating layer as well as the multilayer disk structure

(3) Wavelength sensitive objective lens and optical components

(4) Wavelength tunable or selectable laser diodes in single element or array form with an acceptable wavelength stability over the operating temperature range

These areas of technology development are not currently covered by the optical recording industry. Support for research and development at the national level will be needed. The end result will not only help the optical computing research which requires parallel data processing, but also advance the maturing optical disk industry, by providing a new degree of performance multiplier.

With the adaptation of the fully developed 3-D multilayer disk approach, together with the expected advances of the optical technology, we may anticipate an optical disk drive using such a 3-D disk with an areal storage density of 50 Gigabits per square inch, to achieve a data rate of 10 Megabytes per second and an average access time of 16 milliseconds, within the next seven to eight years.

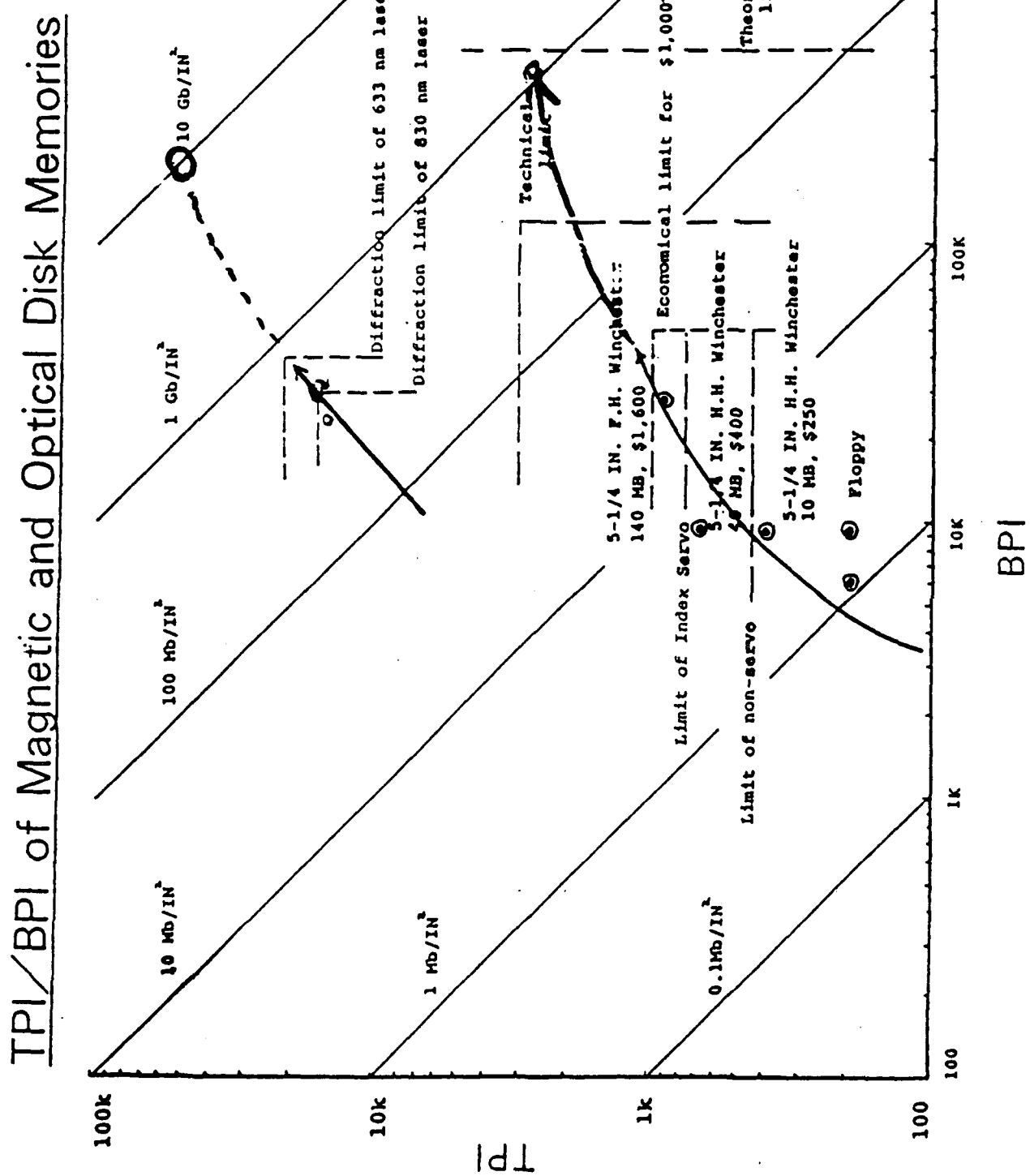
TPI/BPI of Magnetic and Optical Disk Memories
10 Gb/IN²
1 Gb/IN²
100 Mb/IN²
10 Mb/IN²
1 Mb/IN²
0.1Mb/IN²
Diffraction limit of 633 nm laser
Diffraction limit of 830 nm laser
Technical limit
Economical limit for $1,000
Theoretical limit
5-1/4 IN. F.H. Winchester
140 MB, $1,600
5-1/4 IN. H.H. Winchester
40 MB, $400
5-1/4 IN. H.H. Winchester
10 MB, $250
Floppy
Limit of Index Servo
Limit of non-servo
100k
10k
1k
100
TPI
100
1K
10K
100K
BPI

PREDICTED EVOLUTION OF 5.25" DISK CAPACITY

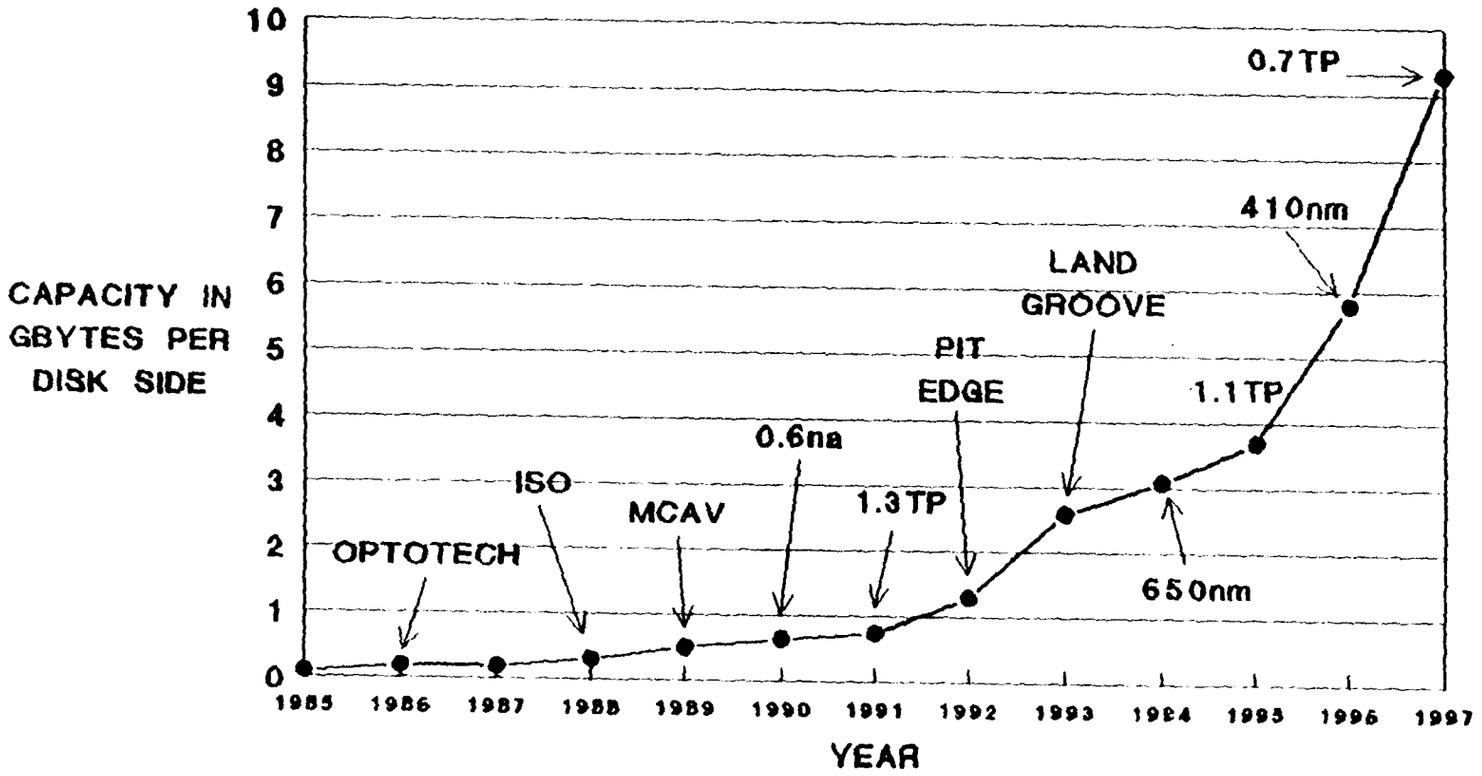

RELATION BETWEEN PERFORMANCE OF OPTICAL DRIVE AND LASER/OPTICAL HEAD CAPABILITY

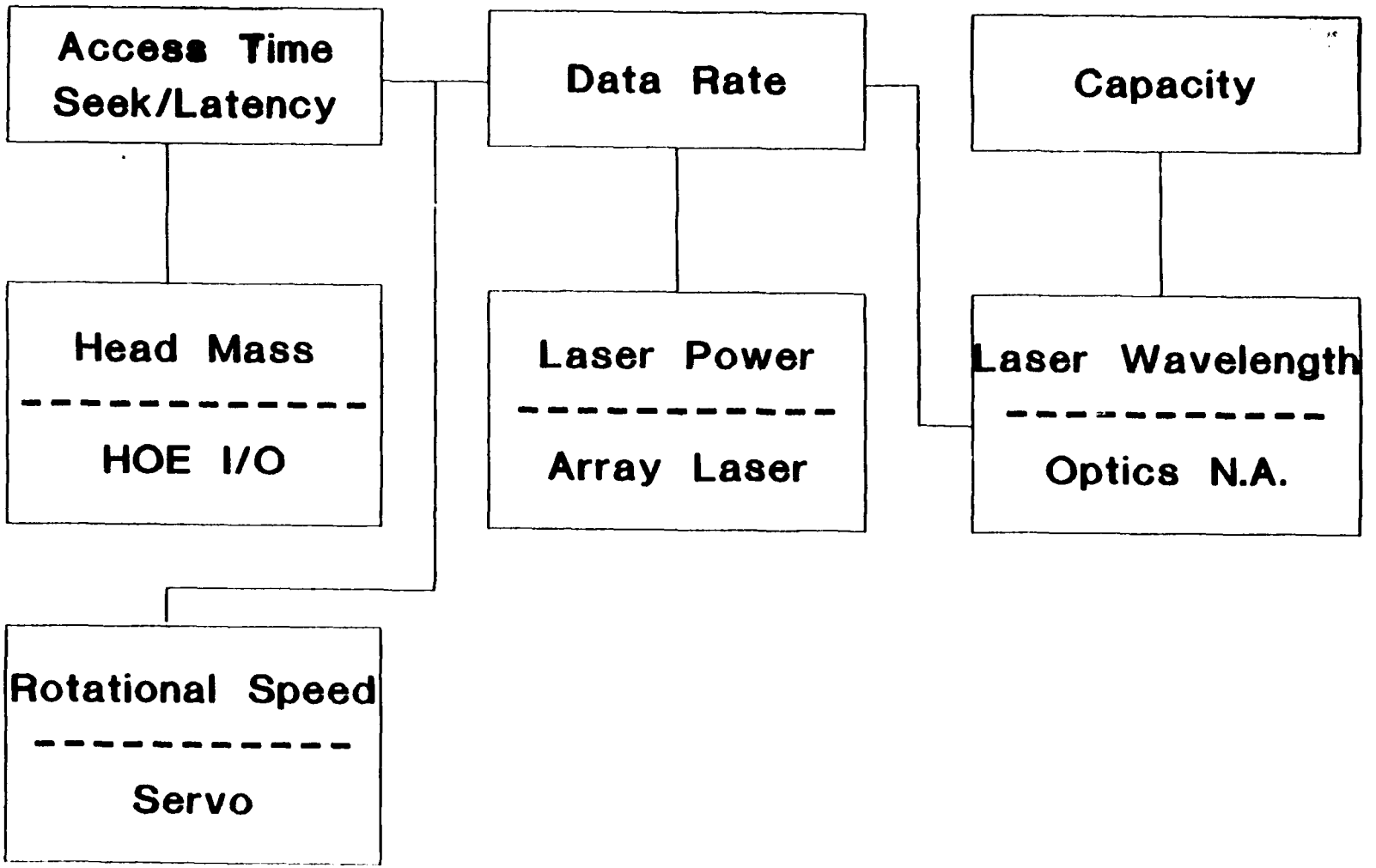

MULTILAYER RECORDING (MLR)

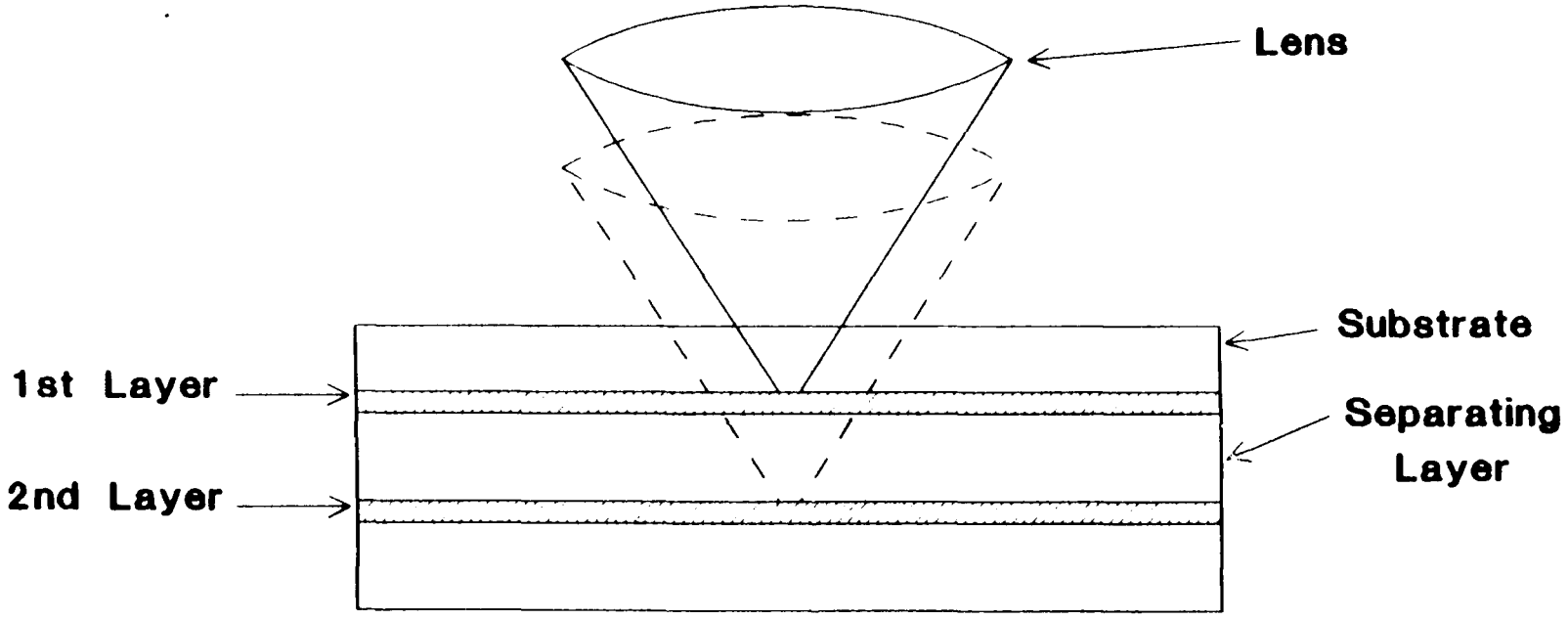

- Recording layers separated in depth by separating layer
- Accessing to each layer by moving the objective lens in depth

CAC 1/90

3D OPTICAL DISK MEMORIES

Approaches	Effort Required			
	Media		Device	
I. Disk Stack	①	Available	⑤	Integrated Head Research
II. Multilayer	②	Develop Multilayer Technology	④	Develop dispersive or multiple hololens
			①	Moving Coil available but not simultaneous Accessible to all Layer
III Volume Hologram	④	Needs Material Research	③	Input device (SLM)
			④	Wavelength Tunable Laser Diode
IV PCH	⑤	Needs Material Research for Room Temp Operation	④	Wavelength Tunable Laser Diode

① ---------- ⑤

Available — Most Difficult

FUTURE RESEARCH IN OPTICAL RECORDING

	Capacity	Access time	Data Rate
Drive Research	• Short wavelength lasers	• Split Optical Head	• High rotational Speed
	• Super Resolution	• Holographic Optical Element	• Efficient code
	• File Library	• Integrated Optical Head	• High power laser
			• Parallel Processing (multiple beam)
Media Research	• High Resolution	• Tolerate High Rotational Speed	• Direct Overwrite
	◦ 3D Recording	◦ 3D Recording	• High resolution
			◦ 3D Recording

CAC 1/90

OPTICAL MEMORY REQUIREMENTS OF VERY LARGE DATA AND KNOWLEDGE BASE SYSTEMS

Pericles A. Mitkas
Department of Electrical & Computer Engineering — Syracuse University
121 Link Hall, Syracuse, NY 13244–1240
email: mitkas@zookeeper.cns.syr.edu

From a simple bank transaction to complex weather prediction, there is an enormous demand for the maintenance and effective manipulation of large volumes of data. Data and knowledge bases with capacity requirements in the order of gigabytes are very common and their expansion to the terabyte range in the near future is a conservative prediction. In addition, fast response is often critical, especially for real-time applications. The conventional Von Neumann computer is no longer sufficient to process such a vast amount of information. Therefore, new, powerful, highly parallel machines have been developed with several orders of magnitude improvement in CPU performance, followed by new intelligent techniques for data and knowledge base management. However, the performance of secondary memory systems does not exhibit an analogous improvement. Further problems are generated by the need for extensive interconnections in a multiprocessor environment.

A common approach to deal with these problems is the incorporation of a data/knowledge base machine (D/KBM). A D/KBM with multiple storage units, multiple processors and the appropriate interconnection network operates as a back-end machine to a host computer undertaking a large part of the total transaction load (Fig. 1). D/KBMs must have very large storage capacity, high degree of parallelism to ensure acceptable data rates, and specialized processing units such as sorting pipes, data filters, relational operators or inference mechanisms. Real-time applications require transfer rates from the secondary memory to the processing units in the order of hundreds of MBytes/sec. Data much richer in information will be transferred to the host at rates lower by at least two orders of magnitude. While electronic processing is acceptably fast, the I/O process remains a bottleneck particularly when a transaction requires a global search through the entire database.

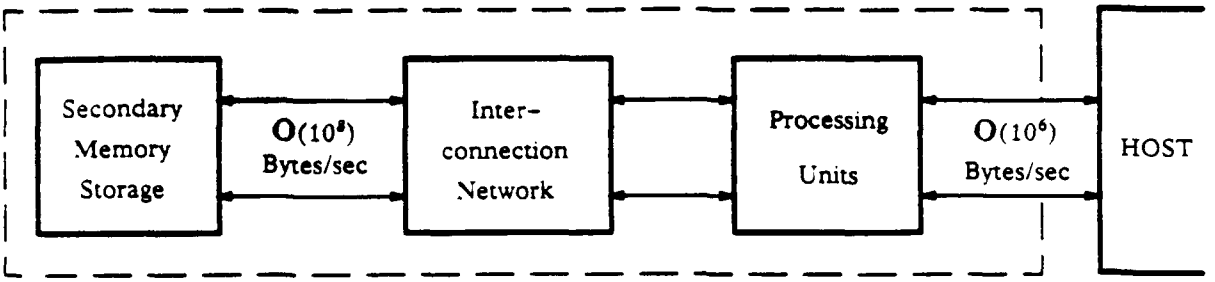

Figure 1. A back-end data/knowledge base machine.

Digital optics is a relatively new technology that may provide alternative solutions to the D/KB problems by replacing electronic signals with light beams [BER87, BER90]. Optical memories, such as optical disks and page or volume holograms, will furnish the required capacity, while optical interconnections can provide the necessary bandwidth. The two-dimensional nature of optical processing will come handy for the associative searching that most data and knowledge base transactions require. For instance, relations in a relational database are nothing but tabular representations of data and thus, can be manipulated in parallel using array processing.

Optical disks offer ultra high recording density in the order of hundreds of Mbits/ cm^2 on a medium that can be replicated at low cost and high speed, and is also erasable and rewritable. Even though their access times are relatively slow, new designs that involve parallel beam read-out, multiple heads, or different wavelengths, are capable of reading multiple tracks simultaneously and will boost the transfer rates into the hundreds of MBytes/sec.

In principal, holographic storage offers a potential improvement in both storage density and access time. In comparison to magnetic and optical disks a higher density can be achieved, because there is no need for mechanically repositioning the read/write mechanism. Access to the data is made by steering a laser beam through an acousto-optic or electro-optic deflector, which is an inertialess operation, unlike that of a moving disk arm. Due to the nature of holography, small imperfections on the recording media are relatively unimportant, because the recorded data are spread out over the recording medium. Holographic memories not only offer a fast, low-cost per bit mass memory system, but also the possibility of providing an inexpensive content addressable memory (CAM). Optical CAMs have been constructed using holograms and they have the desirable search processing properties of electronic CAMs, yet offer a considerably larger storage capacity (10^8 - 10^{10} bytes) and parallel output. Until recently they have been read only but, with the advent of new recording media such as phorefractive crystals, holograms can be

erased and rewritten a limited number of times. Generally, selective changing of information is not possible, unless the hologram is recorded in a page format. In that case the entire page must be erased prior to rewriting. Holography offers the potential of providing enormous transfer rates for data and knowledge base machines, since accessing the data does not involve mechanical movement.

However, these data rates would overwhelm current electronic computers since they have been designed for magnetic disk rates. An alternative approach is to feed the data from the disks into optical fibers and distribute them to remote locations. While this approach takes advantage of the superior speed and parallelism of optical communications, the receiving computers will again have difficulty with such high rates. In a better approach, shown in Fig. 2, optical data are processed by an optical processor prior to conversion and presentation to the electronic computer [BER89]. The electronic computer is then better able to accept a reduced data rate; one that will be richer in content.

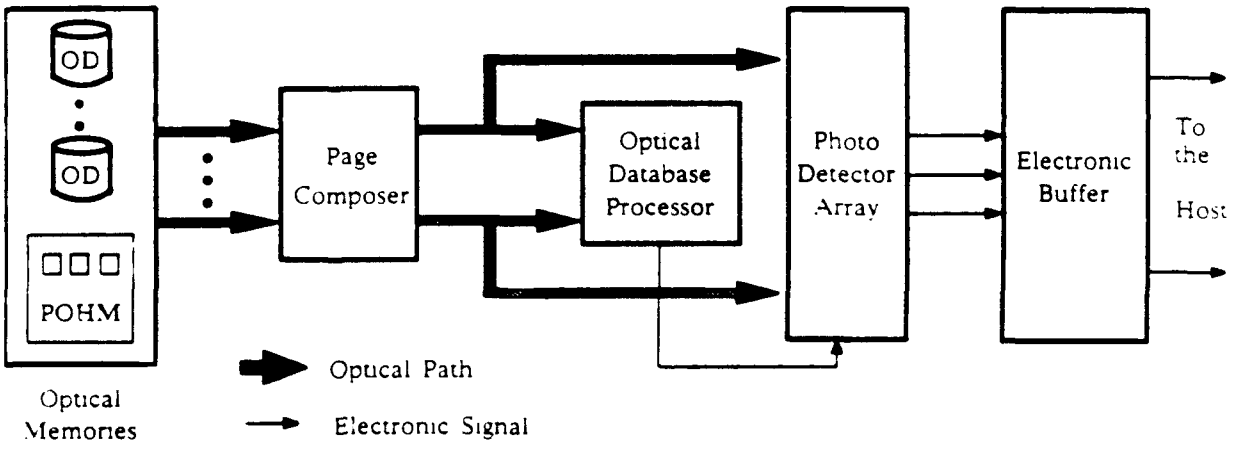

Figure 2. An opto-electronic architecture for database operations.

The goal of this system is to process large volumes of data "on-the-fly" and filter out irrelevant information. The page composer simply converts the output of the optical memory into a two-dimensional pattern and forwards it to the optical database processor where it is temporarily stored in a 2-D spatial light modulator (SLM). The optical database processor compares incoming data with the search argument(s). If a match is detected, a signal is issued to the photodetector array, which enables the cells that correspond to the qualified data. Only these data are transferred to the electronic buffer for further electronic processing, if needed, and transport to the host. In order to avoid bottlenecks, the framing speed of the SLM must be comparable to the time to retrieve a page

from the memory. Current SLMs exhibit framing speeds of a few kHz which are not sufficient to service a very large database. Another possible source of bottleneck is the interface between optics and electronics. If we assume parallel data retrieval, then the potential transfer rate from the detector cells to the electronic buffer requires a considerably wide and fast communication channel. A preferable solution is the integration of the photodetector cells and the electronic buffer, so that the flow of data is confined inside a chip.

In conclusion, the memory requirements of very large data and knowledge base systems can be summarized in the following:

a) Memory capacity in the terabyte level,
b) I/O bandwidth from secondary memory devices in the hundreds of MBytes/sec,
c) SLMs with time-space bandwidth in the order of 10^{12} pixel-operations/sec,
d) Parallel transfer of very long words (1-10 Kbits) into the electronic memory,
e) Integrated photodetectors and electronics.

The first requirement can be met with the use of 3-dimensional memories, such as volume holograms recorded in photorefractive materials. This memory, with a theoretical capacity well into the terabit level, can also provide the large I/O rate, if it is implemented as a page oriented system. If holographic memories are to be used in a D/KBM, however, they must: *first*, exhibit roughly equal write and read times, and, *second*, permit multiple non-destructive read outs; two properties that current holographic memories do not possess. Multiple track reading optical disks are also suitable for D/KBMs. The biggest challenge seems to be in the development of SLMs with 1,000 pixels on the side and a response time of 1 μsec. A possible solution for the temporary storage of data may be the use of SEED arrays, which exhibit both fast response times and low switching powers. The last two requirements are complementary because an integrated photodetector array into an electronic buffer will permit the transfer of an entire record to the buffer in a single step.

REFERENCES

[BER87] P. B. Berra and N. B. Troullinos, "Optical Techniques and Data/Knowledge Base Machines," IEEE Computer, Vol. 20, Oct 1987, pp 59-70.

[BER89] P. B. Berra, A. Ghafoor, P. A. Mitkas, S. J. Marcinkowski and M. Guizani, "The Impact of Optics on Data and Knowledge Base Systems," IEEE Trans. on Knowledge and Data Engineering, Vol. 1, No. 1, March 1989, pp 111-132.

[BER90] P. B. Berra, K.-H. Brenner, W. T. Cathey, H.J. Caulfield, S.H. Lee and H.Szu, "Optical Database Knowledgebase Machines," Applied Optics, Vol. 29, No. 2, 10 Jan. 1990, pp 195-205.

MEMORY IN OPTICAL/ELECTRONIC COMPUTING

B. Keith Jenkins
Signal and Image Processing Institute PHE 306
University of Southern California
Los Angeles, CA 90089-0272

SUMMARY

The requirements on memory in parallel computers is very much dependent on the machine architecture. In this talk we discuss three different classes of architectures and, for each class, some of the architectural and resulting memory issues. The class distinctions are based on models of computing machines, and are: serial, von Neumann machines; parallel graph/network machines; and, parallel shared memory machines. Neural networks also provide a model for parallel computing but are omitted from this talk for reasons of time.

Serial von Neumann machines involve a memory hierarchy with an essentially serial location addressing mechanism at each level of the hierarchy. If we consider the implementation of an algorithm, such as the multiplication of a scalar and a vector to yield a new vector, on a simplified version of such a machine, it becomes apparent that the machine can take a large number of steps to implement the algorithm. In this example, two factors make the number of steps large: the computations can only be done one at a time, and more steps are spent in moving the data between memory and arithmetic logic unit than are spent in actually performing the computation.

The functional memory requirements for a serial von Neumann machine are well understood; the drawback of course is the serial addressing bottleneck. If an optical and/or 3-D memory were to be employed in such a conventional architecture, there are three pertinent issues: (1) compatibility with existing machine architectures and standards; (2) compatibility of bandwidth, i.e., there is no point in overpowering the machine with a larger memory bandwidth than the machine can utilize; and, (3) given these are satisfied, the specifications/capabilities of the memory (vs. more conventional memory implementations. Thus, in effect, the competitiveness of the 3-D/optical memory is determined by a direct comparison of its specifications/capabilities (access time, bandwidth, storage capacity, physical characteristics such as size, weight, power consumption, etc.) with more conventional memory implementations.

Graph/network models of parallel computation consist of a set of PEs and an interconnection network that interconnects them. This class of models covers a wide range of grain sizes, from extremely small and simple PEs to very complex ones. An example of such a machine model is a cellular logic machine, which is a single-instruction, multiple-data stream (SIMD) machine, with a large number of fairly simple PEs, connected by a fixed interconnection network, and under the control of a single control unit that broadcasts instructions to all the PEs in synchrony. The algorithm example given above, for a vector size of 50, can now be done in approx. 8 parallel steps instead of the 500 in the serial machine case, assuming the machine has at least 50 PEs and only nearest neighbor connections. However, we also note that the PE utilization may be poor, in that if the machine has greater than 50 PEs, the extra ones sit idle during this computation.

A multiple-instruction, multiple-data (MIMD) graph/network machine can increase the utilization of PEs. With reconfigurable interconnections, the algorithm given is different than in the SIMD case, and has two potential drawbacks: it assumes that the PEs are selected (which can take actually take many time steps), and it requires each PE to fetch the scalar from the same location, which can cause a contention at that PE, in turn potentially slowing the algorithm down dramatically.

Both of the drawbacks in the MIMD computation example essentially stem from the interconnection and memory addressing bottleneck at each memory. In the SIMD cellular logic array case, a large bottleneck (aside from machine I/O) occurs between the set of PEs and some main memory that stores arrays of data. The typically relatively small number of lines connecting the two in electronic cellular logic implementations causes a speed bottleneck. The use of optical interconnections with a parallel-addressed (for both reading and writing) memory can in principle completely eliminate this bottleneck, in that the main memory becomes functionally equivalent to an expansion of the local memories of each PE. In essence, the graph network models provide a paradigm for parallel computation using conventional, serial location addressed memories. The parallelism is provided by using multiple (perhaps smaller) memories. We can see from the above discussion, however, that this approach to parallelism comes at a price.

Shared memory models of parallel computation incorporate a set of PEs that communicate to a separate set of memory modules via a reconfigurable interconnection network. The speed of computation of the scalar-vector multiplication example, assuming that the PEs are selected, depends on the capability of the specific architectural manifestation. With a suitably general interconnection network, all PEs can communicate with memory modules on a one-to-one basis simultaneously. In addition, in an ideal shared memory machine, any number of PEs can fetch the a value from the same memory location simultaneously. If these capabilities are included, then the algorithm can proceed in just 3 steps; meanwhile, any unused PEs can be utilized for other purposes at the same time. The initial selection of

the PEs can also be performed in a small number of steps if the machine has, for example, the capability of performing simultaneous fetch and adds to a memory cell; this requires not only simultaneous access but also some intelligence in the memory (and, in practice, in the interconnection network).

Thus, in the shared memory model paradigm, to the extent that simultaneous memory access to a given memory cell, parallel memory access, and intelligence in the memory, can be provided, the computation time is reduced. It should also be noted that with this model, the distinction between interconnection network and memory becomes fuzzy, as the interconnection network is providing some of the memory access/addressing function.

From the above discussion, a summary of desired characteristics for a 3-D memory, from an architectural perspective, are: (1) parallel access (different incoming lines accessing different memory cells simultaneously), (2) simultaneous access (different incoming lines accessing the same memory cell simultaneously), and (3) incorporation of some intelligence into each memory cell. In practice, a memory hierarchy will likely be needed, as tradeoffs will inevitably involve the degree to which these desirable characteristics can be incorporated. In addition, we see that memory function and characteristics are very much interdependent on the computing machine architecture and control strategy.

LIMITATIONS OF CONVENTIONAL ELECTRONIC MEMORY AND HOW OPTICS CAN HELP

Miles Murdocca
Department of Computer Science
Rutgers University, Hill Center
New Brunswick, NJ 08903
murdocca@aramis.rutgers.edu

Memory in a conventional digital computer is organized as a hierarchy as shown below:

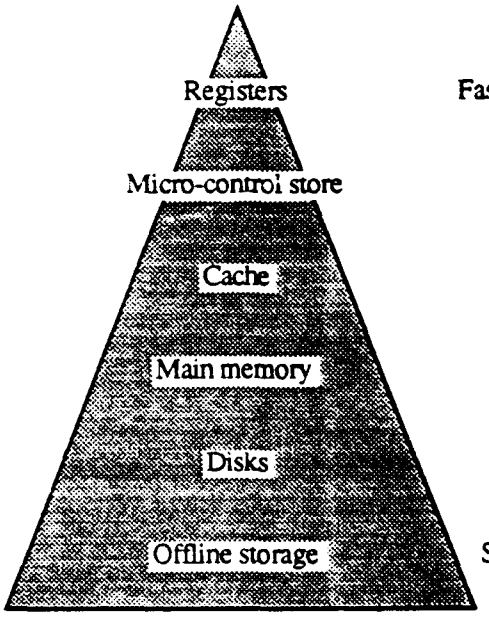

A typical operation in a von Neumann architecture locates two operands in memory, performs a logic operation on the operands in an arithmetic logic unit (ALU) and then stores the results back in memory. For each fetch or store that involves main memory, at least one more machine cycle is needed because main memory is normally slower than register memory. Scientific computation typically involves processing large amounts of data, so that operations involving main memory are frequent and the available computational power of the computer is wasted. For this reason, it makes sense to speed up the access time of main memory.

Another problem related to scientific computing is that when large volumes of data need to be processed only a narrow channel is provided between main memory and the central processing unit (CPU). Typically, an n-bit memory will require on the order of n time units to access the entire memory. This limitation comes about because of pin limitations of electronic packaging and because of the design of electronic random access memory (RAM) (see below).

The bandwidth problem is difficult to solve with conventional technology for a number of reasons, but the primary reason is that in order to increase either the speed of the memory or the number of pins on the packaged chips, density is sacrificed. If we are willing to pack less memory into packaged RAM chips then we can access information faster and in larger chunks *at the chip level*. At the system level, the physical size of the machine becomes larger and the power requirements are

increased. This translates to lower cycle speeds. The whole problem of speeding up RAM comes down to issues in packaging and in architecture. As long as we draw off information through the edges of a chip, there will always be an order of complexity difference in how much information can be drawn off in one cycle. From an architectural viewpoint, as RAM grows in size, deeper decoder trees are needed to access the data, which fundamentally limits the access time of RAM.

A solution to the pinout problem is to draw off information in parallel. Conceptually this is a good idea, but electronically, the fabrication complexity is enormous. The field effects from a large amount of metal carrying high frequency pulses also limit operating speed. Optics can provide a solution, for example using quantum well modulators and detectors for reading and writing data. An example of such an architecture is the S-SEED based processor described in AT&T's recent press release.

A solution to the architectural problem of deeper decoder trees for larger memories cannot be found since the problem is fundamental to RAM. However there are two areas where significant improvements can be made. One area is in improving throughput by using a sequential FIFO (first-in, first-out) memory. For applications that involve processing large amounts of data, where the flow of control is independent of the data, a FIFO is a good method for storing the input and output streams. Commercial FIFO's are available but are normally low in density when compared to RAM implemented in the same technology because each level of storage needs latching logic. Optical logic devices operating in pulse mode eliminate the need for latching because time-of-flight propagation is preserved.

Although the deeper decoder tree problem is fundamental for large RAM, the longer access time does not mean throughput has to decrease. For optical logic devices operating in pulse mode, synchronization is maintained at each level of logic so that the decoder tree can be pipelined at the gate level. The basic idea is that as information moves from one level of the decoder tree to the next, a new memory request is brought in to the top level of the decoder tree on each clock cycle. Thus, a memory access can be satisfied on every clock cycle, even if several clock cycles are needed to complete any one access. This approach addresses the memory needs of new reduced instruction set computer (RISC) architectures since these architectures maintain filled pipelines.

In summary, RAM is an integral part of modern computers, which is limited by access times and word widths (the number of pins on a memory chip) which in turns limits the performance of electronic computers. Arrays of optical logic devices operating in pulse mode offer solutions to the pinout problem by offering completely parallel access and to the access time problem by supporting gate-level pipelining of the decoder tree.

Random Access Memory

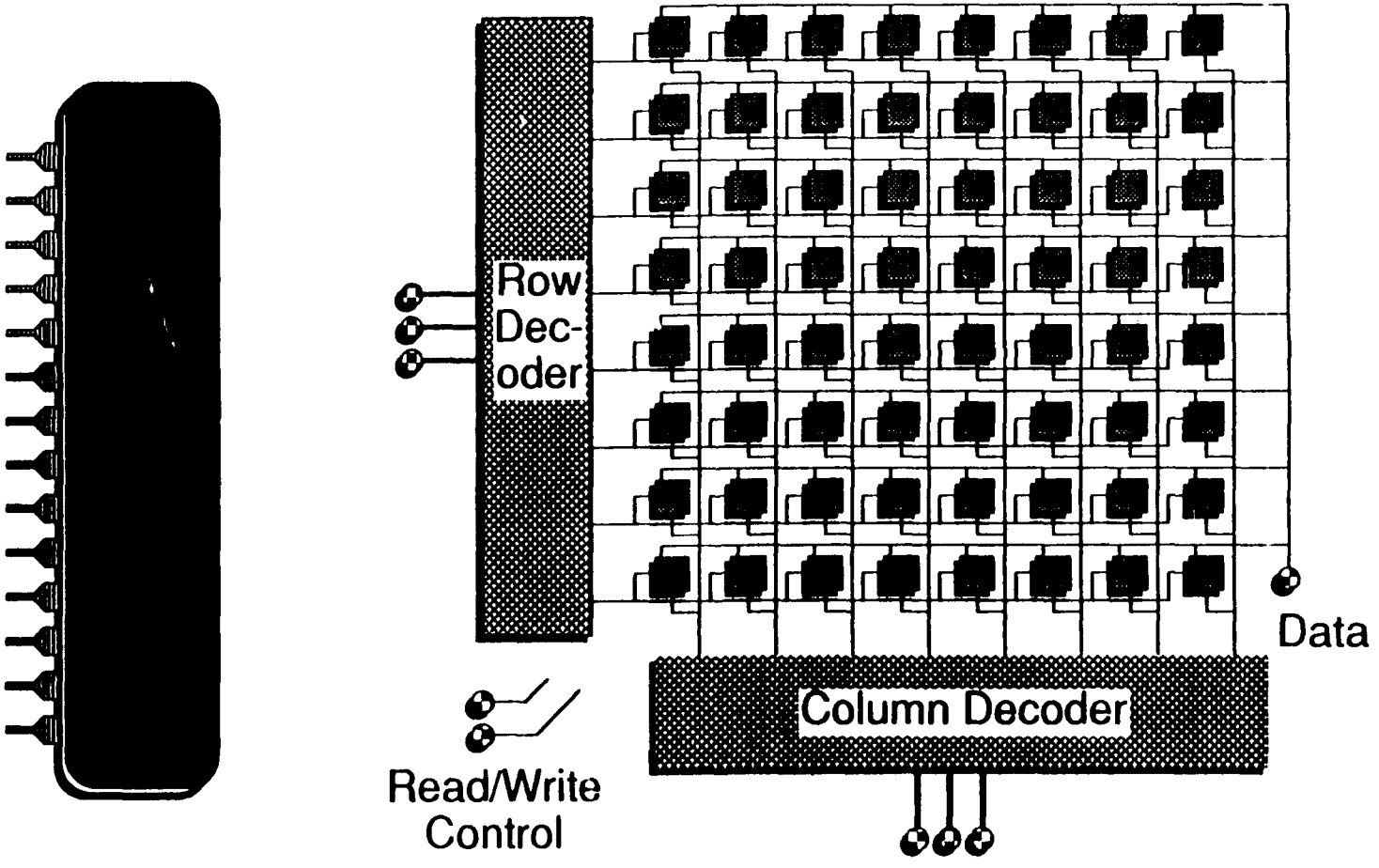

Optical Computing Model

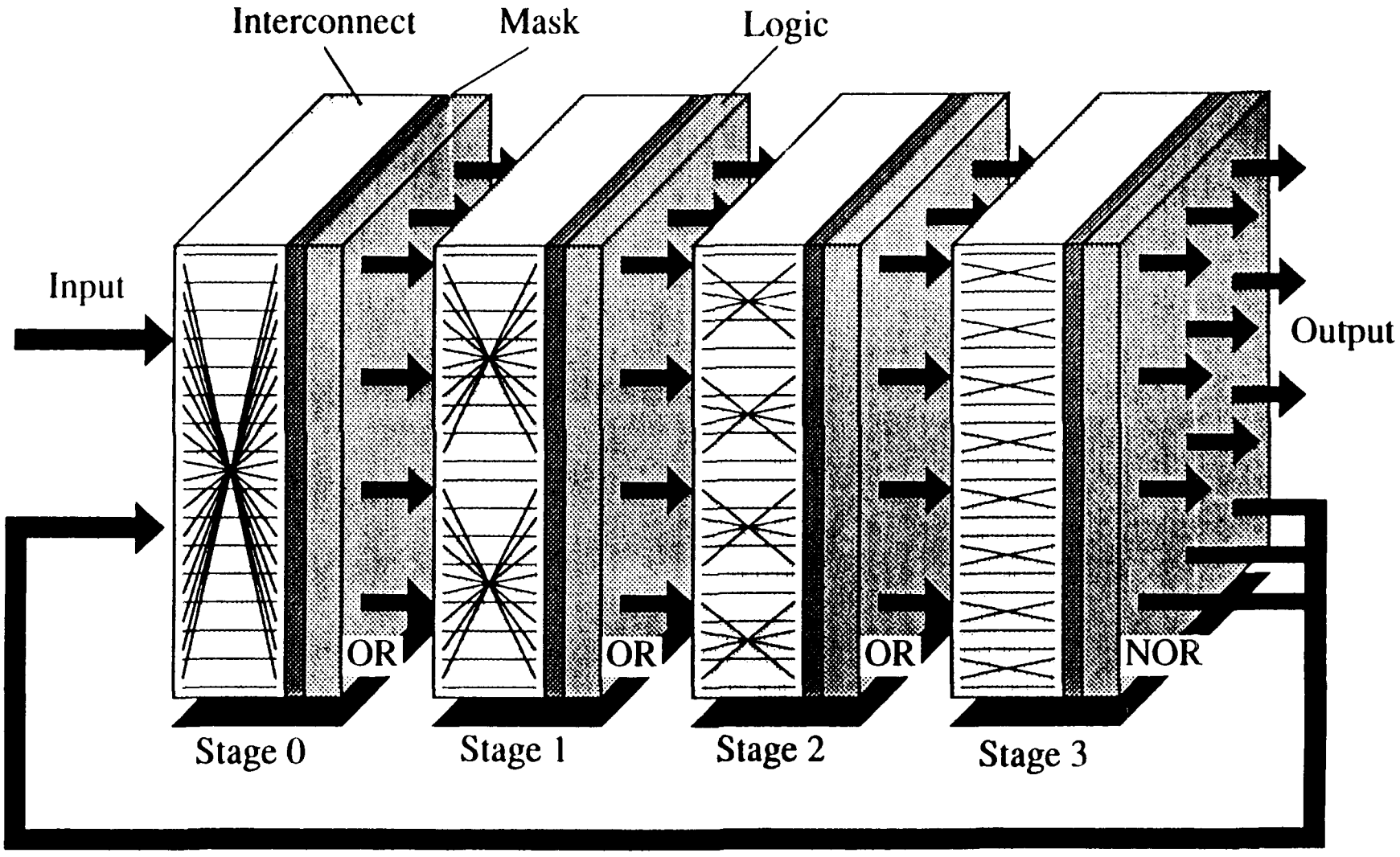

Optical Crossover Interconnects

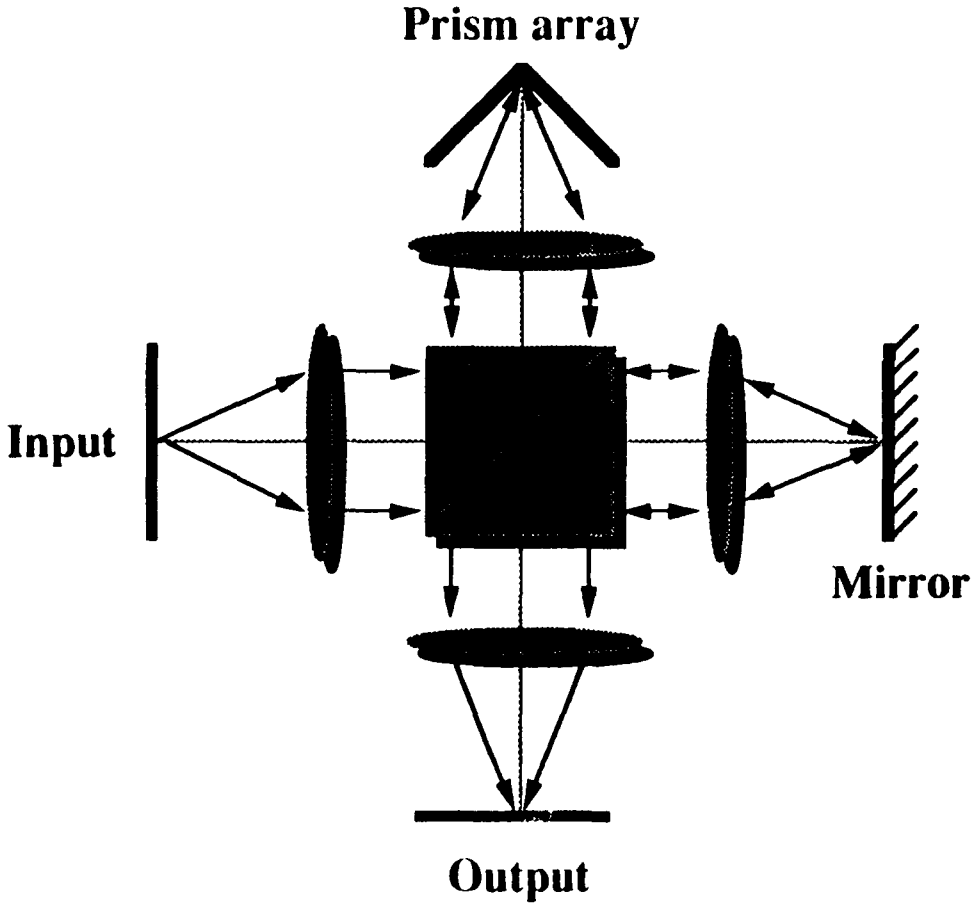

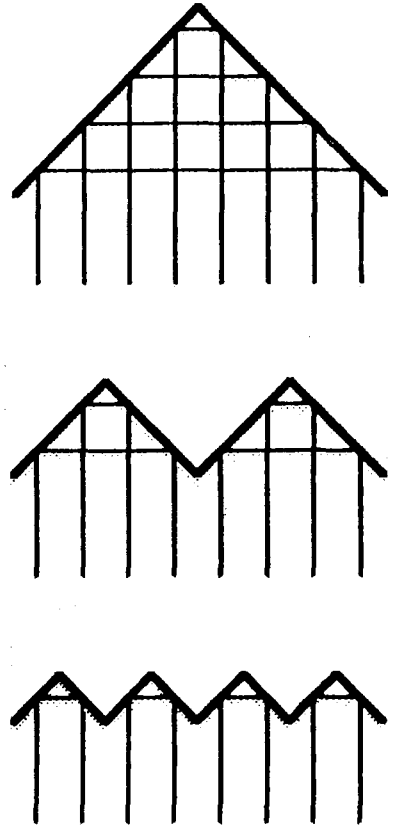

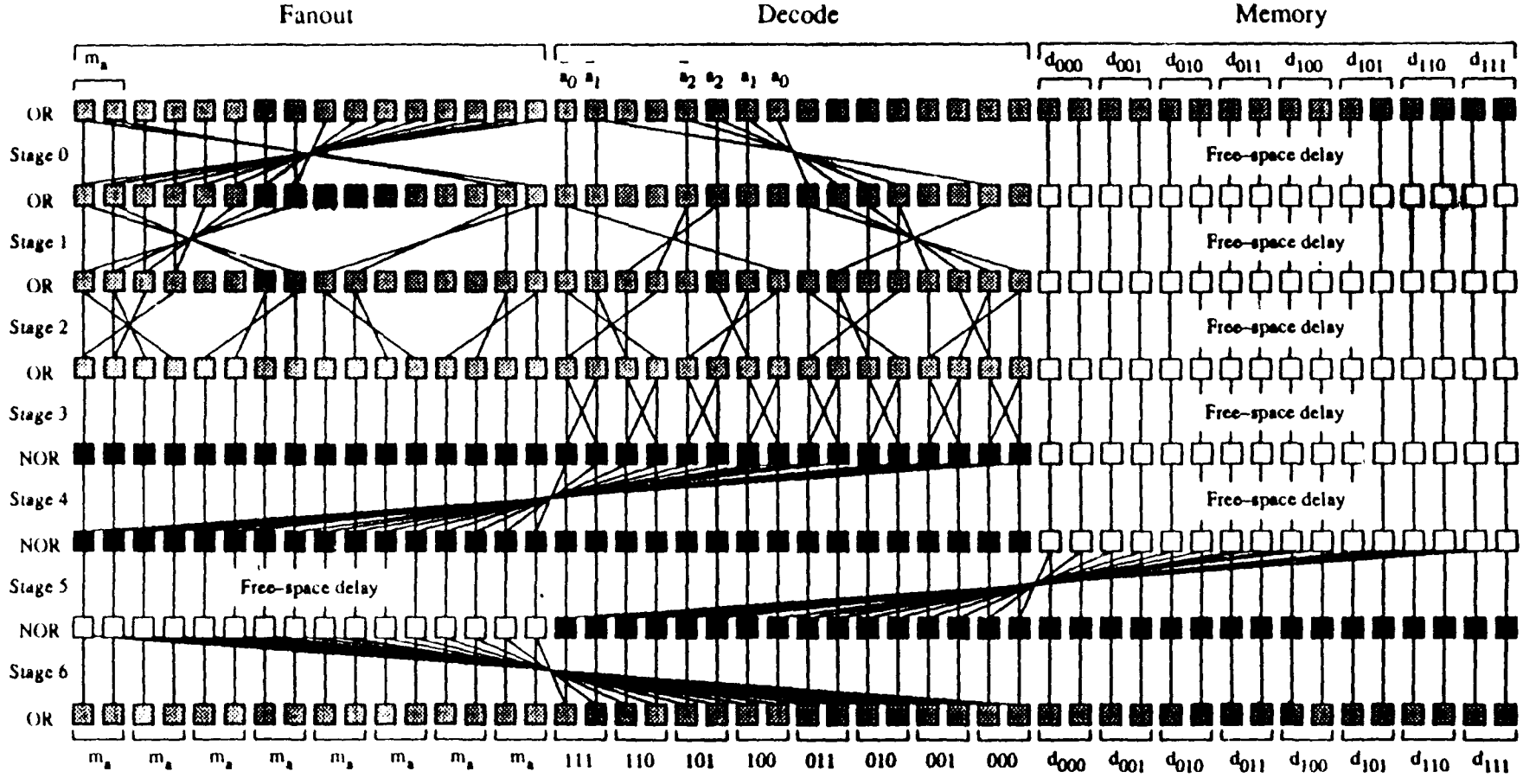
Fanout
Decode
Memory
OR
Stage 0
OR
Stage 1
OR
Stage 2
OR
Stage 3
NOR
Stage 4
NOR
Stage 5
NOR
Stage 6
OR
Free-space delay
Free-space delay
Free-space delay
Free-space delay
Free-space delay
Free-space delay
111 110 101 100 011 010 001 000
Output when reading
New memory when writing
Unchanged memory when reading

Dynamic Fiber Optic Memories

Vincent P. Heuring
Department of Electrical and Computer Engineering
and
Optoelectronic Computing Systems Center
University of Colorado - Boulder
Boulder CO 80309-0425

Dynamic optical memories store bits as bundles of photons. These memories serve an important role in the optical memory hierarchy. When storing bits in a dynamic optical memory, amplitude restoration and bit resynchronization are important considerations that can severely limit the capacity of the dynamic memory. We have designed a dynamic memory using optical fibers and directional couplers that allows a bit stream to be stored indefinitely. Memory capacity is limited by thermal fluctuations unless these fluctuations are compensated for.

1. INTRODUCTION

Most optical memory systems don't actually store bits as bundles of photons, but rather store a *representation* of the bit by using some distinguishable physical state of matter. Common examples include photorefractive materials, liquid crystalline materials, and electroclinic materials. These memories can be classed as static† optical memories. Static in the sense that there is usually no motion in the memory, because the information is stored *via* a physical state of matter. Ultimately, the bits must be retrieved from the static memory, and converted to photons which are then directed to some processing element.

Contrast this kind of memory with a dynamic optical memory. Here, the bit is represented as a bundle of photons, which are kept recirculating in some manner: traveling through free space, or directed in space and time by way of some transmission medium such as optical fibers.

In most optical computing architectures, there is in fact an implicit conversion process, whenever optical information is stored in a static optical memory:

$$Processing \rightarrow DynamicStorage \rightarrow StaticStorage \rightarrow DynamicStorage \rightarrow Processing$$

where the $Processing \rightarrow DynamicStorage$ step signifies that light emerges from some processing step as an optical bit stream, and must be manipulated as such until the bit stream is converted to static storage.

2. DYNAMIC OPTICAL MEMORIES

There are two important problems to be solved in designing a dynamic optical memory: amplitude restoration, and bit resynchronization. The first problem arises because as the bit is recirculating, it is also suffering amplitude loss, and this loss must be compensated for before the bit disappears into the system's noise. The second problem arises because of inevitable jitter in the bit location/time. If not compensated for, these space/time errors will accumulate, and the bit will ultimately lose it's timing with respect to the system clock, resulting in an error. Belovolov[1] found that even with great care, bit lifetimes range from milliseconds to hours if the two problems above are not adequately addressed.

† We use the terms static and dynamic in a different sense than their use in describing electronic memories, where the terms refer to whether the stored bit must be "refreshed" periodically.

2.1. Implementation of a Fiber Optic Delay Line Memory

We have implemented a fiber optic delay line memory using optical fiber and directional couplers. Figure 1 shows the logic of a conventional directional coupler. The control terminal, labeled "C" is normally electronic, but we have added a detector and appropriate electronics to convert the coupler to a 5-terminal optical device. Figure 2a shows its use in a fiber optic delay line memory. Device 1 acts as an amplitude restoration device. Notice that the incoming bit at terminal C serves to switch a fresh copy of the clock into the loop. Figure 2b shows how the terminal C electronics stretches the arriving pulse, removing all jitter below the threshold level allowed by the stretched pulse. The optical splitter allows the data in the loop to be read as desired. Device 2 allows new data to be written into the loop. Associated circuitry includes a counter to keep track of the location of data in the loop, and an address comparator to match the desired address with the current address passing the loop output. This architecture is O(1) in the number of switches, and O(n) in the access time; this is appropriate for systems that have the goal of minimizing the number of active devices at the expense of access time. Other architectures will support logarithmic access time and devices, and constant time with O(n) devices.

3. CAPACITY

A number of factors work to limit the bit storage capacity of uncompensated fiber delay loops. These include thermally induced length changes in the fiber loop, attenuation by the medium, dispersion, internal reflections, and the thermally induced changes in the refractive index of the fiber, among others. An investigation of these factors led us to conclude that the latter factor was dominant when using AT&T type 5-D single mode fiber at 1300 nm. Figure 3 shows the bit capacity of a fiber loop as a function of temperature. Notice that capacity is a meager 30,000 bits if the fiber is in an environment that has a temperature fluctuation of 1 degree C. There are a number of compensation schemes to circumvent this problem.[2]

4. CONCLUSION

Dynamic optical memories serve an important role in the optical memory hierarchy. The design of these memories allows for significant tradeoffs in access time and device count. Practical large-scale memories will require compensation for thermally induced changes in loop capacity.

5. REFERENCES

1. M. I. Belovolov and al., 'Fiber Optic Dynamic Memory for Fast Signal Processing and Optical Computing', *SPIE*, **963**, 90-97 (August 29, 1988).

2. D. B. Sarrazin, H. F. Jordan and V. P. Heuring, 'Fiber Optic Delay Line Memory', *Applied Optics*, **29**, 627-637 (February 10, 1990).

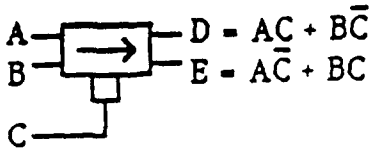

Figure 1. Functionality of the Lithium Niobate Switch

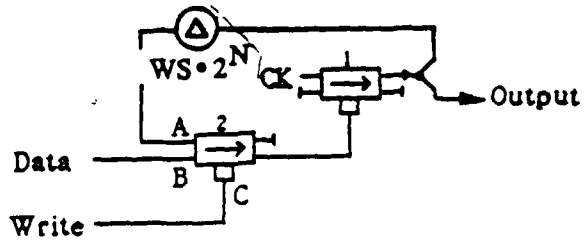

Figure 2a. Fiber Optic Delay Line Memory

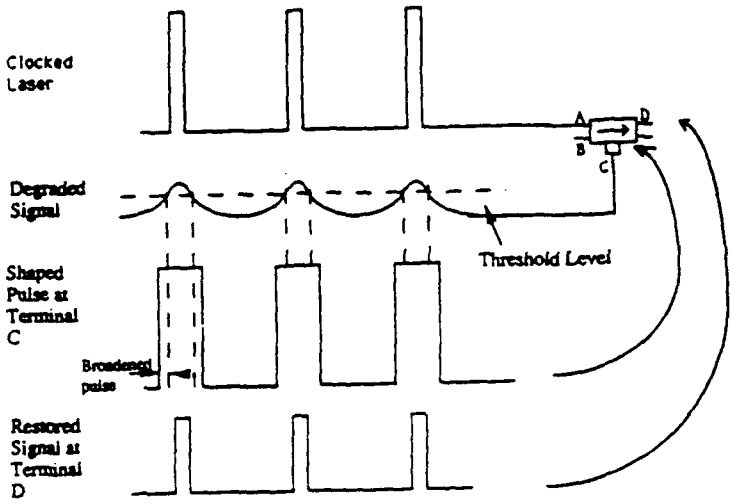

Figure 2b. Use of a Lithium Niobate Switch to Restore Signal Amplitude

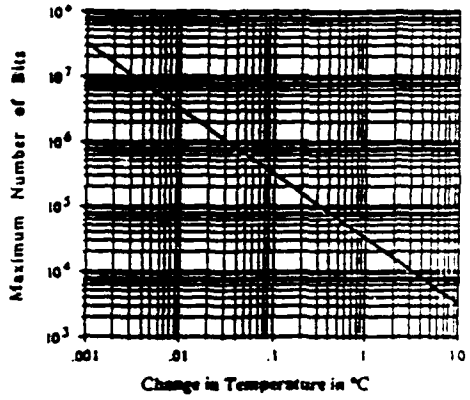

Fig. 3 Maximum number of bits b_{max} as a function of temperature stability ΔT for a lightly doped fiber operating at 1310 nm.

Holographic Data Storage in Photorefractives

Lambertus Hesselink
Stanford University
Stanford CA, 94305-4035

Photorefractives are attractive for data storage applications, because high storage densities can be achieved with low latency and as a result very high throughputs are possible. The theoretical limit on density is computed to be 10^{12} - 10^{13} bits per cm^3 and 10^5 - 10^6 bits can be readout on microsecond time scales using modest laser powers, typically a few mW/cm^2. The density estimates are an upper limit and scattering from striations, crosstalk and erasure from multiple recording tend to lower this number by two to three orders or magnitude. Nevertheless, the potential data throughput is very high on the order of 10^{12} bits/sec, thereby substantially reducing the time required to access large datasets compared with current serial approaches.

There are, however, several issues that need to be addressed before data storage in photorefractives becomes an alternative to conventional magnetic and optical storage approaches. In particular, erasure during readout is a problem that needs to be considered. In the early seventies, data storage in photorefractives was attempted because of the promise of high storage density, not because of low latency and high throughput. As a result, a considerable effort has been expended to find ways to overcome the erasure problem during readout or when writing multiple holograms in the same volume. Several approaches were investigated, including electrical and thermal fixing. Thermal fixing schemes are based on writing a hologram using relatively mobile electrons and forming a mirror space charge field from ions at elevated temperature, so that the mobility is sufficiently large to allow local electric space charge field to establish a corresponding ionic field. The crystal is then cooled and illuminated with a uniform readout beam. The electronic space charge field is erased, revealing the ionic field. Since the mobility of ions at room temperature is low, fixing of the hologram over time periods of days is possible. The disadvantage of this approach is the need for heating of the crystal. This problem may be avoided when using an electrical fixing procedure first outlined by Micheron et al. in 1972. The crystal is poled and illuminated with a

spatially varying intensity pattern until saturation in response is reached. An anti-poling electric field is applied of a certain magnitude depending on the local space charge field and the coercive field for typically 1/2 sec. The hologram is then readout by a uniform beam of extraordinary polarization for SBN. The diffracted beam at first decreases in strength, but then grows in amplitude well above the saturation response and maintains that level for hours. A poling field erases the hologram. This approach has been demonstrated since then in other crystals such as $LiNbO_3$, but no published account has been reported for electrical fixing in SBN since this early effort, despite attempts by several research groups. Redfield and Hesselink demonstrated a procedure by which holograms could be fixed, but not with the high level of efficiency afforded by the electrical fixing approach. In fact, the long term response id rather small, but not negligible and still quite useful for optical data storage. In this approach a hologram is recorded for a certain time period, determined by the materials and geometric arrangement, with ordinary polarization and an applied field of approximately 4 Kv/cm in SBN. The spatial frequency of the grating is approximately 200 lp/mm. The hologram is subsequently readout with extraordinary light. The response initially increases well above the saturation level, but then decays to a small value of a few percent that lingers for hours. This approach allowed Redfield and Hesselink to readout the same hologram at 10 microsecond intervals for 6 hours with a signal to noise ratio exceeding 30 dB.

The approaches described here are useful for fixing of holograms in data storage applications, but some fundamental questions still need to be answered before full utilization of these techniques can be accomplished. Up to now, fixing of holograms has been demonstrated using simple plane waves, but not with multiple, image carrying beams. It is not understood how to optimally fix several image bearing holograms in the same spatial region of the crystal. The origin of the ionic space charge field is not known in one of the most promising materials, namely SBN. The electrical fixing procedure in SBN has not been duplicated and is not understood. To answer some of these questions, detailed studies concerning materials properties and holographic storage is needed. Specific dopant studies are required to examine the nature of the charges involved in charge transport. Such studies must be carried out in close coordination with research efforts concerning data storage architectures, approaches to error correction and I/O operations. Detailed physical models are needed to fully understand the systems and materials

requirements for data storage applications, since these are rather different than those required for optical signal processing systems.

Dynamic 3-D photorefractive optical memories

Y. Fainman
College of Engineering, The University of Michigan
2250 G. G. Brown Bldg., Ann Arbor, MI 48109-2125, tel. (313) 936-0413

Sing H. Lee
Dept. ECE, University of California, San Diego
La Jolla, CA 92093, tel. (619) 534-2413

A large body of work is concerned with applying photorefractive volume gratings to numeric and neural network optical computing problems by utilizing the extremely large storage densities of optical memories. However, success in applying optical memories to optical computing will strongly depend not only on the large memory capacity and the short memory random access time, but also on the dynamic characteristics such as (i) the storage time without degradation of the stored information, (ii) the capability of multiple writing into and reading from the memory without degradation of the material and the stored information, and (iii) erasability, i.e., the ability to replace unnecessary information with new.

Different approaches have been undertaken to optimize the 3-D photorefractive memories with respect to such important dynamic characteristics as erasability and storage time. These existing approaches rely on the properties of the photorefractive materials, but they suffer from a number of disadvantages. For example, the selective erasure [1] approach is based on the superimposed recording of a π-phase shifted image on the image that must be erased. The disadvantages of the selective erasure approach are due to a decrease of the signal-to-noise ratio, which is a result of the coherent accumulation of scattered light, and the gradual optical erasure of stored information by the reading wave. Thermal [2] or electrical fixation [3] approaches have been employed to avoid the problem of readout erasure, but as a consequence, the capability of erasing and rewriting new information is reduced.

To overcome the disadvantages of the material-based approaches to read/write/erasable memories, we propose to employ a system approach called

dynamic or circulating memory [4]. The strategy of the dynamic memory approach is diagrammed in Fig. 1a. The architecture of Fig. 1a is operated in three modes: writing (Fig. 1b), reading (Fig. 1c) , and transfering (Fig. 1d). The input images are stored sequentially in one of the two photorefractive crystals (e.g., PRC1) until the total memory capacity of that crystal is reached (see Fig. 1b). After many readouts (see Fig. 1c) the stored information in PRC1 is degraded. We then transfer the useful part of the information from PRC1 into PRC2 (see Fig. 1d). If the storage capacity of PRC2 is not reached after the transfer, new input images can be recorded in PRC2 in a similar way as that shown in Fig. 1b for storing information in PRC1. Then, the first crystal is optically erased to prepare it for the next cycle, when the memory capacity of the second crystal is overflowed. In contrast to the approach of Ref. 5, where a buffer hologram is used to synthesize a single high diffraction efficiency hologram, this approach produces a dynamic multi-image memory. The dynamic memory approach provides (i) nondestructive readout, i.e., after a large number of readings, the memory can be refreshed by rewriting the still useful information from one crystal into another, and (ii) write/erase capability, i.e., while rewriting the useful part of the information from one crystal to the other, we can also replace some of the old information that must be erased by the new information introduced from the input to the memory. The two crystals are functionally identical, exchanging tasks periodically. An additional advantage of the dynamic memory architecture is provided by the optical gain. Note that memory gain is an important feature for optical computing systems, since they require intensity level restoration.

The optical amplifier must match the format of the input data to the memory. In this regard, it is useful to distinguish between the requirements from the optical amplifiers for input data in a form of a 2-D arrays of intensity distribution (e.g., bit planes for digital optical computing or gray tone images for neural networks) as opposed to data containing amplitude and phase information (e.g., optical interconnections for digital or neural network optical computing). For the former we can employ conventional optically addresses spatial light modulators (OSLMs) based on integration of photodetectors with modulators, while for the latter we require coherent amplifiers that preserve the phase of the input wave, e.g., coherent photorefractive amplifiers [6]. The time response of the photorefractive amplifiers is inversely proportional to the photorefractive sensitivity and the total intensity of the pump and the signal beams. Note that photorefractive crystals

employed in the amplifier can possess higher photorefractive sensitivities (e.g., BSO, [illegible], and GaAs) than the ones employed for storage (e.g., $LiNbO_3$, SBN). Consider a numeric example of a dynamic memory architecture constructed of two SBN:60 and one BSO crystals employed as memory and amplification devices, respectively. Assuming SBN:60 crystals of size 5x5x5 mm, selecting diffraction efficiency of 2 % per image and using typical material parameters for SBN:60 and BSO, we can construct a dynamic 3-D memory with the following characteristics: 2-D memory capacity of $2.5 \cdot 10^7$ and number of volume multiplexed images of 280 provide total memory capacity of more than 5 Gbits; the memory gain of 650; the maximum number of memory accesses before rewriting will be > 10^5; writing and reading memory bandwidths of more than 1 Mbits/sec and 10 GHz/sec, respectively.

We propose to construct the dynamic 3-D photorefractive memory architecture. We will develop techniques to overcome the practical limitations imposed on the 2-D packing densities by the aperture effects of a single lens (e.g., we will design and fabricate holographic optical elements utilizing the approach of diffractive optics, and also use phase conjugation techniques). In order to reach the theoretical limit of the number of multiplexed holograms for 3-D memories, we will study and optimize the efficiency of photorefractive storage in the volume of the material (e.g., using a number of relatively thin crystals as compared to that of a single thick crystal of equal volume). Techniques that will allow to avoid energy coupling during storage in photorefractive materials will be investigated. To optimize the performances of the dynamic memory system we will conduct studies of different memory addressing mechanisms (e.g., angular, wavelength, and random phase coding). We will also investigate parallel recording techniques which will reduce the data transfer time when the memory is operated in the transfer mode shown in Fig. 1d (e.g., parallel data transfer using frequency encoding). By considering the available opto-electronic devices in conjunction with the study of the memory coding techniques, we will be able to further increase the currently achievable reading memory bandwidth with rates of 100 Gbits/sec. By optimizing the writing photorefractive sensitivity, the currently achievable writing memory bandwidth with rates of 1 - 100 Mbits/ sec will be also improved. System related issues such as packaging, power consumption, interfacability, and reliability will be also investigated and utilized in the experimental realization of the dynamic 3-D memory system.

References

1. J. P. Huignard, J. P. Heriau and F. Micheron, "Coherent selective erasure of superimposed volume holograms in lithium niobate," Appl. Phys. Lett., vol. 26, pp. 256-258, 1975.

2. W. J. Burke, D. L. Staebler, W. Phillips and G. A. Alphonse, "Volume phase holographic storage in ferroelectric crystals," Opt. Eng., vol. 17, pp. 308-316, 1978.

3. J. P. Herriau and J. P. Huignard, "Hologram fixing process at room temperature in photorefractive BSO crystals," Appl. Phys. Lett., vol. 49, pp. 1140-1142, 1986.

4. Y. Fainman, "Applications of photorefractive devices for optical computing," Proc. SPIE, vol. 1150, 1989.

5. D. Brady, K. Hsu, and D. Psaltis, "Multiply exposed photorefractive holograms with maximal diffraction efficiency," The 1989 OSA topical meeting on optical computing, Tech. Digest, paper PD2-1, 1989.

6. Y. Fainman and S. H. Lee, "Recent advances in applying nonlinear optical crystals to optical signal processing," Ch. 12 in Handbook of Signal Processing, C. H. Chen, ed., Marcel Dekker Inc., pp. 349-377, 1988.

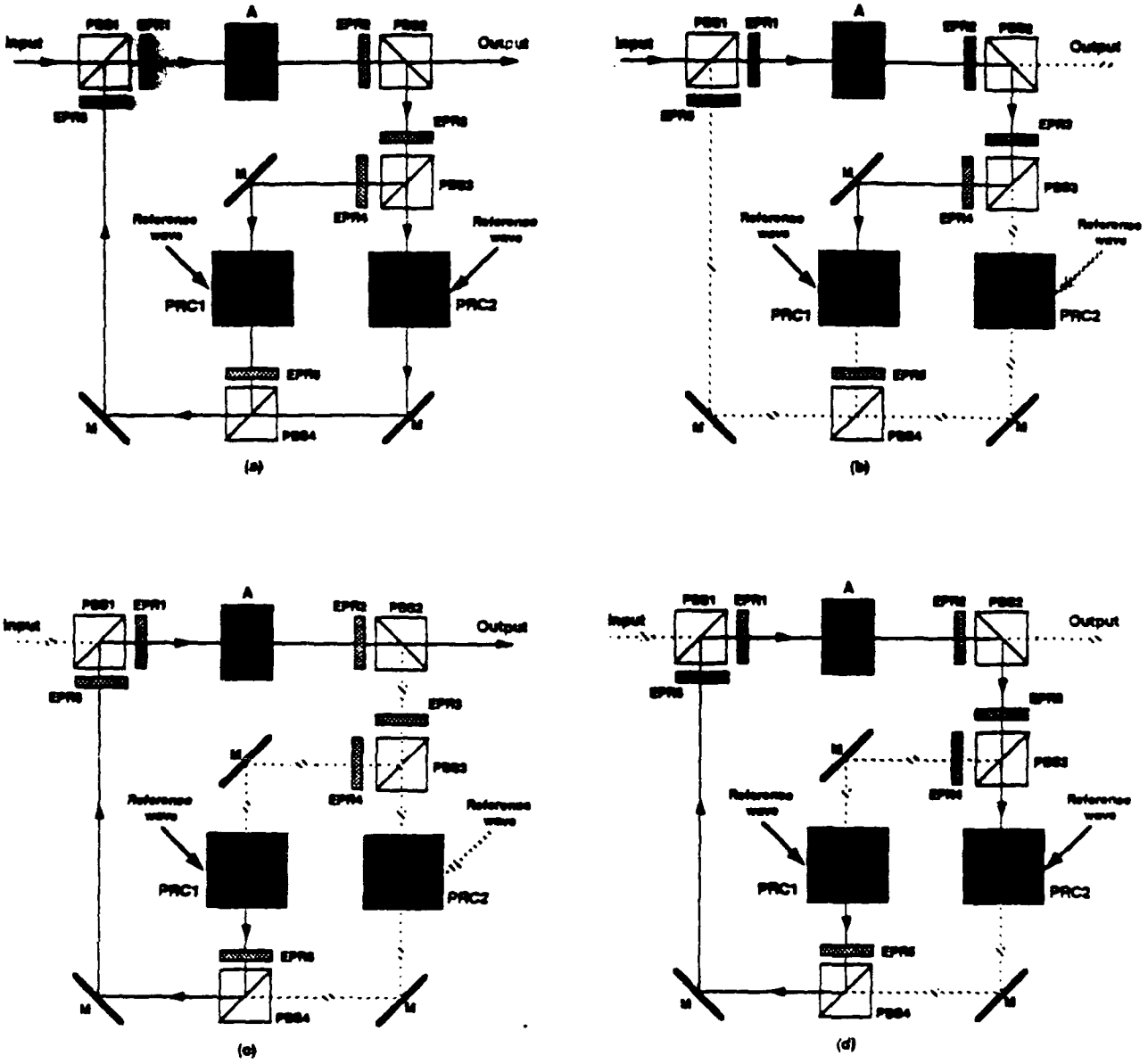

Fig. 1. (a) Schematic diagram of a dynamic 3-D memory architecture. A combination of electronically controlled polarization rotators (EPR) with polarizing beam splitters (PBS) and mirrors (M) to direct information for storage in photorefractive crystals PRC1 and PRC2. In the writing mode, (b), a p-polarized input image is transmitted through PBS1, and EPR1, and amplified by the amplifier, A; the amplified input is then transmitted through EPR2, reflected by PBS2 and PBS3, and is stored in PRC1. The input signal can be directed for storage in PRC2 by turning on EPR3. In the reading mode, (c), the p-polarized reference wave is used to retrieve the corresponding image, which is amplified and channeled to the output of the memory unit by turning on EPR5 and EPR1. In the transfering mode, (d), the information is channeled from the output of PRC1 through the amplifier, A, to the input of PRC2 by turning on EPR5, EPR1, EPR2 and EPR3.

Simulation of 3-D Optical Storage in Photorefractive Crystals and Deposition of Photorefractive Films

Sing H. Lee
Y. Fainman
Sadik Esener

University of California, San Diego
Department of Electrical and Computer Engineering
La Jolla, CA 92093

Photorefractive crystals are the leading material currently available for real-time 3-D optical storage. In 3-D optical storage materials, information can be stored in volume holograms. Since volume holograms store the information distributively, they are more tolerant to material defects. In addition, volume hologram storage offers high diffraction efficiency, angular, and wavelength selectivity. The advantage over thin holograms is higher light throughput, better SNR, and less crosstalk. Finally, in photorefractive crystals information can be recorded and erased in situ in large quantities.

A. Simulations of 3-D Optical Storage in Photorefractive Crystals

What are the storage capacities of different kinds of photorefractive crystals? How is storage capacity dependent on crystal parameters (e.g. dopant level, crystal size and cut) and crystal operating conditions (e.g. applied electric field, temperature control)? How can the storage capacity be optimally utilized (e.g. storage/retrieval system configuration, trade-offs between different system performance parameters such as the number of holograms stored, the complexity of each hologram, the diffraction efficiency, SNR and crosstalk of retrieval)?

To answer these important questions, there are three different approaches: analytical solution, experiment demonstration and computer simulation.

Analytical solutions to the problem have been very elusive. The photorefractive effect has been modeled by two different theories: probability densities (Hopping model) and a series of differential equations (band transport model). Neither of these have been solved without a great deal of approximations. The propagation of light through a volume material of varying index has yet to be solved for more complicated wavefronts than plane-plane wave interactions. The diffraction effect has been expressed as a series of coupled differential equations (coupled mode theory), but the number of equations increases dramatically when considering backscattering and complicated wavefronts.

Experimental investigations are slowed by the large number of crystal and system parameters to monitor. For example, when considering the crystal parameters, it is not easy to change

the impurity concentration in the crystal or cut the crystal in different orientation and thickness. It is even more difficult to remove crystal imperfections, which cause scattering and fanout effects in high gain photorefractives. System parameters that are cumbersome to control include: drift of laser power and frequency, air currents and room temperature, crystal orientations or complex phase codes of the reference beams. All of these system parameters have effects on the exposures of holograms.

Computer simulation can be a valuable alternative to analytical solution or experimental demonstration during the current research and development phase of photorefractives. Based on the current physical models for analytical solutions, computer simulation allows for the investigations of photorefractive behaviors without relying on the many simplifying approximations necessary for an analytical result (e.g. the nature of complexity of the wavefront, the nonlinear interactions in the crystal, etc.). Relationships between photorefractive performance and crystal parameters can be seen as trends, and trade-offs can be assessed more easily. Computer simulations can be faster than experiments in carrying out systematic studies of system parameters because computations can be performed over many long hours or overnight tirelessly with our own VAX or SUN-4. Crystal parameters (e.g. scattering, crystal boundaries, cut and doping concentration) can also be removed/inserted or varied easier in computer simulation than experimentation. We propose to carry out the computer simulation and verify the simulation results against analytical solutions as well as experimental results to establish the accuracy of the simulation model. But, the simulation results can be organized into design rules for optimal optoelectronic system design that utilized photorefractive crystals.

B. Deposition of Photorefractive Films

To increase the memory capacity of a photorefractive crystal, we can increase the dimensions of the crystal. However, increasing the thickness of the crystal is less effective, in practice, than increasing its area because photorefractive crystals possess energy coupling or optical gain (Γ). When these crystals are exposed to optical interference patterns, refractive phase gratings will be formed in the crystals. The refractive modulations of the phase gratings decrease with thickness according to $m(t) = m(0)\exp[-\Gamma t/2]$. For Barium Titanate or Stronium Barium Niobate crystals, $\Gamma = 3$ to $4\,mm^{-1}$. The refractive modulation will be reduced by e^{-1} for the thickness of 500 to 660 μm. Furthermore, the photorefractives with optical gain will cause amplification of noise scattered by imperfections of the crystal. The amplified noise or fanning will reduce the practical number of volume holograms that can be stored in the crystal because the amplified noise consumes available space charges and introduces undesirable crosstalk. Therefore, to increase the storage capacity, it will be more effective to increase the area of the photorefractive material than increasing its thickness beyond $\Gamma/2$.

Photorefractive materials of a large area can be deposited by magnetron sputtering. Sputtering SBN:60 on sapphire is of special interest. We propose to determine the sputtering conditions (e.g. substrate temperature, sputtering source composition, vacuum system pressure) and sputtering rates (related to substrate-source separation and sputtering source power) need to be determined.

Holographic Applications for Optical Data Storage

Raymond K. Kostuk

Optical Sciences Center, and
Department of Electrical and Computer Engineering
University of Arizona
Tucson, AZ. 85721, USA
(602) 621-6172

Abstract

In this paper applications of holography to optical data storage systems are examined. Holography will be considered for use as special purpose optical elements in read/write optical heads of bit serial systems, and as a storage medium for block-oriented data systems. Polarization properties of volume type holographic optical elements are evaluated, and ways of using this characteristic for sensing magneto-optic signals are demonstrated. Application of lithographicaly formed binary phase diffractive gratings are also discussed. Next, the limits of earlier holographic storage systems are summarized and reexamined with reference to new recording techniques and materials.

Introduction

The concept of using holographic techniques for information storage systems was first proposed more than 25 years ago. Initial interest was stimulated by the seemingly high information density which could be interferometrically stored in a volume of optical material[1,2] ($\sim 10^{11}$ bits/cm^3), and the supposition that this information could be retreived. The principle advantage of a holographic approach to data storage is that large blocks or groups of information can be accessed simultaneously. However, early attempts to realize

these systems were limited by the poor performance of available recording materials, beam deflection and detection systems, and by competition from improved magnetic storage systems.

During the past 10 years, bit serial optical disk systems have evolved into high capacity read-write magneto-optical (MO) products. Their performance however, is limited by the relatively slow access times needed to read or write information to the disk. This is due in part to the weight and size requirements for the polarization selective head. Holographic components are an attractive candidate for this application because they can be made in thin, lightweight materials, and several optical functions can be multiplexed in the same medium. These elements can either be generated interferometrically to form volume-type holograms or lithographically to produce binary phase surface-relief gratings.

Another development during the past 5 years has been a renewed interest in associative memory and neural net systems. These rely heavily on the ability to access data in parallel and to perform correlation operations to compress large blocks of data to manageable levels.

This paper begins with an analysis of the polarization properties of volume type holograms and binary phase diffractive elements which may improve the performance of magneto-optic heads. Next, the storage capacity of holographic recording systems are reviewed and their potential performance is updated with new material and device considerations. Finally, new developments in optical data storage systems are presented which feature correlation techniques, photorefractive fibers, and optical disk technology.

I. Application to Data Storage Heads

A typical configuration for a M.O. read/write optical head is illustrated in Figure 1[3]. The head must provide three system functions: i) data detection, ii) focus error detection, and iii) track error detection. Simultaneously accomplishing these tasks and

the requirement to detect small polarization data signals ($\sim 0.5°$ rotation) complicate the design increasing it's weight and the data access time. The higher part count also increases the cost of the overall system.

Holographic optical elements are attractive for this purpose because several optical tasks can be multiplexed into a lightweight and relatively inexpensive medium. Holographic elements can also be easily replicated to reduce manufacturing costs. Several hybrid refractive/holographic head configurations have been suggested[4], and an all holographic head design patented[5]. In order to make full use of holographic elements their polarization properties must be understood. From Kogelnik's coupled wave model[3] the coupling coefficients for an s- polarized reconstruction beam is

$$\kappa_s = \pi \Delta n / \lambda \quad ,$$

where Δn is the refractive index modulation, and λ the free-space optical wavelength of the reconstruction beam. The coupling coefficient for a p-polarized beam is

$$\kappa_p = \kappa_s \hat{r} \cdot \hat{s} \quad ,$$

where $\hat{r}$ and $\hat{s}$ are unit vectors in the direction of the propagation vectors of the reconstruction and diffracted beams respectively. When this angle is 90° the hologram can be made into a polarization beam splitter.

One way to achieve a large interbeam angle in a workable configuration is shown in Fig. 2. In this element the diffracted beam is made to exceed the total internal reflection angle of the substrate material. (For this reason we call this element a substrate-mode hologram.) This construction arrangement allows a full range of s- and p- diffraction efficiencies to be realized as shown in Fig. 3. In particular, a grating can be made insensitive to the polarization of the reconstruction beam by controlling the magnitude of the refractive index modulation. A configuration with an input grating which is not sensitive to the polarization of the reconstruction beam, and a selective output coupling hologram for use

in detecting polarized signal data is shown in Fig. 4. Measured data from a cascaded grating pair of this type of the s-polarized efficiency and p-polarized transmittance are shown in Fig. 5. As indicated, a relatively high level polarization selectivity is possible.

Another important technique for making micro-optical components for use in optical heads is lithographically formed binary phase diffractive elements. These are zero order diffraction elements with binary etch layers approximating the continuous contour of the desired phase function. It can be shown through Fourier analysis[7] that the diffraction efficiency of these elements varies as

$$\eta = \left|\frac{sin(\pi/M)}{(\pi/M)}\right|^2 \quad ,$$

where M is the number of etch levels and equals 2^N with N the number of mask levels. From this expression it can be seen that a 4 mask level process can form a 99 % efficient on-axis element.

Two distinct advantages of the binary phase grating fabrication process are i.) the ability to mathematically specify the reconstructed wavefront, and ii.) the lithographic construction process. The first property allows the formation of optical elements which would be difficult to construct interferometrically by conventional holography methods. It also allows elements to be formed at wavelengths where holographic recording materials are not sensitive. This flexibility has been used to construct elements such as laser diode collimators and beam circularizers[8]. The second property makes micro-optical element fabrication possible for most labs engaged in IC processing. Components may also be integrated with electronic circuits, and large arrays of optical elements can readily be made. Arrays of 60,000 F/5 microlenses in a 5 cm aperture have been realized for use in a rapid optical beam steering system[9]. This device may find use as a replacement for acousto-optic beam steering for holographic storage systems discussed in the next section. This construction process will find increased application in micro-optical systems.

II. Holographic Recording Principles and Capacities

The basic components of a holographic storage and retreival system[10] (Fig.6) consists of a page composer (electro-optic input interface), a Fourier transform lens, recording medium, a beam scanner (to read out data), and a detector array (electro-optic output interface). The stored data can either be encoded in bit or image format[11,12], and Fourier transformed to produce a high density recording. This type of recording makes readout less sensitive to imperfections on the surface of the hologram, and allows readout with a collimated beam. The density of images stored on a non-rotating hologram plane are limited by image projection effects, and the finite aperture of the sub-holograms recorded on the plane[13]. If it is assumed that all bits of data are simultaneously read by the detector array from a single sub-hologram then the capacity of this memory system is given by

$$C = M_h^2 M_d^2 \quad ,$$

where M_h^2 is the number of holograms which fit along the length of the storage plate, and M_d^2 is the number of detectors per length of the detector array.

Assuming a hologram length of 10 cm, a sub-hologram diameter of 1 mm, a hologram-detector separation of 5 cm, and a wavelength of 0.5 μm, results in a worst case diffraction limited spot size projected onto the plane of about 90 μm. A 1 cm square detector array with 90 μm diameter detectors separated by 100 μm is within the capability of current IC fabrication techniques. The capacity of this system becomes

$$C = (100)^2(100)^2 = 10^8.$$

The detector response time will be limited by the time needed to charge the capacitance of the detector to a threshold voltage level. Assuming a CMOS compatible photodiode and

an active load, it can be shown that the power required to charge and discharge a detector and a CMOS inverter is given by[14]

$$\Phi = \frac{3.6(C_D + C_G)V_{DD}f}{R_r} \quad ,$$

where C_D and C_G are the detector and gate capacitance values, V_{DD} is the threshold voltage, R_r the detector responsivity, and f is the operating frequency. The factor 3.6 results from the nature of the biasing circuit. A 100 μm diameter silicon has a capacitance of about 0.2 pF and a responsivity of 0.26 A/W, while the gate has a capacitance of 10 fF (2μm CMOS process) and a threshold voltage of 5V. Using these values, the optical power required to switch the detector at a frequency f is

$$\Phi = 1.45 \times 10^{-5} f(\mu W) \quad .$$

If f = 0.1 MHz, then each of the 10^4 detectors must be illuminated with 1 μW of power. Efficiencies of 20 % were reported for bleached silver halide holograms with a 0.5 mm diameter to form images with 2×10^4 bit patterns[12]. This factor increases the required power to 5 μW/detector for a total laser power of 50 mW. The information rate for this system limited by detector response is

$$R_I = 10^4 \times 10^5 = 10^9 bits/sec \quad .$$

This analysis however did not include the time needed to access a sub-hologram t_A. This term will reduce the information rate of the above system by

$$R_I' = \frac{10^4}{10^{-5} + t_A} bits/sec \quad .$$

Early systems proposed the use of beam steering devices such as mechanical deflectors or acousto-optic (AO) modulators. Current performance of AO beam deflectors allow 0.1 μsec access of up to 1000 points[15], and the transmittance of each device is about 80 %. Two dimensional scanning would therefore drop the total transmittance to 64 %, and increase the required laser power. Another important factor is the cost of these devices (i.e. several

thousand dollars/scanner). For these reasons the beam deflector remains an important obstacle to practical holographic system realization.

III. Current Holographic Storage Systems

i. Data Compression System

Two inherent advantages of optical systems are that blocks of two dimensional information can be handled in parallel, and that correlation operations can be performed between these blocks. If these features are used in inventive ways, large amounts of data can be filtered to produce a desired result in an efficient manner. An example of an instrument of this type is an in-process wafer inspection system[16]. These systems require a stepper driven microscope system to scan and sample the area of a wafer. In the holographic system a filter is made of the desired wafer pattern. Then a hologram is recorded of light reflected from a wafer under inspection after it has passed through the filter. The hologram is then re-illuminated and light from the hologram falls on the inspected wafer. Since the images represent light which pass through the reference filter, it corresponds to defects on the wafer. This procedure has successfully been used to locate 0.5 μm defects on a 6 inch wafer.

ii. Photorefractive Read/Write Systems

The holographic storage systems discussed in Section II were of the read-only variety. Many efforts have been made to store 2-D data in photorefractive crystals in order to realize a read/write memory system[17-20]. Early attempts at achieving this goal were limited by the efficiency, grating volatility, speed, capacity, and cost of optical quality photorefractive crytals. Recently many of these properties have been improved by optimizing crystal growth techniques[21], finding a new method for non-destructive readout[22], and by making

arrays of photorefractive fibers which are much easier and less costly to manufature[23]. These advancements have rekindled interest in photorefractive storage systems. A page-oriented system based on cerium doped SBN fibers is currently under investigation at Stanford University and MCC. The targeted performance parameters are: 10,000 bit pages; 1-10 μsec latency; and a capacity of 200 -1000 Mbytes.

iii. Holographic Disk Systems

The development of rotating disk technology has opened many new possibilities for holographic storage systems. The spatial resolution ($\sim$ 1 μm)of current read-only disk systems along tracks is sufficient to store optical gratings with high information content. Two difficulties of using conventional disks for this task are poor cross track registration and phase uniformity over the surface of the disk. D. Psaltis and his research group at the California Institute of Technology in conjunction with Sony Corp. of Japan have made progress in solving these problems and have successfully stored and retreived 2-D data from optical disks[25,26]. The availabilty of this technology implies that blocks of data can be read out in parallel by rotating the disk, while beam steering need only be carried out in one direction which greatly simplifies the task of data acquisition. It also increases the store of data which can be presented for readout as discussed in Section II.

This system has so far been used to demonstrate a variety of image correlation operations in which an incoming signal must be matched to a large library of data for identification. The projected correlation rate of this system 100×100 pixel images is 40,000/sec , which would be difficult to accomplish electronically. This system is also being used for storage and read out of weight levels for a neural net processor[27]. These systems require very large capacity memories for successful operation.

Conclusions

In this paper an attempt was made to present several aspects of holographic optical elements and recording which show potential for use in optical storage systems. First, the use of both volume type holographic elements and lithographically formed binary phase gratings have many desireable features for use as micro-optical components in M.O. heads. Next, the capacity limits of holographic storage systems were reviewed, and the main obstacle to practical implementation identified as the lack of a high resolution, wide angle beam steering device. Finally, several emerging optical data storage systems were introduced which take advantage of new techniques for holographic storage.

Acknowledgements

The author would greatly like to thank the Optical Data Storage Center and IBM for support and interest in some of the areas discussed in this paper. The author also expresses appreciation to Yang-Tung Huang, Dale Hetherington, and Masayuki Kato for help in fabricating and measuring the volume holograms discussed in Section I.

References

1. P.J. van Heerden, "Theory of optical information storage in solids," Appl. Opt., 2, 393 (1963).

2. P.J. van Heerden, "Note on optical information storage in solids," Appl. Opt., 2, 764 (1963).

G.T. Sincerbox, "Miniature optics for optical recording," SPIE 935, 63 (1988).

4. Y. Kimura, S. Sugama, and Y. Ono, "High performance optical head using optimized holographic optical element," Int. Symp. on Optical Memory, Tech. Digest 16-18 Sept. 1987, p.195.

5. G.T. Sincerbox, U.S. Patent 4,497,534 (1985).

6. H. Kogelnik, "Coupled wave theory for thick hologram gratings," Bell Syst. Tech. J..

48, 2908 (1969).

7. G.J. Swanson, "Binary Optics Technology: The theory and design of multi-level diffractive optical elements," MIT Lincoln Lab Tech. Report 854, 14 Aug. 1989.

8. J.R. Leger, M. Holtz, G.J. Swanson, and W.B. Veldkamp, "Coherent laser beam addition: an application of binary-optics technology," Lincoln Lab. J., 1, 225 (1988).

9. W. Veldkamp, W. Goltsos, and M. Holtz, "Binary optics for rapid optical beam steering (ROBS)," MIT Lincoln Lab Final Report, 15 July 1989.

10. A. Vander Lugt, "Design relationships for holographic memories," Appl. Opt., 12, 1675 (1973).

11. Y. Tsunoda and Y. Takeda, "High density image-storage holograms by a random phase sampling method," Appl. Opt. 13, 2046 (1974).

12. Y. Takeda, "Hologram memory with high quality and high information storage density - Hologram Memory - ," Jap. J. Appl. Phys., 11, 656 (1972).

13. H. Kiemle, " Considerations on holographic memories in the gigabyte region," Appl. Opt., 13, 803 (1974).

14. R.K. Kostuk, Y-T. Huang, D. Hetherington, and M. Kato, "Reducing alignment and chromatic sensitivity of holographic optical interconnects with substrate-mode holograms," Appl. Opt., 28, 4939 (1989).

15. See for example Crystal Technology Model 4080 Acousto-optic beam scanner specifications.

16. T.H. Jeong, "Holography takes on a practical look," Laser Focus, p.89, July (1989).

17. G.A. Alphonse and W. Phillips, "Iron-doped lithium niobate as a read-write holographic storage medium," RCA Review, 37, 1976.

18. L. d'Auria, J.P. Huignard, C. Sleazak, and E. Spitz, " Experimental holographic read-write memory using 3-D storage," Appl. Opt., 13, 1974.

19. B.R. Reddersen and L.M. Ralston, "Digital optical data storage and retrieval," Opt. Eng., 19, 1980.

20. J.E. [redacted]ver and L.M. Gaylord, "Evaluation experiments on holographic storage of binary data in electro-optic crystals," Opt. Eng., **20**, 1981.

21. R.R. Neurgaonkar, W.K. Cory, J.R. Oliver, M.D. Ewbank, and W.F. Hall, " Development and modification of photorefractive properties in the tungsten bronze family crystals," Opt. Eng., **26** , 392 (1987).

22. S. Redfield and L. Hesselink, "Enhanced nondestructive holographic readout in strontium barium niobate," Opt. Lett., **13**, 880 (1988).

23. L. Hesselink and S. Redfield, " Photorefractive holographic recording in strontium barium niobate fibers," Opt. Lett., **13**, 887 (1988).

24. L. Hesselink, "Photorefractive fibers for optical data storage and processing," IEEE Intl. J. Optoelectr., 1990.

25. D. Psaltis, M.A. Neifield, and A. Yamamura, " Image correlators using optical memory disks," Opt. Lett., **14**, 429 (1989).

26. A. Yamamura, M. Neifeld, S. Kobayashi, and D. Psaltis, " Application of optical disk technology to optical information processing," SPIE 33rd Ann. Symp. on Opt. and Opt.-Electr., San Diego, Ca., Aug. 1989.

27. D. Psaltis, M.A. Neifeld, and A. Yamamura, "Optical memory disks in optical information processing," Appl. Opt., **29**, 1990.

To be published in
Proceedings of SPIE - The International Society for Optical Engineering
Volume 639 Advances in Optical Information Processing II (April 1986)

Convolution, correlation, and storage of optical data in inhomogeneously broadened absorbing materials

W. R. Babbitt, Y. S. Bai, and T. W. Mossberg

Department of Physics, Harvard University
Cambridge, Massachusetts 02138

Abstract

We discuss the light signals that are coherently emitted by some optical absorbers subsequent to excitation by a series of three laser excitation pulses. In some cases, the light signal emitted by the material duplicates the temporal shape of one of the laser input pulses. In other cases, the emitted signal represents the convolution or cross-correlation of two of the laser input pulses. In principle, digitally encoded signals of multi-gigahertz bandwidth can be convolved in real time, or, in suitable materials, stored for long periods. Output signals on the order of a few percent as intense as the inputs are possible. We provide experimental demonstrations of these effects, and discuss their implementation in optical signal processing and data storage systems.

Introduction

The effects described in the title and abstract above are possible because of the special properties of Inhomogeneously Broadened optical Absorbers (IBA's). These materials are characterized by absorption profiles that are wider, often much wider, than the absorption profiles of the atoms of which they are composed. This situation comes about, as shown in Figure 1, when the absorption profiles of individual atoms are shifted relative to one another throughout the sample. A dilute gas is a good example of an IBA. Individual atoms have well-defined narrow absorption frequencies, but the atoms move at different velocities and are thereby Doppler shifted relative to each other. It turns out that variations in the local electric fields within solids can also result in strong inhomogeneous broadening. The material and atomic absorption bandwidths described above are referred to, respectively, as the inhomogeneous and homogeneous absorption bandwidths of a given IBA.

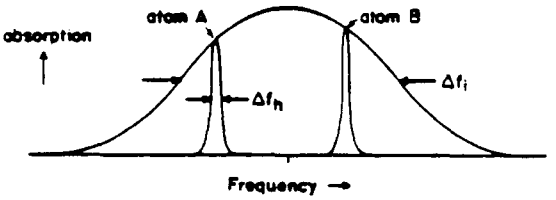

Figure 1. Absorption versus frequency. Wide curve: overall material absorption profile. Narrow curves: absorption profiles of two atoms within the inhomogeneously broadened absorber.

Consider, as shown in Figure 1, an IBA that has an inhomogeneous absorption bandwidth, Δf_i, and is composed of absorber atoms with a smaller homogeneous absorption bandwidth, Δf_h. If a monochromatic laser of frequency f_o is made incident on certain spatial region of the absorber, it will excite only those atoms that lie within the excited spatial region and within a frequency bandwidth Δf_h centered about f_o. As a result, atoms within the IBA can be addressed on the basis of both their spectral and spatial locations. The number of frequency channels independently addressable is determined roughly by the ratio $\Delta f_i/\Delta f_h$. In some materials, this ratio approaches a million. Ultra-high-data-density optical memories have been proposed[1,2] in which spatially and spectrally addressable "holes" are burned in IBA's. The burning of holes in this case actually refers simply to modifying, by photochemical or other means, the absorptivity of the sample.

By virtue of their multitude of frequency channels, IBA's can be used as spectrum analyzers. In fact, as described below, when an IBA is illuminated by a temporally structured laser pulse it automatically records the pulse's Fourier transform. When three pulses excite an IBA, the material emits an output signal whose temporal shape evolves as the inverse transform of the product of the Fourier spectra of all three input pulses.[3] Optical pulse-shape storage/recall[3] and convolution/cross-correlation[4] follow as special cases of this basic result. We now describe the interaction of temporally modulated light pulses with IBA's in more detail. We pay special attention to the physical quantities within the IBA's that represent the Fourier spectra of the input pulses, and to the necessary operating conditions. Actual experimental results are described that verify the basic features of our calculations.

Physical principles

Atoms within the absorbers of interest here may have a variety of internal energy level

schemes. In Figure 2a, we show the simplest. ground and excited state, and incident light causes atoms to move back and forth between these levels. In this simple case, all three laser pulses interact with the same transition, A, and information can be stored in frequency-dependent orderings of level populations[3,5] or a similar ordering of the coherence between the two levels. The coherence between the two levels is important, because it corresponds to the atom's optical electric- or magnetic-dipole moment. If this quantity is nonzero, the sample may emit coherent optical radiation. The properties of the light coherently emitted by the sample are determined by calculating the properties of the atomic coherence.

In this case, the atom possesses simply a

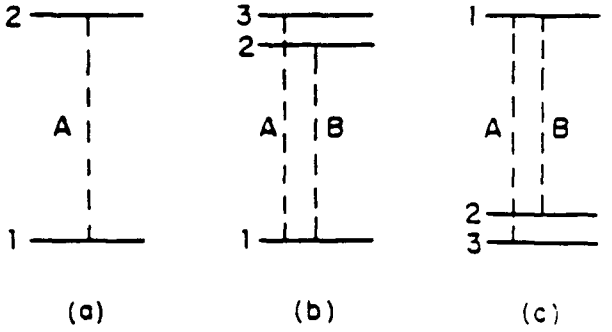

Figure 2. Possible absorber energy-level configurations.

More complicated but perhaps more useful energy level schemes are shown in Figures 2b and 2c. The energy levels 2 and 3 are assumed to be very closely spaced relative to their separation from level 1. In these systems, the transitions A and B may be distinguished by the laser frequency or polarization, and each laser pulse interacts with only a particular one of the transitions. The ability to distinguish light resonant with a particular one of the transitions is useful in detecting the material signal in the background of the laser pulses. In these three-level systems, information may be stored in a spectrally ordered coherences involving any pair of the three levels,[6] or in spectral orderings of population of any one level.[3] For simplicity, we discuss excitation of the two energy level system of Figure 2a, but some of the data presented later was obtained in systems similar to those shown in Figures 2b and 2c.

Consider three laser pulses having electric fields of the form

$$E_p(\vec{r},t) = \varepsilon_p(t-\tau_p)\cos[\omega_0(t-\tau_p)], \qquad (1)$$

where $p = (1, 2, 3)$ denotes the p^{th} pulse in time, $\varepsilon_p(t)$ is a modulation envelope, $\tau_p = (\hat{k}_p\cdot\vec{r})/c + t_p$, $\hat{k}_p$ is the unit wave vector of pulse p, and t_p is the time that pulse p passes the arbitrary location $\vec{r} = 0$. As stated above, we assume for simplicity that all three pulses are resonant with a single inhomogeneously broadened transition (see Figure 2a).

As the first pulse passes through the material, a coherence representing $E_1(\omega)$ is generated, where $E_p(\omega)$ is the Fourier transform of $E_p(t)$. If the second pulse passes through the material before the coherence created by pulse 1 has relaxed, i.e., is delayed by an interval less than Δf_h^{-1} from pulse 1, both energy level populations are modified so as to represent the product $E_1(\omega)E_2(\omega)$. Since the spectral distribution of populations tends to be fairly stable, the interval between the second and third excitation pulses can be fairly long compared to the interval between the first and the second. The permissible delay time can be increased by somehow "destroying" those atoms in the excited state so that they cannot decay back to the ground state and thereby restore thermal equilibrium. This destruction can be accomplished by various photochemical means[1] which convert the excited state atoms to a stable optically inactive chemical species. The second-to-third pulse interval is the one which is used for long term storage of optical pulseshapes.[3] Delays as long as years may be possible in cryogenic solid-state IBA's.[1] During the pulse 2 - pulse 3 interval in three-energy-level systems, the transform product is stored in coherences between the closely spaced energy levels of Figures 2b or 2c.[6] These coherences, as opposed to those involving optically separated levels, can also be fairly stable.

The third pulse creates a new atomic coherence proportional to the product $E_1^*(\omega)E_2(\omega)E_3(\omega)$, and this coherence radiates a signal field of the form[3]

$$E_s(\vec{r},t) \propto \int_{-\infty}^{\infty} E_1^*(\omega)E_2(\omega)E_3(\omega)\exp[i\omega(t-\tau_s)]g(\omega)d\omega, \qquad (2)$$

where $g(\omega)$ represents the inhomogeneous absorption profile of the material with width Δf_h and $\tau_s = \tau_3 + \tau_2 - \tau_1$. The perturbation theory calculation leading to Eq. 2 is only valid in the limit of low intensity excitation pulses. Experimentally it is found that the shape of the output signal deviates from that expected on the basis of Eq. 2 when the intensity of any input pulse exceeds the level necessary to transfer about half of the atomic population in any frequency channel to the excited state. In cases, as detailed below, where a particular input pulse is required to be very short, it is only important that the effect of the pulse be the same on all atoms. In such cases, it turns out that the intensity of the short pulse can be increased to optimize the intensity of the output signal without

affecting the temporal properties expected on the basis of Eq. 2. We also note that the introduction of phase noise onto an amplitude encoded signal is a good way of increasing the maximum attainable signal intensity. The introduction of the phase noise makes it possible to increase the input pulse intensities without violating the condition given above. However, once the bandwidth of a temporally structured pulse exceeds Δf_i or the bandwidth of any needed short input pulses (see below), further increasing it will not result in increased output signal size and may cause distortions in the output signal.

The signal described by Eq. 2 can be regarded as a generalized stimulated photon echo, or a generalized free-induction decay.[7,8] The three laser pulses generate other echo-type signals that occur at various times relative to the excitation pulses and the output signal. These extraneous signals and the excitation pulses themselves must be discriminated against in the process of detecting E_s. Various means are useful in eliminating background signals. The excitation fields may be angled so that E_s is directionally isolated. This approach works well in solids, but beam angling leads to reduced signal intensity in gases. In three-or-more energy level systems, polarized input pulses and polarization selective detection optics are helpful. Finally acousto- or electro-optic shutters may be employed to actively block unwanted background signals.

If we assume the modulation bandwidth of the excitation pulses is narrow compared to Δf_i, the $g(\omega)$ factor in Eq. 2 can be treated as a constant. We can then use Eq. 2 to write the temporal envelope of the output signal, ε_s, in terms of the envelopes of the input pulses, i.e.

$$\varepsilon_s\,(t-\eta_s) = \int_{-\infty}^{\infty} \varepsilon_1(\xi) \left[\int_{-\infty}^{\infty} \varepsilon_2(v)\, \varepsilon_3[\{\xi + (t-\eta_s)\} - v]\, dv \right] d\xi. \qquad (3)$$

This expression indicates that ε_s is the cross-correlation of pulse 1 with the convolution of pulses 2 and 3.

Various special cases are of interest. a) If pulse 1 is short, i.e., a temporal delta function, ε_s is the convolution of pulses 2 and 3. b) If pulse 2 (pulse 3) is a temporal delta function, ε_s is the cross-correlation of pulse 1 with pulse 3 (pulse 2). c) When two of the input pulses are temporal delta functions and the other is temporally structured, the envelope of the output signal duplicates the envelope of the temporally structured input pulse or its time reverse. The time reversal occurs when pulse 1 is the temporally structured one. d) Less obviously, if one of pulses 2 and 3 is temporally structured and the other two pulses are long, of constant intensity, and frequency chirped (swept) across the bandwidth of the temporally structured pulse, the output signal duplicates the temporally structured input pulse. When pulseshape storage/recall is performed according to (c), relatively intense short pulses are needed to optimize the output signal size. If long, frequency-chirped, pulses, as described in (d), are used, relatively low intensities are sufficient to maximize the output signal intensity. It should be noted that the envelope ε_s is not observed directly unless homodyne detection is used. Generally the intensity, which is proportional to $|\varepsilon_s|^2$, is the observed quantity.

In all of the cases described above, if the temporally structured input pulses referred to contain temporal features shorter than Δf_i^{-1}, the IBA will not have sufficient bandwidth to record them. Similarly, the total duration of a temporally structured pulse cannot exceed Δf_h^{-1}, since if it does the IBA will not have enough frequency resolution to record it. Also as mentioned above, pulses 1 and 2 should not be separated in time by more than the limiting pulse duration, i.e., Δf_h^{-1}. When pulses are assumed to be temporal delta functions, they need only be sufficiently short so that their transform is relatively flat over the modulation bandwidth of the temporally structured pulses. The use of short pulses of non-negligible width in pulseshape storage/recall has the effect of suppressing the high frequency components of the temporally structured input pulse.

Experimental implementation

Apparatus

In Figure 3, we show the major components of an apparatus capable of generating the various types of signals described above. Three laser sources, L1-L3, are modulated by modulators M1-M3, and polarized by polarizers P1-P3, respectively. The laser beams are then made incident on the IBA in such a manner that the vector phase-matching condition

$$|\vec{k}_s| = \frac{\omega_s}{c} \qquad (4a)$$

is satisfied, where

$$\vec{k}_s = \vec{k}_3 \pm (\vec{k}_2 - \vec{k}_1), \qquad (4b)$$

$\vec{k}_p$ is the wavevector of pulse p, ω_s is the angular frequency of the output signal, and c is the speed of light. In a solid-state IBA, the plus sign in Eq. 4b is possible. In a gaseous sample, the output signal is progressively degraded in intensity as the input pulses deviate from collinearity or anticollinearity. The output signal travels along the direction $\vec{k}_s$. Extraneous signals travelling in the direction $\vec{k}_s$ are eliminated by the combined action of the polarization selector PS and the acousto- or electro-optic gate (shutter) G. In some implementations, a single laser source may be capable of generating all three input beams. The laser source(s) may be cw dye lasers or preferably semiconductor diode lasers. The modulators may employ traditional acousto- or electro-optical devices, or in the case of semiconductor diode lasers any of the recently developed high-speed modulation schemes.

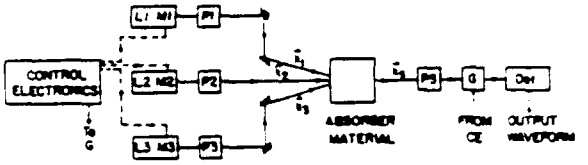

Figure 3. Generalized experimental apparatus.

Materials

Two classes of absorbers appear to be promising. In situations where long term data storage is unimportant, gas phase samples, including in particular atomic vapors, may be very useful. These systems have inhomogeneous and homogeneous absorption bandwidths on the order of a gigahertz and a megahertz, respectively, and therefore provide about 1000 frequency channels. In gaseous samples, diffusion of atoms out of the excitation beams limits sample memory to the time scale of microseconds. With near gigahertz allowable modulation rates, however, a considerable amount of data can still be processed by convolution/cross-correlation on the available time scale. Atomic barium vapor appears to be an appropriate gaseous material to use with semiconductor diode lasers.

Cryogenic solid-state materials form a second potential class of useful absorbers.[1] In these systems, inhomogeneous and homogeneous widths vary enormously. Inhomogeneous widths of tens or hundreds of gigahertz are not uncommon. Homogeneous widths from tens of kilohertz to tens of megahertz are known and fall into the useful range. Furthermore, spectral information stored in populations can be stored for very long times. The disadvantage of these solid-state systems is the need to cool them to the liquid helium temperature range. At much higher temperatures, the homogeneous widths become too large to be useful. While much is known about these solid-state materials and they appear to be very promising for the applications of concern here, pulseshape studies have not yet been performed in them.

Experimental observations

Introduction and general experimental discussion

In this section, we present actual experimental results demonstrating the effects described above. Our description will be necessarily brief, but details can be found in the references cited. All data described below was obtained in a gas phase sample of atomic Yb vapor. Generally speaking, output signals are maximum when the absorber absorbs about half of the excitation pulses' energy (in the absence of saturation). In the Yb system, this means that a 5 cm absorption cell must be maintained at about 450 degrees centigrade. All excitation pulses were derived from the output of a single cw ring dye laser tuned to resonance with the 555.6 nm, $(6s^2)\ ^1S_0 - (6s6p)\ ^1P_1$ transition of ^{174}Yb. The maximum time scale of the experiment was set by the combined effects of upper level natural decay (875 nsec) and the motion of atoms out of the millimeter size excitation volume (2 - 3 microsecond transit time). The modulators of Figure 3 were acousto-optic modulators with 135 to 200 Mhz carrier frequencies and 15-20 nsec rise times. The modulators were the bandwidth limiting factor in our experiments. In some of the cases discussed below, magnetic sublevels of the $^1P_1$ energy level were employed to form a three-level system like that shown in Figure 2b. In all cases, the three excitation beams were collinear. As a result, the output signal was generated in the same direction as the excitation pulses and it was necessary to block the latter by polarization selective optics and an acousto-optic shutter. Occasionally the shutter alone provided sufficient discrimination.

Short-pulse storage of pulseshape information

Population storage. In Figures 4a - 4c, we show the temporal intensity profiles of input

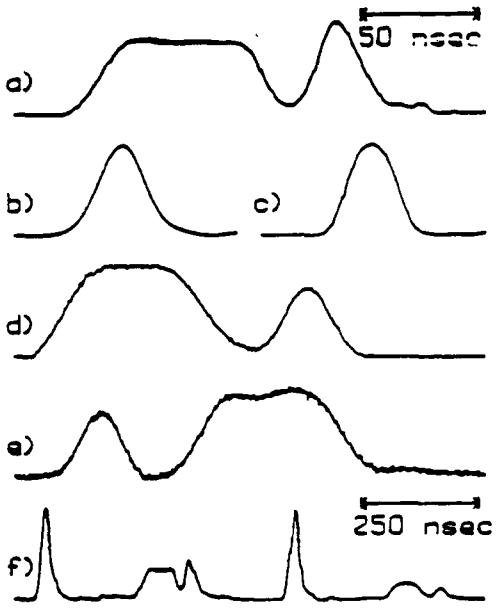

Figure 4. Storage/recall of pulseshapes from the spectral distribution of population in a single energy level.

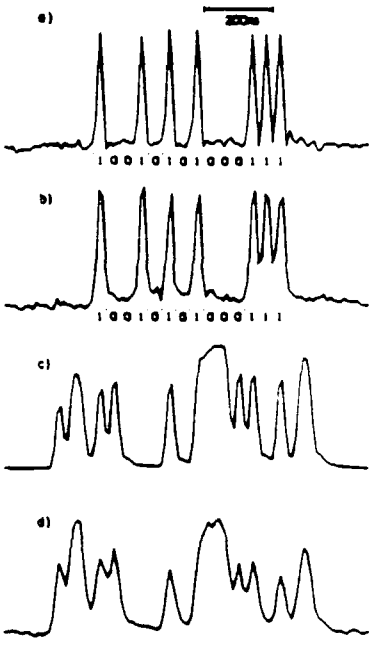

Figure 5. Complex input pulses (traces a and c) and observed output signals (traces b and d). Trace b is a single-event recording.

pulses used to demonstrate, for the first time, that optical pulseshapes can be stored in and recalled from spectral information encoded into the population of a single energy level. In this experiment, performed in a level system like that shown in Figure 2b, the first two excitation pulses excited one transition, say A, while the third excited transition B. In this scheme, the third pulse only samples information stored in the lower energy level. Trace d of Figure 4 is the output signal (intensity) observed when the temporally structured input pulse (trace a) occurs second in the excitation sequence. Trace e is the output signal observed when the temporally structured input pulse is the first excitation pulse. Trace f depicts the three input pulses (left) and observed output signal as used to generate trace d. (In trace f, relative intensities are not accurately portrayed.) All traces were measured using a gated boxcar integer whose 3-5 nsec sampling window was scanned across the profile of many repeating output signals. Reproduction of the stored analog waveforms is quite good. In fact, it is better than expected when the non-negligible widths of the "short" pulses are taken into account. We believe that a frequency chirp, introduced unintentionally onto the raising and falling edges of the short pulses by the acousto-optic modulators used to create them, makes the pulses act shorter than they really are. In this experiment, the signals observed were about 0.1 percent as intense as the input pulses. The signals were estimated to have been degraded by a factor of ten from their potential magnitude by potentially avoidable relaxation effects.

Sublevel coherence storage. A related experiment was reported[6] that demonstrated the storage of pulseshape information in spectrally ordered coherences involving closely spaced levels like those shown in Figures 2b and 2c.

Storage of complex and digitally encoded pulseshapes. In Figure 5, we show[7] temporally structured input pulses, traces a and c, and the corresponding output signals, traces b and d. In these experiments, the pulseshape information was stored in a sublevel coherence involving closely spaced sublevels of the Yb $^2P_1$ state. The other two excitation pulses were in each case short, intense, pulses of about the same duration as the narrowest subpeaks shown in traces a and c. Trace b is a high speed transient digitizer recording of a single output signal. The accuracy of the reproduction is excellent and appears only to be limited by the non-negligible width of the two short excitation pulses. Trace d was averaged over 10,000 output pulses, and reproduces a great deal of information about the input pulse. The smoothing observed is again apparently due to the width of the two short excitation pulses, as well as the 50MHz bandwidth of our digitizer.

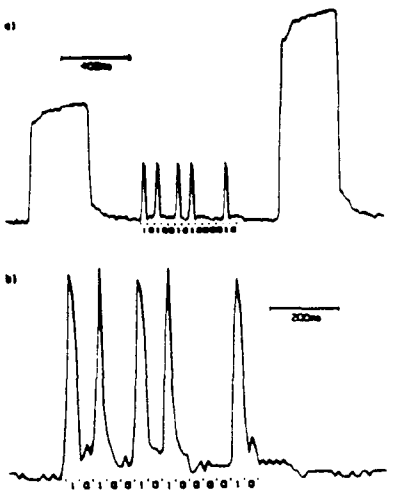

Figure 6. Pulseshape storage/recall with frequency-chirped pulses. Trace a: input pulses. Trace b: single-event output signal.

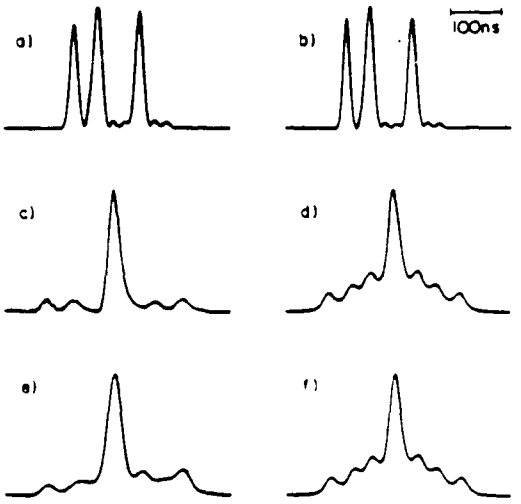

Figure 7. First demonstration of real time cross-correlation using the present techniques (see text).

Chirped-pulse storage of pulseshape information

In Fig. 6a, we show an excitation pulse sequence consisting of (left to right) a long, frequency-chirped pulse, a digitally encoded temporally complex pulse, and finally another long, frequency-chirped pulse. The long pulses were frequency-chirped (linearly) over 40 Mhz by inserting an electro-optic crystal in the cw dye laser cavity. In trace b, we show the single-event output signal.

Convolution and cross/correlation

Initial demonstration. In Fig. 7, we present results obtained in the first experimental study of output pulseshapes generated with multiple temporally structured input pulses. Traces a and b in the figure show the temporal intensity profiles of the pulse 1 and the pulse 3 used in this demonstration. Pulse 2 had the form of a single intense pulse of about the same duration as the subpeaks of pulses 1 and 3. As discussed above, the output signal should have a temporal intensity profile proportional to the square of the cross-correlation of the pulse 1 and pulse 3 electric-field envelopes. The observed output signal is shown in trace c, and the mathematically calculated cross-correlation is shown in trace d. Traces c and d are similar but not identical. In an effort to understand why the output signal did not show precisely the expected behavior, we did exact numerical calculations of the expected output shape which took account of atomic nonlinearities neglected in Eqs. 2 and 3. At excitation intensities above the acceptable level discussed after Eq. 2, our calculation predicted an output signal like that shown in trace e. The same calculation, performed assuming pulses satisfying the post Eq. 2 intensity condition, predicted the output signal of trace f. The former calculation predicts an output quite close to our observed one, while the latter predicts an output in agreement with the predictions of Eqs. 2 and 3. Unfortunately, we were unable to repeat this experiment at lower excitation intensities, but it seems reasonable to conclude that the deviations observed resulted from the use of excess excitation intensity. Observed output signals were 0.1 to 0.4 percent as intense as the input signals.

Mixed binary multiplication using real-time optical convolution. Output signals produced with multiple temporally structured input pulses have been studied more extensively in the context of optical processing.[19] In Figure 8, we schematically depict the input pulses and output signal expected in an experimental scheme to perform mixed binary multiplication. In (a), the numbers 14_{10} and 12_{10} are encoded in binary into the envelopes of the second and third input pulses. The first pulse is short so that in this case the output, the convolution of pulses 2 and 3, should represent the mixed binary product of $14_{10} \times 12_{10}$. In mixed binary, digits correspond to multipliers of powers of two as in binary, but their values are not restricted to 0 and 1. In (b), a third number is encoded (backward) in the first pulse. The output in that case represents the mixed binary product of all three

encoded numbers. In the experiment, a fast shift register was programmed with the numbers to be multiplied. Its serial output was fed, under the control of a 20 Mhz clock, into the acousto-optic modulators that created the input pulses.

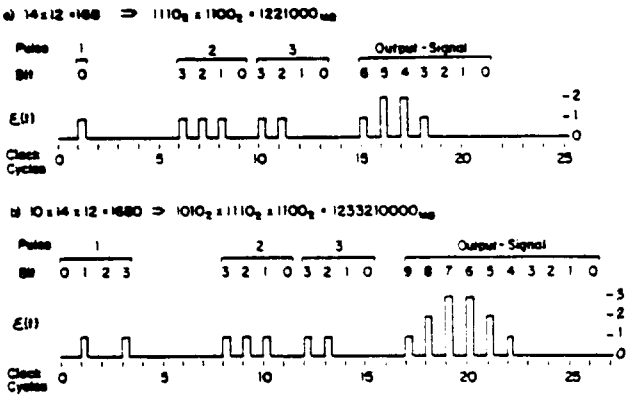

Figure 8. Input and output pulses expected in schemes to perform mixed binary multiplication. (a) Two number multiplication. (b) Three number multiplication.

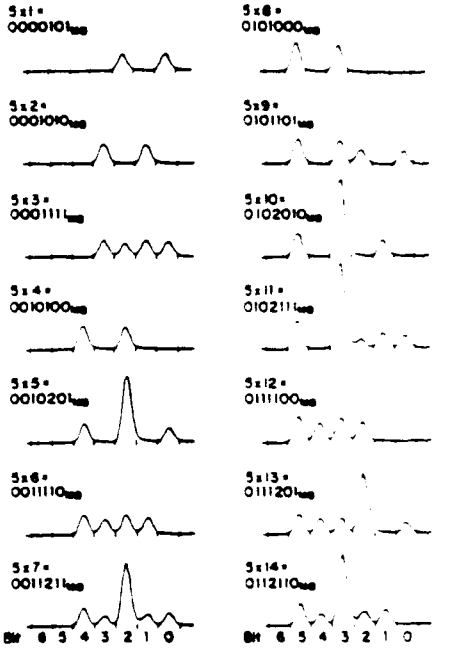

Figure 9. Observed mixed binary products of the numbers indicated by each trace.

In Figure 9, we show observed output signals representing the mixed binary products of the numbers shown. The tick marks shown represent the 40 nsec clock periods. Because we measure the output's intensity rather than its electric field, mixed binary levels are 1, 4, 9, etc. rather than 1, 2, 3, etc. In all cases, the output represents the correct product. Further analysis revealed that most of the peak height variation observed within a given mixed binary level results from material relaxation effects. By operating on a time scale fast compared to material relaxation (by using faster modulators) most of the variation could be eliminated.

Summary

We have presented a new means of storing and processing optical waveforms. This means provides for ultra-fast operations and, in the case of storage, ultra-high data densities. In the absence of material relaxation, output signals can be optimized to be one to several percent as intense as the input pulses. In the demonstrations presented, using rather strongly relaxing materials, output signals 0.1 percent as intense as the input pulses have been realized. With the successful development of generally useful absorber materials, we believe the effects described here will play an important role in future optical technology.

Acknowledgement

We gratefully acknowledge the support of the U. S. Army Research Office (DAAG29-83-K-0040) and the Joint Services Electronics Program (N00014-84-K-0465).

References

1. Moerner, W. E., J. Molec. Elec. 1, 55 (1985).
2. Castro, G., Haarer, D., Macfarlane, R. M., and Trammsdorff, H. P., U. S. Patent 4,101,976 (1978), and Szabo, A., U. S. Patent 3,896,420 (1975).
3. Mossberg, T. W., Opt. Lett. 7, 77 (1982).
4. Bai, Y. S., Babbitt, W. R., Carlson, N. W., and Mossberg, T. W., Appl. Phys. Lett. 45, 714 (1984).
5. Carlson, N. W., Bai, Y. S., Babbitt, W. R., and Mossberg, T. W., Phys. Rev. A 30, 1572 (1984).
6. Carlson, N. W., Babbitt, W. R., Bai, Y. S., and Mossberg, T. W., J. Opt. Soc. Am. B 2, 908 (1985).

7. Shen, Y. R., The Principles of Nonlinear Optics, Wiley, N. Y., 1984, chap. 21.
8. Mossberg, T. W., Kachru, R., Hartmann, S. R., and Flusberg, A. M., Phys. Rev. A 20, 1976 (1979).
9. Babbitt, W. R., Bai, Y. S., and Mossberg, T. W., to be published.
10. Babbitt, W. R., and Mossberg, T. W., Appl. Opt. March 1986.

STIMULATED ECHO OPTICAL MEMORY

R. Kachru
Molecular Physics Laboratory
SRI International
Menlo Park, California 94025

High speed, high capacity, random access memories play an increasingly vital role in computers, telecommunications, image analysis, and other applications requiring large memory capacity and high read/write rates. Traditional memory approaches are based on long-lived magnetic polarization and on short-lived electronic logic circuits. The rapid progress in these technologies is leading to increasing storage density and data transfer rates.

Substantial additional improvements can be expected as the technology is developed for using optical rather than electronic means of data encoding and transfer. The simplest and most familiar example is the digital compact audio disk (CD), in which the high spatial resolution of the laser is used to read bits stored as pits on the surface of a substrate. This approach, which allows data storage densities of 10^7 to 10^8 bits/cm^2 and data input/output rates as high as 2×10^7 bits/s, is beginning to be actively exploited by the computer industry for archival data storage.

The optical memory techniques described above use only one feature of a laser: the ability to generate a high intensity in a small focal area. To take effective advantage of the laser's potential, we also need to encode information by using its spectral and/or temporal profile. One of the earliest proposals to increase the areal density of optical information storage, and to attempt to achieve true volumetric (rather than surface) storage, was to use the spectral resolution of the laser to record multiple bits in the same focal volume, these bits being labeled by the wavelength or frequency of the laser.[1] This approach, called photochemical hole burning (PCHB), is under investigation in several laboratories. It relies on bleaching (or hole-burning) selected molecules that happen to absorb at the incident laser wavelength The selected laser-excited molecules undergo a chemical change that precludes them from absorbing any more laser light at the original wavelength. This reduction in absorption creates a hole in the absorption profile, that leaves an imprint of the laser excitation frequency. The reduction in absorption is monitored by a reading laser beam. The major limitations of this approach are high energy cost of bleaching a sufficient fraction of the absorbing molecules and the long writing time.

During the last three years, several groups elsewhere have been investigating a new,[2] inherently parallel read/write volumetric optical memory concept called the stimulated echo memory.[3-9] When the memory medium is coherently excited by a train of laser pulses, the time history of excitation is recorded as follows. The data to be stored are encoded as a train of short-duration laser pulses, with 1's and 0's being represented by the presence or absence, respectively, of an individual pulse in the train. These "data pulses" enter the sample from one direction, followed in time by a single counterpropagating laser pulse, called the "write pulse." Because the various laser pulses constructively and destructively interfere with each other in exciting the atomic dipoles in the recording medium, the time separations and phase relationships between the laser pulses are holographically impressed on the absorbing atoms, eventually resulting in storage of information in the form of modulations in population in the hyperfine sublevels as a function of the absorption frequency. The information storage is thus absorption frequency selective, unlike that for the compact disk. The frequency selective nature of recording acts as the fourth dimension of the existing three spatial memory dimensions, and it consequently increases the memory density by at least a factor of 10^3 over that of a CD.

When the memory medium is later excited by a single laser pulse, called the "read pulse," the remembered population differences are reexpressed as holographic phase relations between the emissions of the atoms at the various sites. The resulting constructive and destructive interferences produce spatially collimated bursts or pulses of coherent emission. Thus the output appears as a temporally delayed replica or "echo" of the information stored previously.

Our approach shares one feature with the PCHB scheme described above. We depend on the fact that, in a solid sample at low temperature, the distribution of different site environments means that many distinguishable absorption wavelengths are available within the interaction volume. However, rather than scanning the laser between these recording wavelengths, we present the sample with a complex temporal laser profile consisting of many individual pulses and depend on the individual atoms to perform what is effectively a Fourier transformation from the time domain to the frequency domain. As we have briefly described above, the mechanics of reading the memory are especially simple, yielding output in a form identical to the input. In microscopic terms, the atoms have performed the reverse Fourier transformation from the frequency domain back to the time domain.[12]

We can begin to evaluate the potential storage density and read/write speeds for our stimulated echo memory approach by considering the restrictions placed on the laser pulses by the spectral properties of the absorbing atoms. The first requirement is that the laser pulses be separated by enough time that they are distinguishable. The minimum temporal separation between

neighboring pulses is given by $\tau_p = (\pi\delta_I)^{-1}$ where δ_I (called the inhomogeneous linewidth) is the spread in the absorption frequencies of the atoms in the various sites in the sample.

The second requirement is that the last data pulse must arrive while the excited atomic dipoles can still compare it with the first data pulse. The maximum time between the first and last data pulse is given by $T_2 = (\pi\delta_H)^{-1}$ where δ_H (called the homogeneous linewidth) is the effective absorption linewidth of an atom at a specific site. T_2 is also called the dephasing lifetime. Its maximum value is the radiative lifetime of the excited state.

Thus at most T_2/τ_p bits of information can be stored in a single spot and the read/write rate is just $1/\tau_p$. For Pr^{3+} doped in YAG,[10] the best-studied but certainly not the which yield active material, we have $\tau_p \equiv 6$ ps and $T_2 \equiv 5$ μs, obtaining a read/write rate of greater than 10^{11} bits/s and a storage density of more than 10^5 bits per spot.

From the existing data on the fluorescence yields of Pr^{3+}:YAG and estimated echo intensities, we concluded that the minimum number of atoms required per bit was about 10^7, which at a maximum doping of about 10^{19} atoms/cm^3 gave an estimated storage density of 10^{12} bits/cm^3. At that doping, the optical depth is about 200 μm, so the "spot" would have an area of about 5×10^{-6} cm^2, giving (for comparison with a CD) a *surface storage density* of 2×10^{10} bits/cm^2. Already, it is clear that the stimulated echo memory approach offers improvements of multiple orders of magnitude over other techniques. Thus far we have been able to store up to 45 bits of digital information in a single spatial location. Our goal is to store 10^3 bits. In addition we have found that in Eu:YAℓO$_3$ information can be stored for more than five hours.[8]

The discussion above has used the simple model of a single, spatially uniform laser beam that has been temporally modulated. Recently, we have demonstrated that dramatic increases in data throughput are potentially available by encoding additional information on the spatial profile of the laser beam.[4,5] We refer to this process as image storage. In principle, a different two-dimensional image could be encoded on each laser pulse, each pixel of which could be considered as an individual bit. If we suppose that 10^5 pixels can be used for each image, we estimate that a read/write rate of over 10^{15} bits/s could be achievable. Thus we might be able to store 10^5 images, each containing 10^5 pixels, in 10^{-5} s in an area of 1 cm^2.

Although there has been substantial increase in our understanding of the stimulated echo memory concept, and the material characterization, there are two broad areas of research that must be addressed before a practical device can be made. These areas of research are:

1. Characterization of memory performance by optimization of multiple-bit digital and image storage prototypes, with special attention to fidelity and signal/noise ratios.

2. Optimization of memory characteristics by materials studies on various ions and hosts, investigation of the effects of temperature and applied magnetic fields, and studies of the mechanisms that control the signal size.

Given its potential high speed and high density, and the limited storage lifetime of the order of days, the stimulated echo optical memory is most suited to applications such as a main or cache computer memory, dynamic memory for a fast computer. In addition this memory will be very suitable for those applications requiring fast input/output, direct image storage and image processing. Conversely, the rare-earth doped crystal materials discussed above make it unsuitable as a permanent, archival, disk type memory. In addition the fast input/output speed inherent in the materials we are investigating require some thinking about how this memory can be interfaced with the current and future computer architecture.

REFERENCES

1. F. M. Schellenberg, W. Lenth, and G. C. Bjorklund, Appl. Opt. **25**, 3207 (1986).
2. T. W. Mossberg, Opt. Lett. **7**, 77 (1982).
3. Y. S. Bai and T. W. Mossberg, Opt. Lett. **11**, 30 (1986).
4. M. K. Kim and R. Kachru, J. Opt. Soc. Am. B **4**, 305 (1987).
5. M. K. Kim and R. Kachru, Otp. Lett. **12**, 593 (1987).
6. M. Mitsunaga, M. K. Kim, and R. Kachru, Opt. Lett. **13**, 536 (1988).
7. W. R. Babbitt and T. W. Mossberg, Optics. Commun. **65**, 185 (1988).
8. M. K. Kim and R. Kachru, Opt. Lett. **14**, 423 (1989).
9. M. K. Kim and R. Kachru, Appl. Opt. **28**, 2186 (1989).
10. R. M. Macfarlane and R. M. Shelby, "Coherent Transient and Hole-burning Spectroscopy of Rare Earth Ions in Solids," in *Spectroscopy of Solids Containing Rare Earth Ions*, A. A. Kaplyanskii and R. M. Macfarlane, Eds. (North Holland 1987).

a reprint from Applied Optics

Potentials of two-photon based 3-D optical memories for high performance computing

Susan Hunter, Fouad Kiamilev, Sadik Esener, Dimitri A. Parthenopoulos, and Peter M. Rentzepis

The advent of optoelectronic computers and highly parallel electronic processors has brought about a need for storage systems with enormous memory capacity and memory bandwidth. These demands cannot be met with current memory technologies (i.e., semiconductor, magnetic, or optical disk) without having the memory system completely dominate the processors in terms of the overall cost, power consumption, volume, and weight. As a solution, we propose an optical volume memory based on the two-photon effect which allows for high density and parallel access. In addition, the two-photon 3-D memory system has the advantages of having high capacity and throughput which may overcome the disadvantages of current memories.

I. Introduction

Sequential computers are approaching a fundamental physical limit on their computational power.[1] To achieve higher performance, computers are increasingly relying on parallel processing and require memory systems with high capacity and fast parallel access.[2,3] Present memory technologies such as semiconductor memories,[4] optical disks,[5] rigid and flexible magnetic disks,[6] and magnetic tape[7] store information across a planar surface. Due to their 2-D nature, these storage devices are not able to provide parallel access, and in addition their access time grows with increasing capacity. The use of these devices in parallel computers can lead to an unbalanced situation where the cost, volume, and power requirements of the memory system greatly exceed that of the processors.[8]

To overcome the restrictions imposed by present memory devices, research has been seeking alternate means for storage, including 3-D optical memory devices.[9] Three-dimensional optical storage devices have higher theoretical storage capacity than present memory devices, because information is stored in volume. For example, the maximum theoretical storage density for an optical disk is $\rho_{2\text{-}D} = 1/\lambda^2 = 3.5 \times 10^8$ bits/cm^2 assuming that 0.5 μm wavelength of light is used to access the information. On the other hand, assuming the same wavelength of light, the maximum theoretical storage density of a 3-D memory device is $\rho_{3\text{-}D} = 1/\lambda^3 = 6.5 \times 10^{12}$ bits/cm^3. In addition, 3-D optical memory devices have the potential for parallel access, because an entire bit plane can be read or written in a single memory access operation. However, the difficulty in addressing the individual memory bits without data interaction and crosstalk with other bits has obstructed the development of 3-D optical memory devices.

We describe two-photon optical materials, device architecture, and potential applications for a bit-oriented two-photon 3-D optical memory device. Unlike other schemes which have been proposed for 3-D optical memories, such as the photorefractive effect (for holographic storage),[10] spectral hole burning,[11] and optical echo,[12] the two-photon effect[13,14] provides a means of storing data into separate bit locations throughout the entire volume without affecting the neighboring bit locations. In addition, the two-photon process has the benefits of high sensitivity, high speed, and the ability to work near room temperature. As discussed in this paper, a 3-D memory based on the two-photon effect can achieve very high capacity as well as parallel access of up to 10^6 bits/memory access operation. Finally, the two-photon 3-D memory can potentially have a low cost per bit because the material it uses can be made as an inexpensive polymer.

The paper is organized in three parts. Section II presents the physical principle behind the two-photon effect and describes the characteristics of two-photon materials that make them uniquely suited for 3-D

Dimitri Parthenopoulos and Peter Rentzepis are with University of California, Irvine, Chemistry Department, Irvine, California 92717; the other authors are with University of California, San Diego, Electrical & Computer Engineering Department, La Jolla, California 92093.

Received 27 June 1989.
0003-6935/90/142058-09$02.00/0.

memory. Preliminary experimental results are also given to substantiate these characteristics. In Sec. III the two-photon 3-D memory device is described, and the feasibility of its critical components is studied. Finally, in Sec. IV the two-photon 3-D memory device is compared with existing memory technologies, and its application in existing and future parallel supercomputers is discussed.

II. Principles of the Two-Photon Process

This section describes the nature of the two-photon effect and discusses how it can be incorporated into an optical volume memory due to the unique addressing capabilities. Experimental data are presented on the read and write cycles of the spirobenzopyran, a two-photon material.

A. Two-Photon Absorption and Its Relevance to Memory Functions

Two-photon absorption refers to the excitation of a molecule to an electronic state of higher energy by the simultaneous absorption to two photons. The first photon excites the molecule to a virtual state, while the second photon further excites the molecule to a real excited state. Since the intermediate state is a virtual state, the two-photon process is different from a biphotonic process where a real intermediate state is present.[15]

The wavelengths of the two beams are such that, although neither beam is absorbed individually, the combination of the two wavelengths is in resonance with a molecular transition. Therefore, both beams must temporally and spatially overlap for two-photon absorption to result.

As shown in Fig. 1, the two beams, of equal or different wavelengths, are directed along different directions to select any region inside the material. Since the two-photon process is localized to the small region of overlap, all points in the volume can be individually addressed. Depending on the wavelengths of the two beams, which are incident on the material, the addressed location can be written or read, as discussed in the next section. In addition, since the two-photon is based on molecule transitions, the material is theoretically able to operate in the picosecond regime. Finally, the small size of the molecule and low crosstalk between neighboring bits should theoretically be able to reach the optical diffraction limit of $\sim 1\ \mu m$.

B. Material Feasibility Studies

A prototype photochromic molecule has been used to demonstrate the feasibility of 3-D optical memory based on two-photon processes.[16] The photochromic molecule, a spirobenzopyran,[17] initially absorbs only in the UV region; on excitation it undergoes structural changes and it subsequently absorbs in the visible region also. A schematic energy level diagram is presented in Fig. 2. The spirobenzopyran, embedded in a polymer matrix in the form of a 100-μm film, has been irradiated simultaneously with two beams of 30-ps pulses at 532 and 1064 nm and a total energy density of

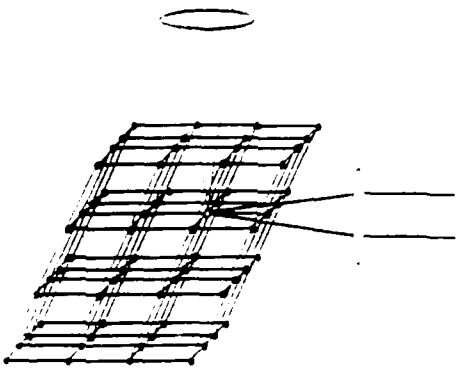

Fig. 1. Optical addressing of data inside a volume using two orthogonal beams incident on the two-photon material.

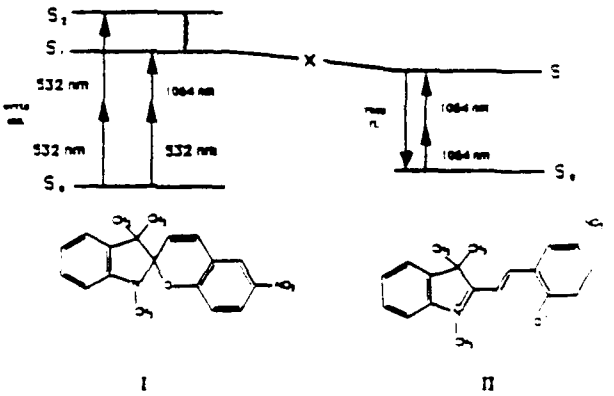

Fig. 2. Schematic energy level diagram of the write and read forms of the photochromic molecule. "X" is an intermediate to the isomerization of the spirobenzopyrans. The structures of the two forms of SP as well as the laser wavelengths used for writing and reading are shown also.

$<10\ nJ/\mu m^2$. Although initially the spirobenzopyran does not absorb in the visible or near IR, two-photon absorption of the two beams resulted in coloration of the films. The absorption spectrum of the written colored molecule is shown in Fig. 3.

The read process is also based on two-photon absorption of laser light. The written form of the molecule was excited with two beams of 1064 nm resulting in two-photon absorption of the IR photons and emission of fluorescence from the written form. The two-photon-induced fluorescence spectrum of the written form is shown in Fig. 4. The intensity of the observed fluorescence shows a square dependence on the excitation pulse energy, as shown in Fig. 5, which unequivocally demonstrates the two-photon nature of the process. Thus the read cycle, which can be as fast as a few tens of picoseconds, is also based on a two-photon process allowing 3-D reading of the stored information.

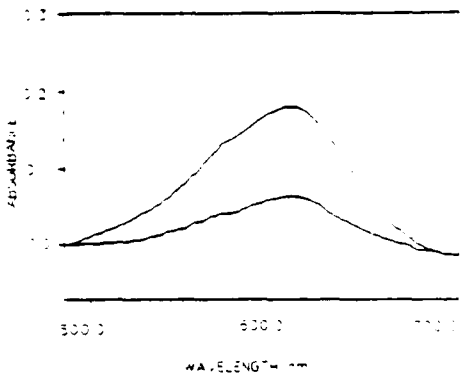

Fig. 3. Room temperature visible absorption spectrum of 1% SP in a PSt film. Upper curve: after irradiation for 5 s with 355 nm, pulse fluence, 4 mJ/cm². Lower curve: after irradiation for 60 s with 532 and 1064 nm; total pulse fluence, 20 mJ/cm²; beam diameter d = 1 cm.

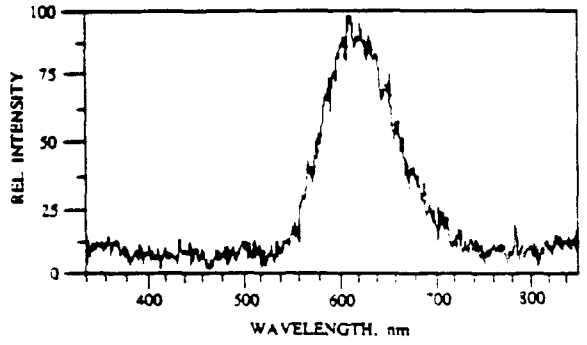

Fig. 4. Room temperature two-photon-induced fluorescence spectra of the colored merocyanine form of 1% SP in PMMA. Excitation wavelength, 1064 nm; pulse fluence, 1.5 mJ/cm²; beam diameter d = 2 mm.

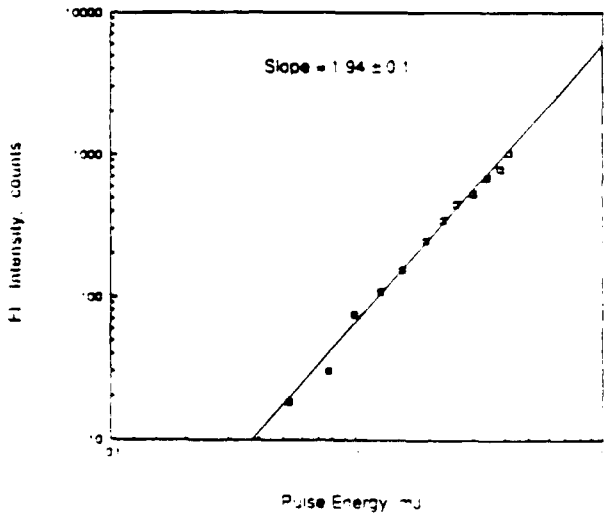

Fig. 5. Log-log plot of the two-photon fluorescence intensity vs excitation pulse energy. A slope of 2 within experimental error is observed.

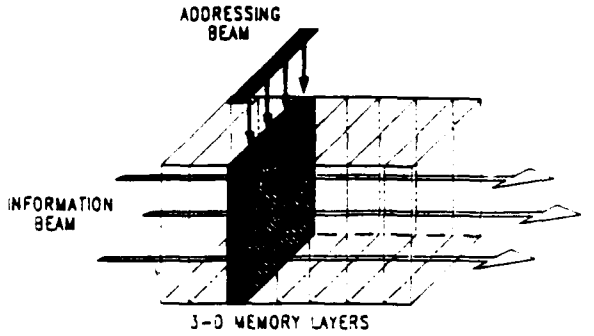

Fig. 6. Addressing a two-photon volume storage material. The dark regions indicate the written bits.

Since the read cycle is based on fluorescence rather than changes in absorbance, higher sensitivity is obtained. The written form persists at room temperature for several minutes. When the written form is placed in dry ice the written form persisted for several days. A complete discussion of the experimental results based on a spirobenzopyran molecule is presented elsewhere.[18]

III. Two-Photon 3-D Memory Device

Now that the behavior of the memory material has been explained, a complete description of the proposed two-photon 3-D memory device is provided. The critical components in the proposed device are then discussed.

A. Three-Dimensional Memory Device Description

The actual memory unit can be described as a multilayer storage system, with each layer composed of a large 2-D array of bits. As shown in Fig. 6, the desired memory layer is selected and illuminated with the addressing beam. At the same time, the data are sent into the memory on the information beam. Due to the two-photon nature of the material, the data can only be stored in the selected layer, as shown by the darkened regions in Fig. 6. A very important characteristic of this system is the fact that as high performance spatial light modulator arrays become available and the two-photon materials are optimized for smaller writing energies, the entire array of bits in a single layer can be accessed simultaneously, allowing the memory system I/O to have a parallelism up to 10^6.

The complete two-photon 3-D memory device architecture is shown in Fig. 7. The 3-D memory unit has been drawn to show the orientation of the individual memory layers. The connection between this memory system and the computer which is addressing the memory is via the input and output arrays and the address manager. The optical components, such as the dynamic focusing lens (DFL), polarizers, and retardation plate, provide the necessary imaging between the input/output arrays and the selected memory layer. The system uses a Nd:YAG diode pumped solid state laser as the optical power supply.

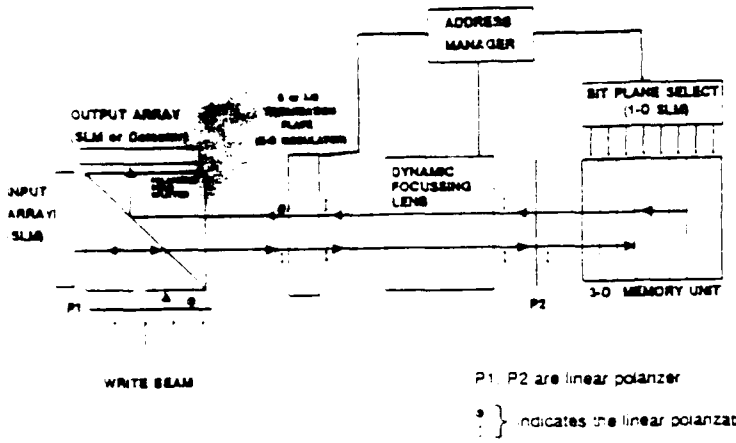

Fig. 7. Two-photon 3-D memory system. The memory I/O is achieved via the input and output SLMs. The address manager controls the internal components to assure proper imaging between the data arrays and the correct memory layer.

Both the write and read cycles have been drawn to show the flow of information into and out of the 3-D memory unit. For the write cycle, it is desired to take the information which is contained on the input spatial light modulator (SLM) and store it at a particular memory location. The first step of the write cycle is for the host computer to send the memory address to the address manager. The address manager then communicates with the bit plane select (to illuminate the correct memory plane) and the DFL (to establish a proper imaging system between the input array and memory location). Next, the host computer puts the desired bit plane information onto the input array. The final step is for the write beam to enter through the polarizing beam splitter (PBS) and be deflected toward the input SLM. The SLM will modulate the polarization of the optical field in direct correspondence with the desired information plane. On reflection back through the PBS, only the modulated parts are allowed to go straight through and will be imaged onto the selected memory layer.

For the read cycle, the bit plane select array illuminates a particular layer of the memory. This causes light to be generated by two-photon fluorescence at each of the written bits. This light is then polarized by $P2$ and imaged onto the output array using the DFL. To steer the information through the PBS and onto the output plane, the polarization must be rotated by 90°. This is achieved with the activation of the electrooptic $\lambda/2$ retardation plate during each read operation. The address manager controls all the essential components (dynamic focusing lens, bit plane select, $\lambda/2$ retardation plate) to guarantee that the information is imaged onto the output detector array.

It is desirable for the memory system to have the highest possible access speed and parallelism. In the proposed two-photon 3-D memory system, the speed and parallelism are limited by the response time, size, and sensitivity of the input and output arrays and the DFL rather than by the very high inherent speed of the two-photon materials. Therefore, the design of these components is critical and is now discussed.

B. Critical Component Feasibility

The input and output devices which are used in the memory system depend on the type of computing system which is accessing the memory as well as the desired access time for the memory. For electronic computers, the input and output devices must perform high speed electronic–optical conversions so that the access times can be made as short as possible. Such a conversion can be carried out at the output with the use of a sensitive optical detector array, while the input device can be an electronically addressed SLM. Note that the output array must be sensitive enough to detect the fluorescence of individual bits. Also, the input array should be able to supply enough energy per pixel to write to each bit. For future optoelectronic computers, the input and output arrays must be optically addressed SLMs. We are envisioning the utilization of sensitivity enhanced silicon PLZT SLMs (S-PLZT)[19] for these applications.

The DFL is also an important component in the system since it provides the interface between the SLMs and memory unit. Although dynamic focusing lens systems have been used for many years (in microscopes, zoom lenses), the high speed and accuracy required for this application are unique in that they preclude the use of mechanical adjustments. In addition to the microsecond speed, the DFL must be able to image 1 μm^2 spot arrays to any memory bit plane. To meet these requirements, we can combine an electrooptic dynamic focusing lens with a holographic dynamic focusing lens (HDFL) that is presently being developed at UCSD.

The HDFL works on the idea that a hologram can be used to store several lens functions, each of which can be individually recalled. Initially, a multiplexed hologram is recorded using the method of random phase encoding.[20] Random phase encoding was chosen since the code can be generated on a phase-only SLM. Therefore, the selection of the correct hologram is limited only by the speed of this device. The HDFL setup is shown in Fig. 8. The hologram is placed at the plane S_1 and contains each lens function L_i and its

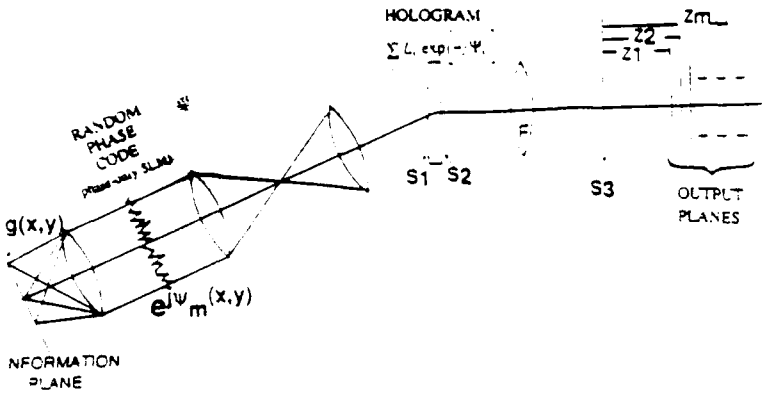

Fig. 8. Design for the holographic dynamic focusing lens. The system provides imaging between the information plane and any one of the desired output planes. The hologram has been made using random phase codes to achieve a multiplexed hologram of all the desired lens functions. An individual lens function is selected by presenting the correct phase code on a phase-only SLM.

associated random phase pattern $[\exp(-j\Psi_n)]$. The information is placed at S_1 and picks up the phase code $\exp(j\Psi_m)$ at S_2. This phase code allows for the selection of the lens function L_m, which will focus to the output plane located at Z_m. Therefore, this system creates an imaging system between S_1 and any of the output planes by placing the phase code of the desired lens function onto a phase-only SLM. Moreover, the reciprocal nature of this linear optical system allows the same HDFL to be used for the input and output to the memory unit.

One attractive feature is that any focal length lens can theoretically be produced. Unfortunately, the total number of superimposed images will be limited due to the increase in the noise with each additional stored lens function. To achieve a large number of memory bit planes, the final design of the DFL requires a combination of an electrooptic DFL (such as the liquid crystal lens)[5] and the HDFL. In such an arrangement, the HDFL would focus to several positions throughout the length of the memory, while the electrooptic DFL could provide more precise focusing capabilities. This arrangement is very advantageous, since the complementary characteristics of HDFL and electrooptic DFL can be combined to achieve the desired results.

The throughput of the two-photon 3-D memory system is, therefore, governed by the SLMs used for the input and output arrays, the DFL, the energy requirements of the two-photon materials, as well as the optical power supply technologies that are available. Using SLM technologies that will be available in the early 1990s, a DFL device as described above, and optimized two-photon storage materials, the two-photon 3-D device can have an IO bandwidth as large as 0.25 Tbits/s, assuming 512 × 512 SLMs operating at a frame rate of 1 MHz. One important fact is that these same technological limitations apply to the performance of future optoelectronic computers, since such computers will rely on similar SLM technologies. It is, therefore, believed that two-photon memories will remain compatible with optoelectronic processing for many years to come, since both of these technologies will progress at approximately the same rate.

IV. Comparison and Application of 3-D Optical Memory

This section compares the projected performance of the two-photon 3-D memory device with the performance of existing memory devices and describes potential applications of 3-D optical memory in parallel computers. We show that the proposed 3-D optical memory device can be effectively used in present parallel computers and will be required for the success of future optoelectronic and 3-D VLSI parallel computers.

A. Two-Photon 3-D Memory vs Present Memory Technologies

The performance of the two-photon 3-D memory device is compared with present memory devices in Table I. The two-photon 3-D memory device provides the highest storage density and the largest parallelism (bandwidth) of any existing memory device. As shown in Fig. 9, existing memory devices are projected to increase their storage capacity, but their bandwidth is expected to grow at a very slow rate. This fine parallel access capability of the two-photon 3-D memory device will not be achieved by existing memory devices. As shown in Fig. 10, the access time of the two-photon 3-D memory device is between the access times of semiconductor memory and magnetic disk devices. Therefore, with low cost per megabyte, two-photon 3-D memory can potentially become a more cost-effective mass storage technology than magnetic and optical disks.

B. Potential Applications of Two-Photon 3-D Memory

The potential uses of the two-photon 3-D memory device in existing and future parallel computers are described in Table II. The data from Table II are graphically presented in Figs. 11 and 12. Figure 11 shows that the bandwidth of the 3-D memory device either exceeds or meets the bandwidth requirements of existing and future parallel computers. On the other hand, the data transfer rate of existing memory devices is far below the required bandwidth, thus requiring the use of many of these devices in parallel to achieve a higher bandwidth. Figure 12 shows the cycle times of parallel computers vs the number of processing ele-

Table I. Two-Photon 3-D Memory and Its Comparison with Other Memory Devices (per 1989 Data)

Device	Capacity	Cost Per Mbyte	Access Time	I/O Bandwidth	Volatile Storage?	Future Trends and Other Comments
Two-Photon 3-D Memory	$\sim 10^{14}$ bits	$0.1 - $10	1 ms - 1 μs	1 Gbit/sec-1Tbit/sec 10^6 Channels Parallel	No	Device at research/development stage. Expect prototype in late 90's
Static RAM (BiCMOS) [4]	256 Kbit	$1,000	10 nsec	100 Mbit/sec Serial	Yes	Expensive and fast memory, used in caches and supercomputers. Expect 1Mbit with same cost by 1995.
Dynamic RAM (CMOS) [4]	1 Mbit	$100	100 ns	10 Mbit/sec Serial	Yes	Used for main memory. Expect 64 Mbit DRAM by 1995. Beyond 64Mbit, a breakthrough in technology is needed.
Solid-State Disk Drive [29]	1.28 Gbits	$300	200 μs	24 Mbit/sec Serial	Yes	Solid-state disk fills the gap between main memory and disk drives.
5.25" Optical Disk Drive [30]	10 Gbits	$5.25	20 ms	20 Mbit/sec Serial	No	Density is expected to double every 2.5 years. Other parameters grow at slower pace.
5.25" Magnetic Disk Drive [30]	10 Gbits	$1	10 ms	20 Mbit/sec Serial	No	Density is expected to double every 2.5 yrs. Other parameters grow at slower pace.
IBM 3390 Disk Drive [7]	120 Gbits	$10	10 ms	36 Mbit/sec Serial	No	Used in supercomputers. Trend is to replace these with an array of 5¼" drives, since they are more cost effective.
Digital Tape Recorder [7]	2000 Gbits	$.0025	Sequential	150 Mbit/sec Serial	No	Used for off-line data storage. Does not support random access.

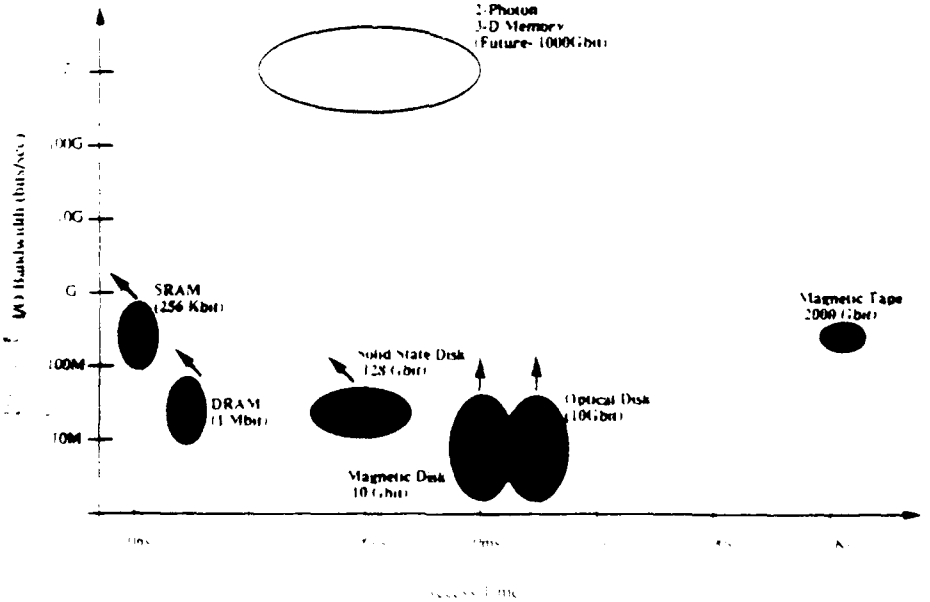

Fig. 9. Comparison of the two-photon 3-D memory device to other memory devices on the basis of access time and data transfer rate (bandwidth). The two-photon 3-D memory device provides a much higher bandwidth than present memory technologies due to parallel access.

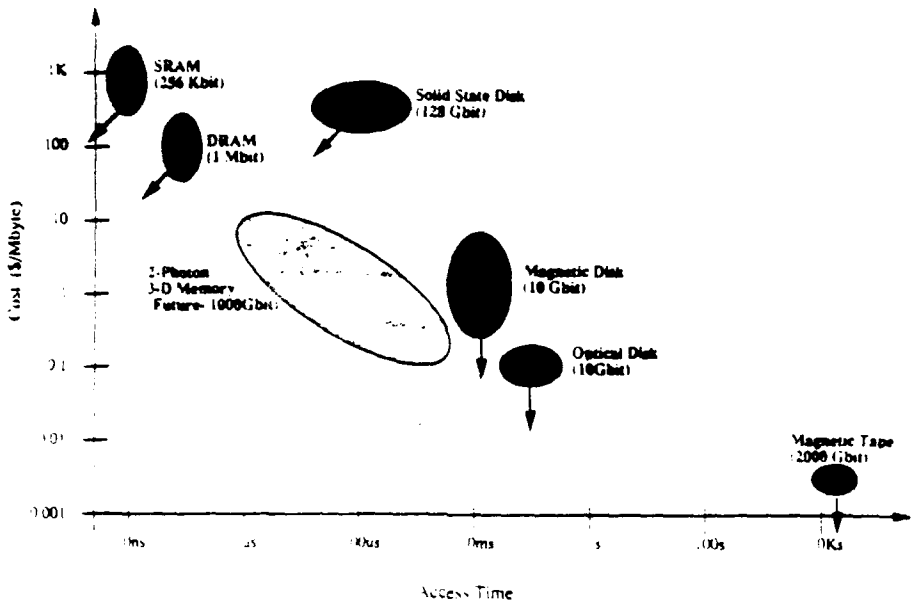

Fig. 10. Comparison of the two-photon 3-D memory device with other memory devices on the basis of access time and cost per megabyte. The two-photon 3-D memory device can potentially compete with magnetic and optical disk storage by providing faster access, higher density, and lower or equivalent cost per megabyte.

Table II. Two-Photon 3-D Memory for Parallel Computers

Computer	Approx Price	No. of Processors	Architecture	Cycle Time/ Peak Performance	I/O Bandwidth	Potential Use of Two-Photon 3-D Memory
Cray Y/MP [21]	$10M	8	MIMD BUS	6 nsec 2.7 Gflops (64-Bit)	40 Gbit/sec to Secondary Storage	Access time, low cost and high density make two-photon 3-D memory useful as a secondary storage device.
NEC SX-X [21]	$10M	4	MIMD BUS	2.9 nsec 22 Gflop (64-Bit)	8 Gbit/sec to Secondary Storage	3-D media is removable and thus it can be used for off-line storage.
Intel IPSC/2 [1]	$1M	128	MIMD HYPERCUBE	100 nsec 2.6 Gflops 32-Bit)	3 Gbit/sec to Secondary Storage	3-D memory can reduce the cost of supercomputers.
NCUBE-10 [1]	$1M	1,024	MIMD HYPERCUBE	100 nsec 500 Mflops (64-Bit)	6 Gbit/sec to Secondary Storage	Two-photon 3-D can capture data from parallel sensors for later processing by a supercomputer
DAP610 Array Processor [24]	$100K	4,096	SIMD MESH	100 nsec 200 Mflops 32 Bit)	40 Gbit/sec to Main Memory	SIMD synchrony is well suited to bit plane access of 3-D memory
Blitzen Array Processor [25]	Research Prototype	16,384	SIMD MESH	100 nsec 450 Mflops 32 Bit)	90 Gbit/sec to Main Memory	Ideally suited for 3-D image and signal data storage
Connection Machine 2 [23]	$3M	65,536	SIMD HYPERCUBE	100 nsec 20 Gflops 32 Bit)	700 Gbit/sec to Memory 3 Gbit/sec to Secondary Storage	Potentially cost effective memory for these types of computers.
Hughes 3-D Computer [26]	Late 1990's	262,144	SIMD 3-D MESH	10 nsec 9 Gflops 32 Bits)	5 Gbit/sec to Secondary Storage	For SIMD format. Use as a secondary or primary memory
CSD POEM Computer [28]	Future 2000	262,144	SIMD Reconfigurable interconnects	10 nsec 9 Gflops 32 Bit)	2000 Gbit/sec to Main Memory	Compatible with POEM system Cost-effective solution for computer weight, size power dissipation.

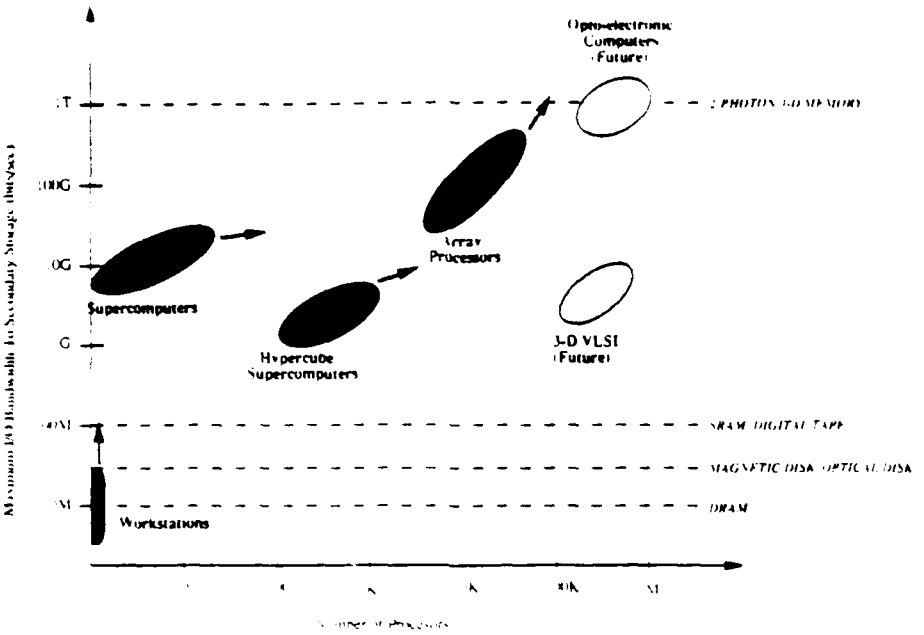

Fig. 11. Maximum I/O bandwidth to secondary storage for parallel computers. Horizontal dashed lines indicate the bandwidth provided by various memory technologies. The two-photon 3-D memory device bandwidth far exceeds the data transfer rate of existing memory devices.

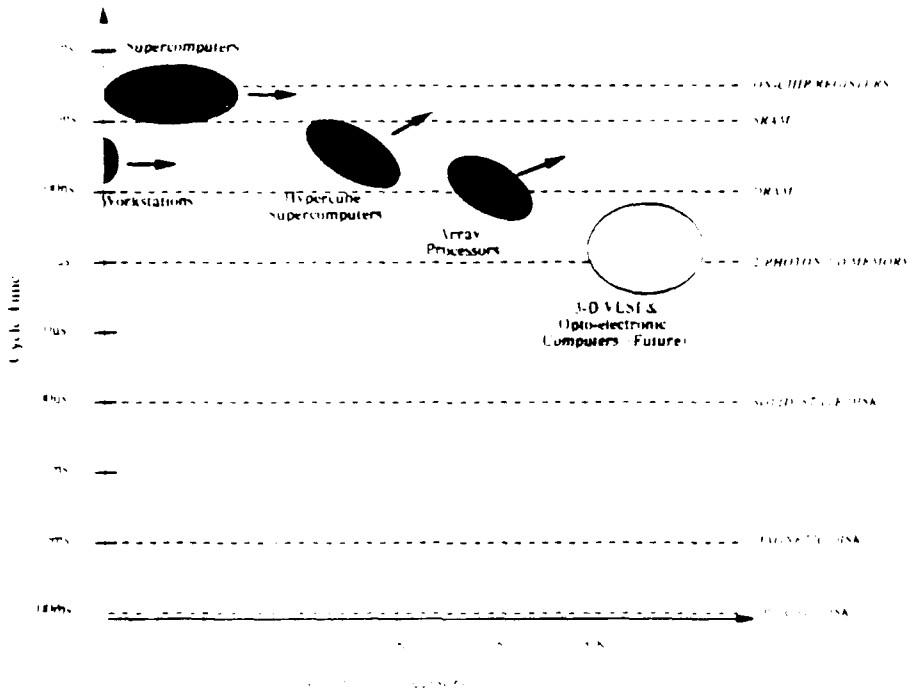

Fig. 12. Clock cycle time for parallel computers. Dashed lines indicate the access time for the two-photon 3-D memory and other memory devices. For future optoelectronic parallel computers based on the POEM architecture, the two-photon 3-D memory device can serve as the main memory storage.

ments. In existing supercomputers and hypercube parallel supercomputers, the two-photon 3-D memory device can be used as a cost-effective replacement for magnetic and optical disks as a secondary storage system. In addition, the potential removability of 3-D memory media makes it well suited for off-line storage. We can also envision applications where the parallel access capability of the proposed memory is used to

gather data from 2-D image sensors and loaded into the supercomputer for processing at a slower rate.

In SIMD array processors,[23-25] the two-photon 3-D memory can potentially be used as the main memory. Since these computers operate on bit planes of information synchronously, their memory access pattern fits the access pattern for the two-photon 3-D memory device. Also, since array processors use inexpensive VLSI processing elements, the potential low cost per megabyte of the two-photon 3-D memory makes it very attractive for use in these computers. In the future, there will be massively parallel computers based on 3-D VLSI[26,27] or optoelectronics technologies.[28] For these systems, two-photon 3-D memory will become a necessary component because of its large degree of parallelism and high storage capacity. Using wafer scale integration and 3-D packaging, these computers promise to deliver unprecedented computing power with very small cost, size, and power consumption. However, using present storage technologies for secondary memory in these computers is not practical due to the overall cost, weight, power, and size of the required memory system. Fortunately, the two-photon 3-D memory is well suited to this type of system and will be able to efficiently satisfy the bandwidth and capacity requirements of these future computing systems.

V. Conclusion

Two-photon 3-D memory stores information in volume and allows parallel access to a plane of information, thus increasing the memory bandwidth by orders of magnitude over present 2-D memory devices. In addition, because the data are stored in a volume, very high capacities can be achieved within a very small area. The fast access time and expected low per megabyte cost can potentially make two-photon 3-D memory a competitor to magnetic and optical disk for mass storage applications. We have shown the 3-D memory system to be a critical component to the success of future parallel supercomputers based on optoelectronic and 3-D VLSI technologies.

This work has been funded by RADC through Call/Recall Corp. Additional funding has been provided through the Office of Naval Research Graduate Fellowship program. The authors would like to acknowledge help with magnetic and optical recording information from John C. Mallinson, who is the director of the Center for Magnetic Recording Research at UCSD.

References

1. A. L. DeCegama, *Parallel Processing Architecture and VLSI Hardware* (Prentice Hall, Englewood Cliffs, NJ, 1989).
2. B. Robinson, "Grand Challenges to Supercomputing," Electron. Eng. Times (18 Sept. 1989).
3. R. H. Ewald and W. J. Worlton, "A Review of Supercomputer Installations' Mass Storage Requirements," IEEE Symp. Mass Storage Syst. 83 (1985).
4. H. E. Maes, G. Groeseneken, H. Lebon, and J. Watters, "Trends in Semiconductor Memories," Microelectron. J. 20, Nos. 1-2, 9-37 (1989).
5. W. P. Altman, G. M. Claffie, and M. L. Levene, "Optical Storage for High Performance Applications in the Late 1980s and Beyond," RCA Eng. 31, 46–55 (1986).
6. A. E. Bell, "Critical Issues in High-Density Magnetic and Optical Data Storage: Part 1," Laser Focus 19, 61–66 (1983).
7. J. Mallinson, UCSD Center for Magnetic Recording Research; private communication.
8. K. R. Wallgren, "Optical Disks and Supercomputers," Proc. Soc. Photo-Opt. Instrum. Eng. 529, 212–216 (1985).
9. D. Chen and J. D. Zook, "An Overview of Optical Data Storage Technology," Proc. IEEE 63, 1207–1230 (1975).
10. J. E. Weaver and T. K. Gaylord, "Evaluation Experiments on Holographic Storage of Binary Data in Electro-Optic Crystals," Opt. Eng. 20, 404–411 (1981).
11. U. P. Wild, S. E. Bucher, and F. A. Burkhalter, "Hole Burning, Stark Effect, and Data Storage," Appl. Opt. 24, 1526–1530 (1985).
12. L. d'Auria, J. P. Huignard, C. Slezak, and Spitz, "Experimental Holographic Read-Write Memory Using 3-D Storage," Appl. Opt. 13, 808–818 (1974).
13. N. W. Carlson, L. J. Rothberg, and A. G. Yodh, "Storage and Time Reversal of Light Pulses Using Photon Echoes," Opt. Lett. 8, 483–485 (1983).
14. P. Lambropoulos and S. J. Smith, Eds., *Multiphoton Processes* (Springer-Verlag, Berlin, 1984).
15. R. M. MacFarlane, "Photon Aided Spectral Hole Burning," J. Luminesc. 38, 20–24 (1987).
16. P. M. Rentzepis, "3-Dimensional Optical Memory," U.S. Patent Application No. 07/342,978 (1989).
17. R. C. Bertelson, "Photochromic Processes Involving Heterolytic Cleavage," in *Techniques of Chemistry: Photochromism*, Vol. 3, G. M. Brown, Ed. (Wiley-Interscience, New York, 1971), p. 45.
18. D. A. Parthenopoulos and P. M. Rentzepis, "Three Dimensional Optical Storage Memory," Science 245, 843–845 (1989).
19. S. H. Lee, S. Esener, M. Title, and T. Drabik, "Two-Dimensional Si/PLZT Spatial Light Modulator Design Considerations and Technology," Opt. Eng. 25, 250–260 (1986).
20. E. L. Kral, J. F. Walkup, and M. O. Hagler, "Correlation Properties of Random Phase Diffusers for Multiplex Holography," Appl. Opt. 21, 1281–1290 (1982).
21. S. T. Kowel, D. S. Cleverly, and P. G. Kornreich, "Focusing by Electical Modulation of Refraction in a Liquid Crystal Cell," Appl. Opt. 23, 278–289 (1984).
22. IEEE Scientific Supercomputer Subcommittee, "Special Report on Supercomputing," Computer 22, No. 11, 57–68 (1989).
23. L. W. Tucker and G. G. Robertson, "Architecture and Applications of the Connection Machine," Computer 21, No. 8, 26–38 (1988).
24. C. G. Winckless, "Massively Parallel Computer for Signal and Image Processing," in *Proceedings, IEEE International Symposium on Circuits and Systems*, Portland, OR, 8–11 May 1989), pp. 1396–1399.
25. R. A. Heaton and D. W. Blevins, "BLITZEN: A VLSI Array Processing Chip," in *Proceedings, IEEE Custom Integrated Circuits Conference*, San Diego, 1989), pp. 12.1.1–12.1.5.
26. M. J. Little and J. Grinberg, "The Third Dimension," Byte 13, 311–319 (Nov. 1988).
27. Y. Akasaka, "Three-Dimensional Integrated Circuit: Technology and Application Prospect," Microelectron. J. 20, Nos. 1-2, 105–112 (1989).
28. F. Kiamilev, S. Esener, R. Paturi, Y. Fainman, P. Mercier, C. Guest, and S. H. Lee, "Programmable Optoelectronic Multiprocessors and Their Comparison with Symbolic Substitution for Digital Optical Computing," Opt. Eng. 28, 396–409 (1989).
29. L. Curran, "Wafer-Scale Integration Arrives in Disk Farm," Electron. Design (26 Oct. 1989).
30. J. Vaughan, "Peripheral Memory Options Multiply," Special Supplement on Computers & Peripherals: Storage, Electron. Design News (30 Nov. 1989).

2D STACKED MEDIA FOR 3D MEMORY APPLICATIONS

Workshop on 3D Memories
March 12 - 13, 1990

Snowbird, Utah

Presented By
Haim M. Haskal

SPARTA, INC
24 Hartwell Avenue
Lexington, MA 02173
(617) 863-1060

SPARTA INC.

INTRODUCTION

- Examine in detail the capability of a 2D stack as a 3D memory medium (Simulation)
- Determine if holograms can be written in dye-in-polymer films (Experiment)
- Devise some memory concepts using the 2D stacked medium

STATIONARY OPTICAL MEMORY CONCEPTS

SPARTA INC.

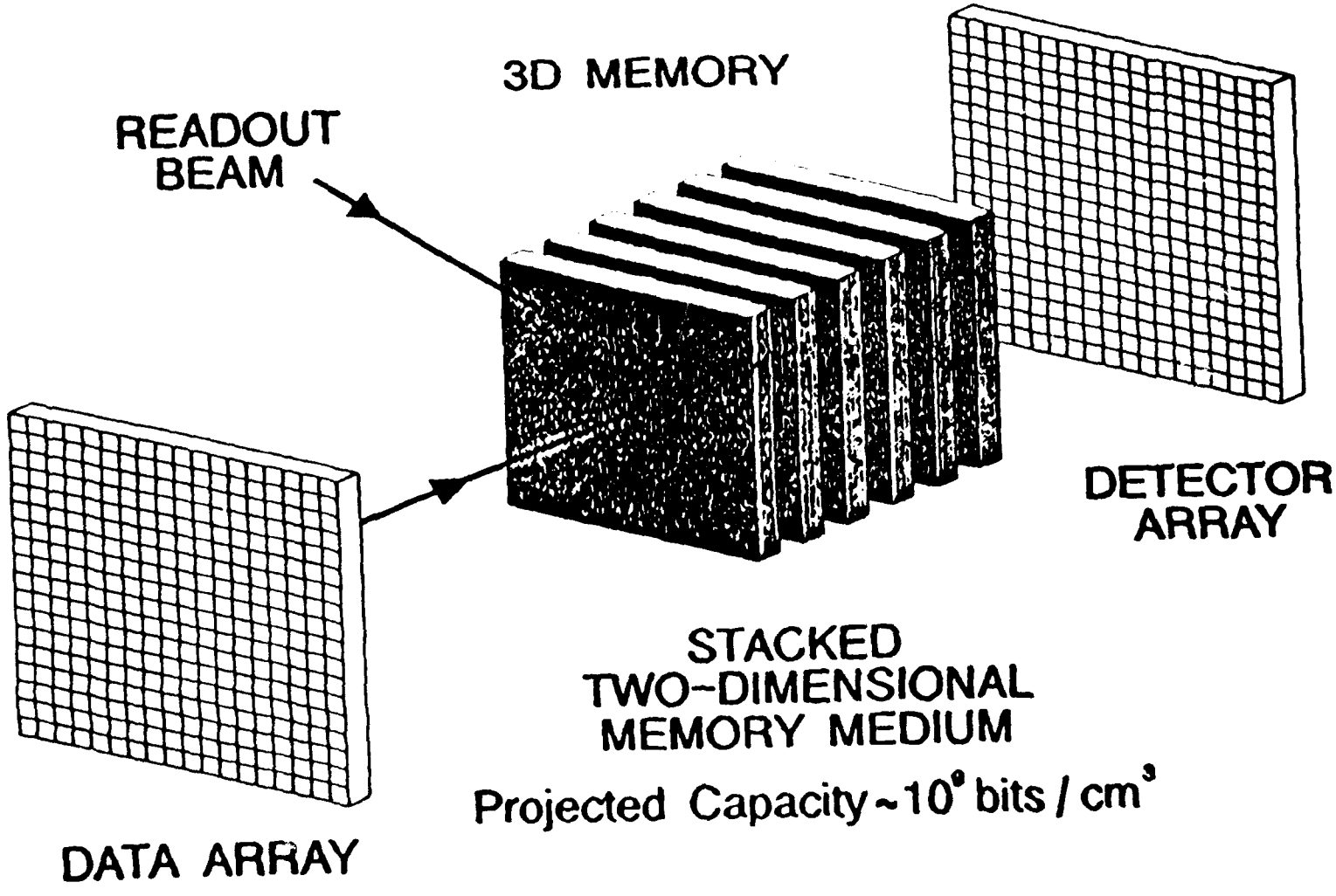

DYE POLYMER MEDIA

SPARTA INC.

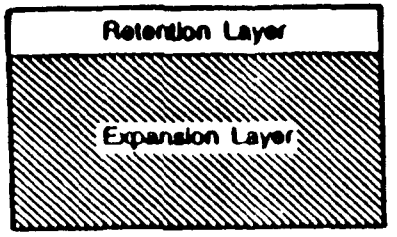

The Unperturbed Material

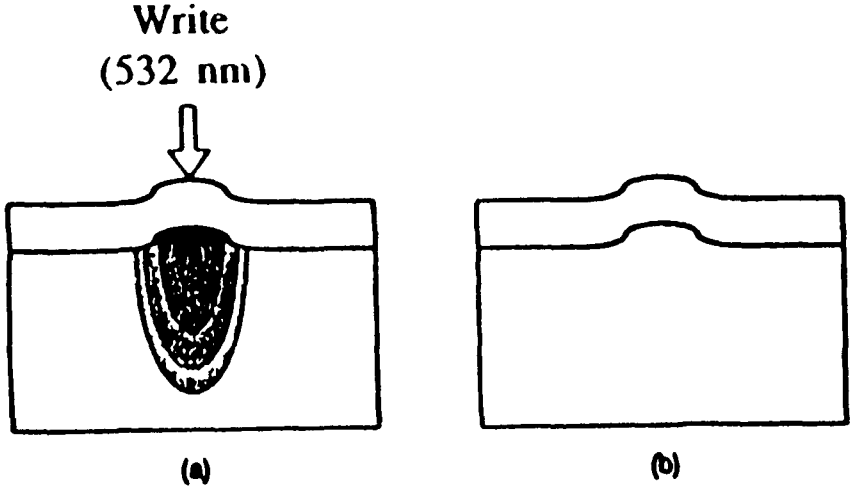

The Writing Process. a) Expansion During Heating. b) Contraction After Cooling.

EXPERIMENTAL SET-UP

SPARTA INC.

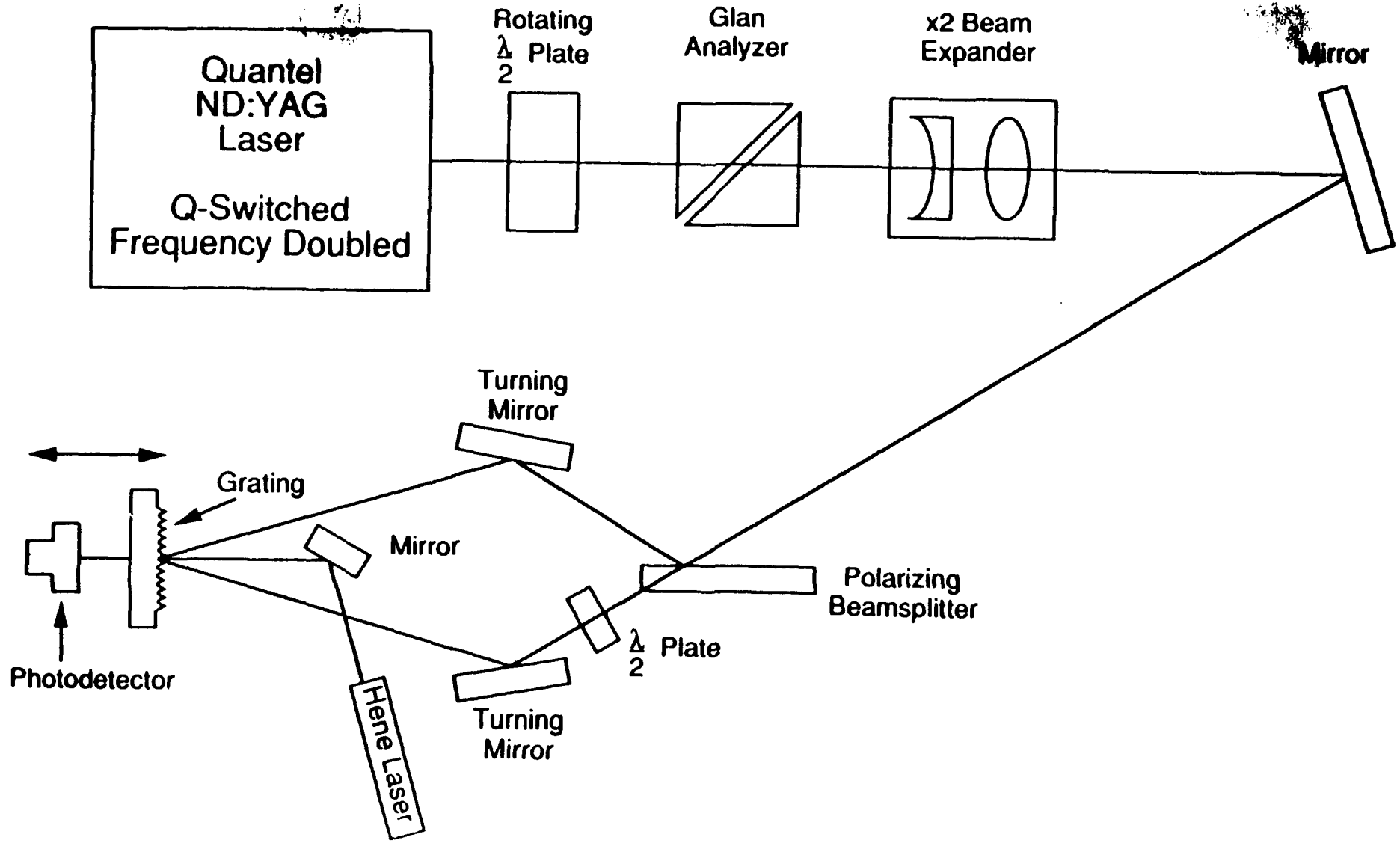

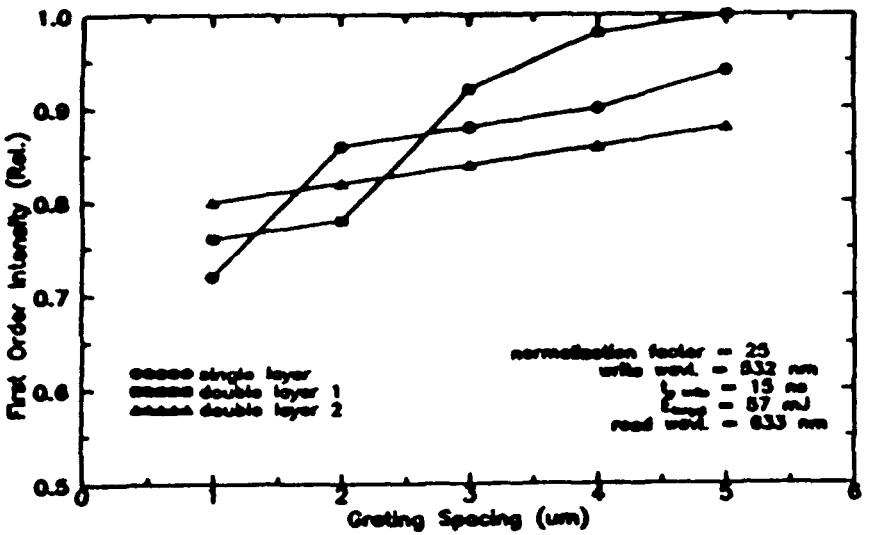

(a)
First order diffracted read beam relative intensity

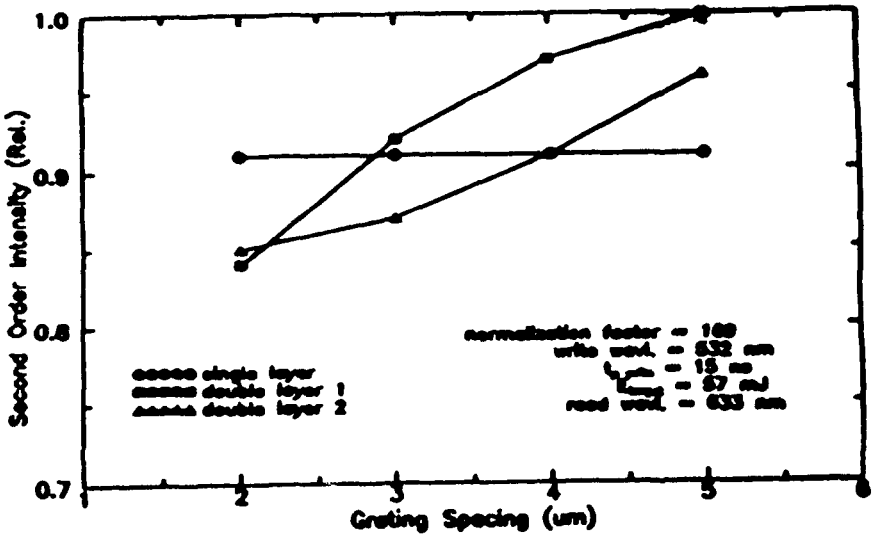

(b)
Second order diffracted read beam relative intensity

First and Second Order Diffraction Efficiency.

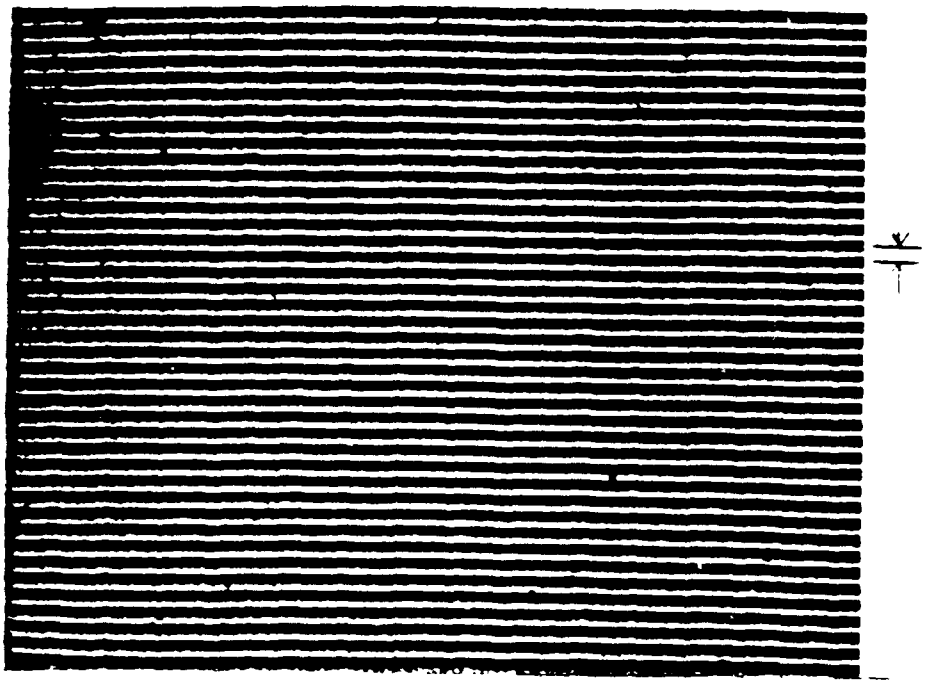

(a)

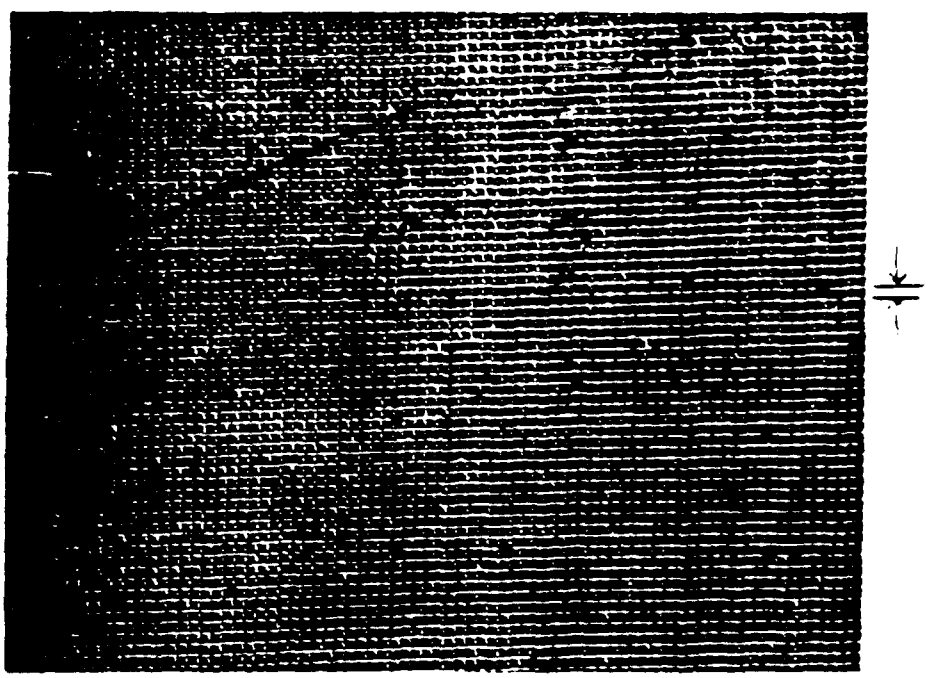

(b)

Nomarski photomicrographs of diffraction gratings in polymer film (a) single relief grating, 3um spacing and (b) two relief gratings crossed at 90°, 5um spacing.

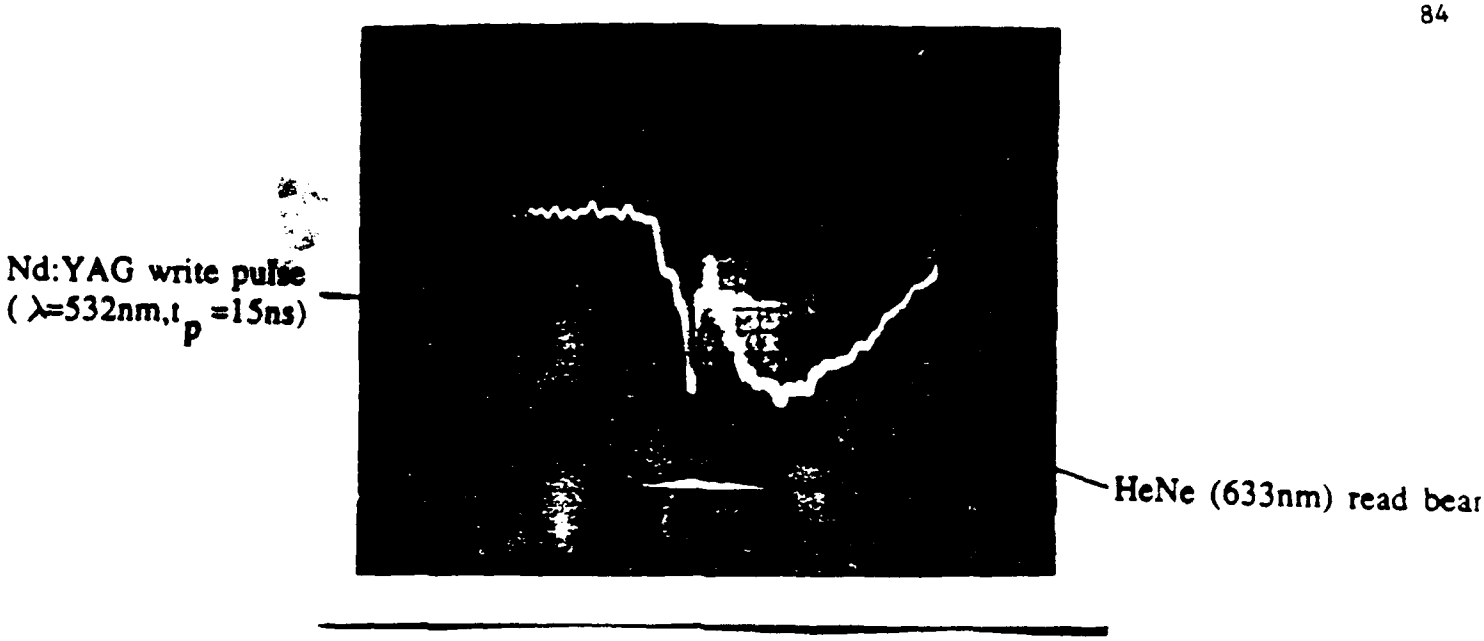

10 nanoseconds/division

(a)

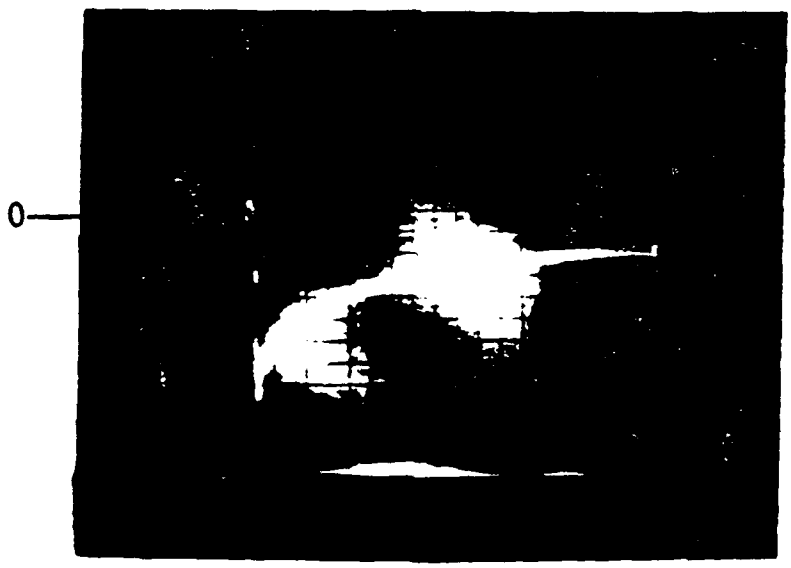

100 nanoseconds/division

(b)

Real time grating formation (a) summation of write pulse and first order diffracted read beam and (b) first order diffracted read beam only.

SPARTA INC.

Stack of Thin Gratings

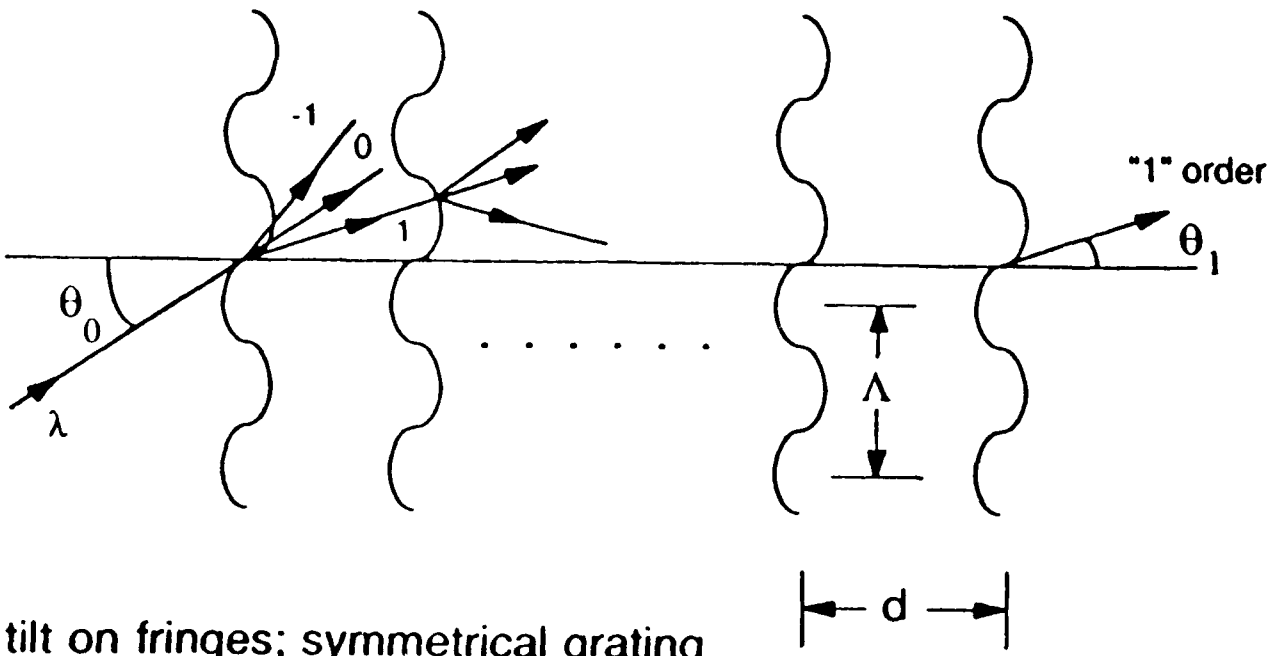

- No tilt on fringes; symmetrical grating

- A stack of 2-D storage media to approximate a 3-D storage medium

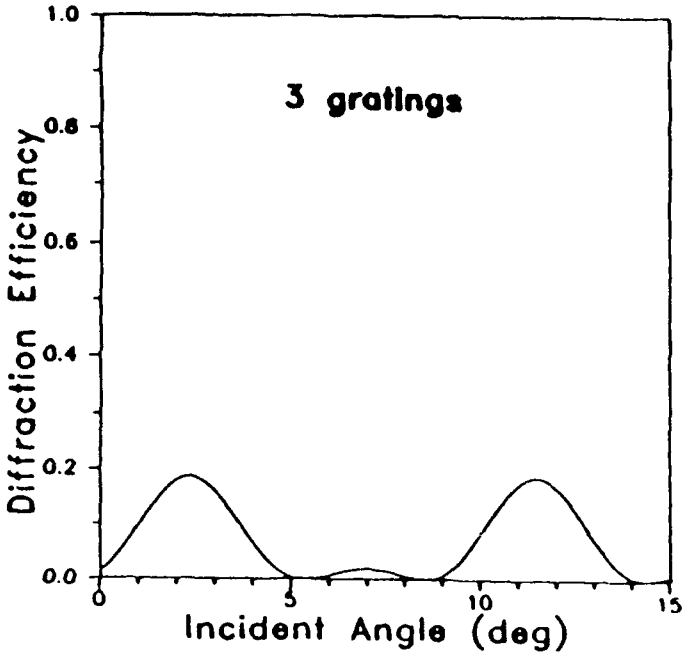

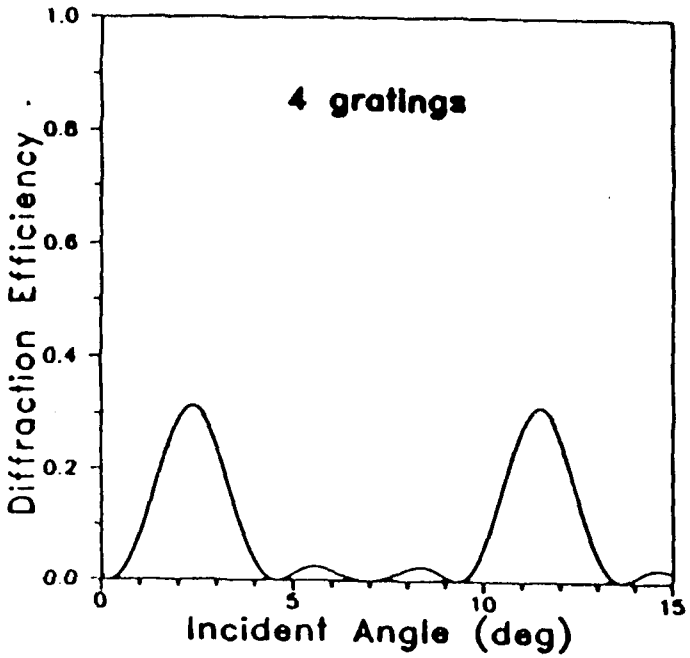

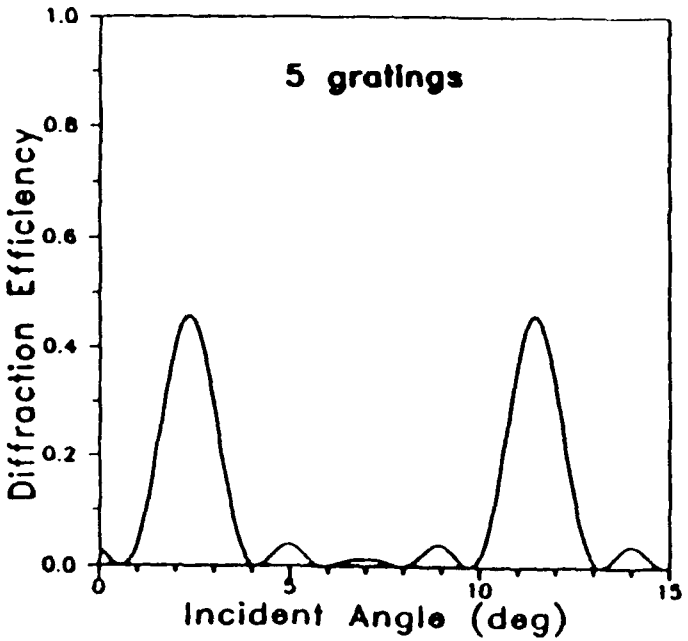

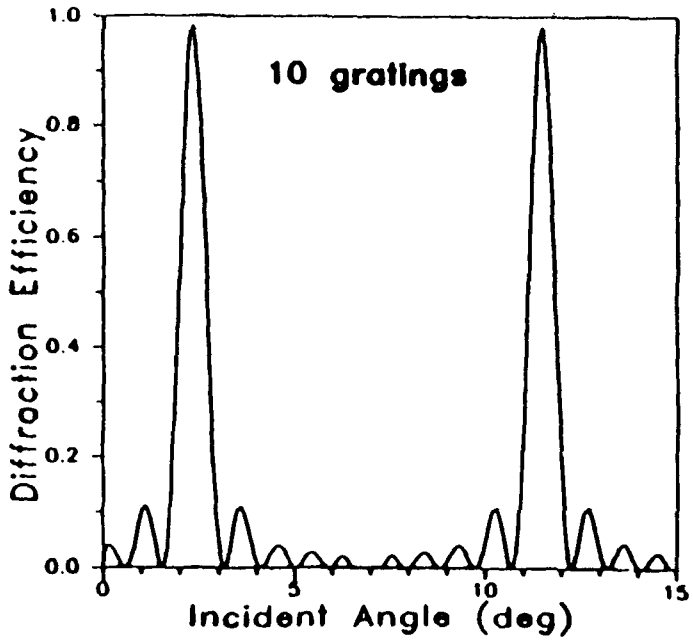

- Angular width varies as $1/Nd$

Grating strength = 0.3
Grating separation = 62.5 microns
Grating spacing = 10 microns
Wavelength = 0.8 microns
Fringe tilt = 0

Set Grating Strengths Individually
Vary Grating Separation

SPARTA INC.

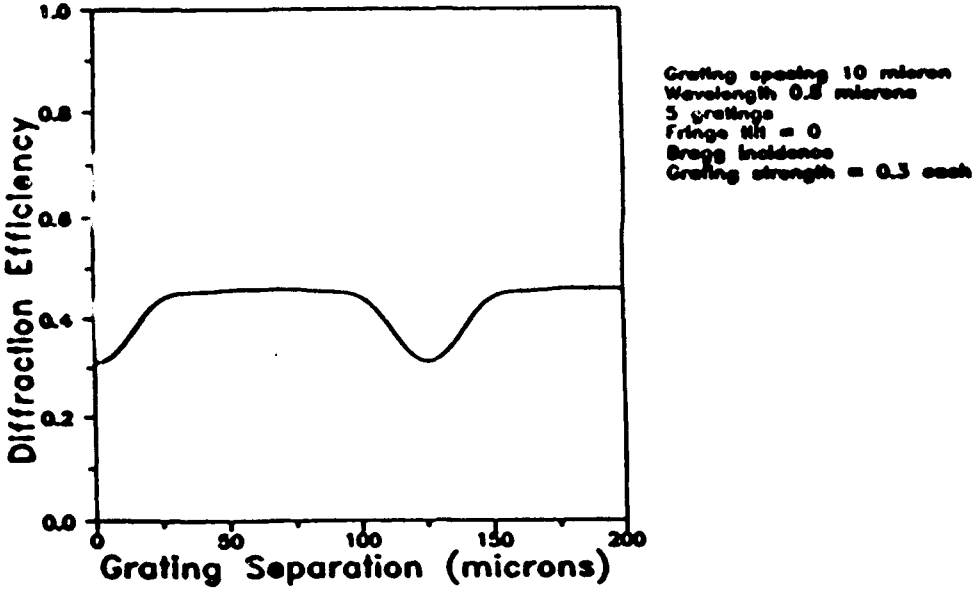

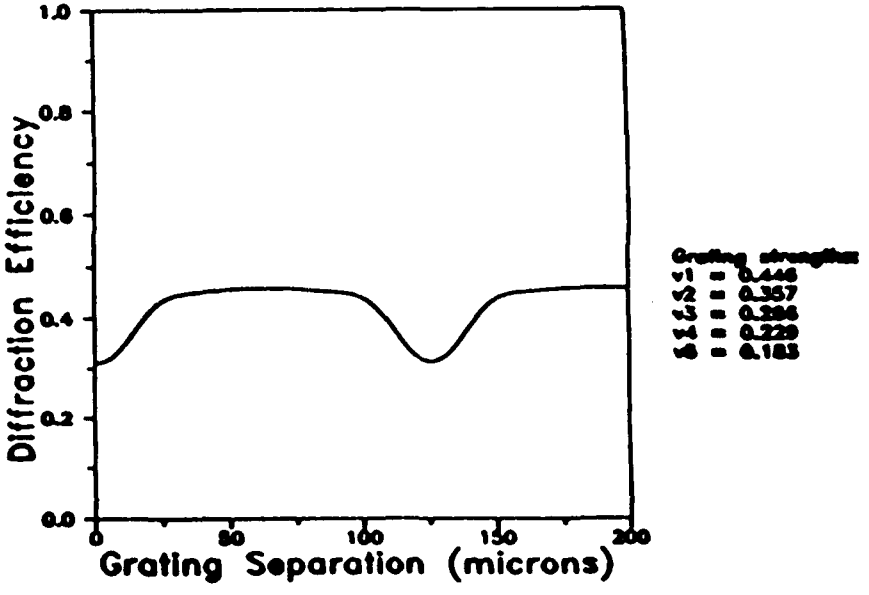

SPARTA INC.

CONCLUSIONS

- It is Possible to Write a Hologram in this Material
- Grating Formation Begins about 12 ns into Write Pulse
- Grating Reaches peak Height in about 10 ns
- Grating Bump Height Rises to 371 nm Before Relaxing to 160 nm
- Total Formation and Relaxation Time for Grating to Steady State is about 700 ns

SPARTA PROPRIETARY

Product Goals for (Optical) Mass Storage

Philip D. Henshaw
Robert F. Dillon
SPARTA, Inc.
24 Hartwell Avenue
Lexington, MA 02173
(617) 863-1060

1 Introduction

Most researchers would agree that the long-term goal of any research and development program is to conceive and develop something useful. In fact, without this goal, most R&D programs will not *be* long-term. This paper suggests an evaluation criterion for computer mass storage technologies that can be used to argue convincingly the merits of a specific approach. This criterion is *cost/megabyte*.

As an example, we apply this criterion to mass storage technologies geared to rapid data access. A summary of mass storage requirements for several applications is presented in Table I. Each of these applications requires a short access time, either directly, because of short timelines, or indirectly, because of the effect of access time on data rate. (See Appendix A for a discussion of effective data rate.) We have chosen access time as the vehicle for our discussion of mass storage goals for several reasons: it is a clear cut "market niche" which is currently unfilled, it clearly illustrates the importance of cost/megabyte, and it appears to be a problem which could be solved by developing new mass storage devices.

Table I. Mass Storage Requirements for Several Applications

Applications / Characteristics	Relational Database	Interactive Video	Telephone Services	Distributed (Teraops) Computing
Capacity (Mbytes)	≥1000	≥1000	7600 [1]	10^6 [2]
Data Rate (Mbytes/s)	0.1 - 12	6	1	1000
Access Time (ms)	<20	<5	1	?

2 Applications

Many significant military applications involve the implementation of software decision aids for wartime where large data bases must be searched for rules, associations, etc. based on rapidly changing inputs. This application may also require the added feature of removable media for classified data bases.

Rapid access to data on optical disks has the potential to play an important role in communication (telephone voice mail), interactive video, and relational database applications. In

each case, the average access time is a key parameter which determines the limit of system performance.[3] The performance of relational database systems is currently limited by access time and effective data rate.[4] In addition to rapid access, a device based on our concept would share the advantages of removable media, immunity to head crashes, and large capacity common to all optical disk storage devices.

Boston Technologies develops equipment for telephone company central offices which allows users within a local area to have personal mailboxes for voicemail and FAX, and call and FAX forwarding from office to home, among other features.[1] The telephone company bills users $3 per month for these services. A trial installation near Philadelphia resulted in a very high subscription rate. For a typical central office, 10 disk drives, with a total capacity of 7.8 GBytes are used to store the menu messages and mailbox contents. Accessing a specific individual's mailbox to leave a message requires 27 disk accesses to the master system disk, and the total timeline should be kept under 3 seconds. In a typical central office system the presence of 120 to 150 simultaneous users results in noticeable delays, limited by disk access time. This load is equivalent to a disk access rate of 1000 accesses per second. Although this problem can be solved by arrays of Winchester magnetic disks, this solution has not been used because of reliability concerns. Currently this problem is solved by using large capacity semiconductor memory caches, however, this solution is expensive and complex, and limits the ultimate capacity of the system. A rapid access optical disk system could provide both cost and reliability benefits, however, the cost of our rapid access disk drive will be a key issue for this application.

The Media Lab at MIT is examining how a convergence of information technologies will have a profound effect on our society, and interactive video is central to most of these effects.[5] Interactive video has many interesting applications: training aids, entertainment, editing of video sequences, and video newspapers, for example.

Reducing the total access time required to retrieve any piece of information from a large data base is a key to achieving interactive video. Interactive video is implemented by "coding" a video database – annotating the time, place, activities, and participants for any sequence of video frames, for example.[6] The code database is then used to determine which frames to retrieve based on interaction with a user. Very large data bases can be created very quickly in this environment. During operation, choosing which frame to retrieve from a database may involve a number of accesses to the code data base. For example, to retrieve frames showing fighting in the Middle East, accesses to determine which frames contain war scenes, city scenes, and middle east participants might have to be intersected to determine the number of possible frame sequences which apply. If the search finds more than one "hit," then the most recent sequence might be selected and shown if the application is a video newspaper. Ideally, all these accesses will take place and the frame sequence will begin in a time interval shorter than a single frame. In this example, five accesses in less than 30 msecs leads to a required access time of less than about 5 msec.

Currently, when disk storage with high on-line capacity and a high data rate is desired, "disk farms" – arrays of low-cost Winchester magnetic disks – can be configured to achieve these goals.[7]These configurations have been developed by companies such as Thinking Machines, Inc., and they are cost-effective because of the low cost of current Winchester drives as a result of their widespread use.[8] The limitation of "disk farms", however, centers around concerns of reliability and the cost inefficiency associated with maintaining multiple copies of data to reduce access time. This use of disk arrays suggests that cost/megabyte of on-line storage is a key issue

for comparing our rapid access disk drive concept to the competition.

3 Analysis

The competition for a potential rapid access mass storage product comes from two directions: low-cost Winchester disk technology and extremely rapid access semiconductor RAM. Semiconductor RAM boxes with capacities of 60 megabytes are available[9]and 130 megabyte capacities are planned. The results of a recent survey of Winchester disk products[7] is shown graphically in Figures 1 and 2. Cost/megabyte, shown in Figure 1, ranges from $3 to $30 for current products, and access times, shown in Figure 2, range from 12 to 20 msec.

SPARTA has examined the cost/megabyte and average access time for optical jukebox, optical and magnetic disk systems, and semiconductor RAM storage. These systems and a goal for a rapid-access system are shown in Figure 3. We have assumed that an average access time greater than 5 msec is too slow for certain time-critical applications, and that a cost per megabyte greater than $100 is too high. These lines are, of course, movable depending on the specific applications, but they indicate the desirable region for rapid access mass storage devices. The line extending up to the right from the single-disk ovals indicate the performance that can be achieved with disk arrays. This line was derived by noting that a narrow band of tracks could be used to minimize seek time, and the data could be written multiple times around the disk to reduce the latency. Because the seek time and latency for current disk systems are similar, both problems must be attacked, leading to a reduced capacity (equivalent to an increased cost/megabyte) proportional to the square of the reduction in access time. This severe penalty has prevented the current use of low-cost disk arrays to solve the problem of slow access to data which currently limits important real-time applications such as decision aids and interactive video. This chart shows clearly that at a cost of $30/Megabyte a mass storage concept would bridge the gap between today's slow disk technology and expensive RAM technology.

Short access time is not the only market niche which must deal with the cost/megabyte of competing technologies. For example, reliability can be traded for cost/megabyte by duplication of data, duplication of storage units, or encoding of data. In each case, increased reliability can be achieved with existing mass storage devices and an increased cost/megabyte. If the cost per megabyte of the competing technology is low enough, then R&D to develop a competing, high-technology solution will not provide a useful result. Similarly, increased data rate can be achieved by duplicating hardware to implement parallel transfer. In this case, the penalty in cost/megabyte is almost insignificant but the competition is clearly significant. Finally, capacity can be increased by simply buying more memory devices. The cost/megabyte will determine how much memory can be afforded for a given application. If form factor is not an issue, then the low-cost technology wins. (We have not analyzed whether form factor issues, such as compactness, ruggedness, and power consumption, can be addressed by using low-cost/megabyte hardware.)

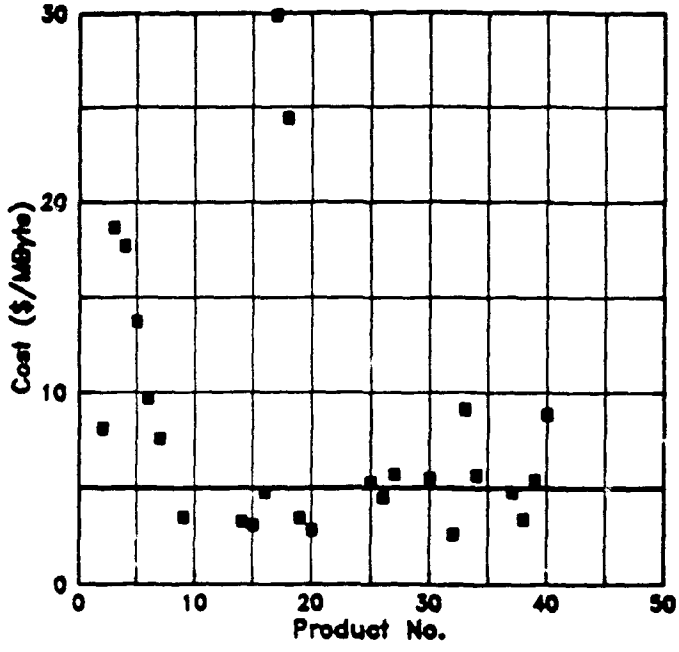

Figure 1. Cost/megabyte for Winchester drive products.

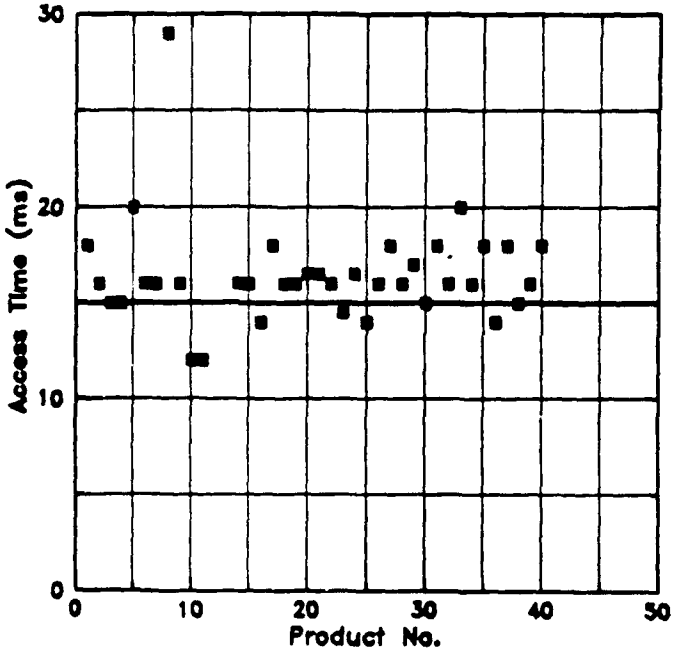

Figure 2. Access time for Winchester drive products.

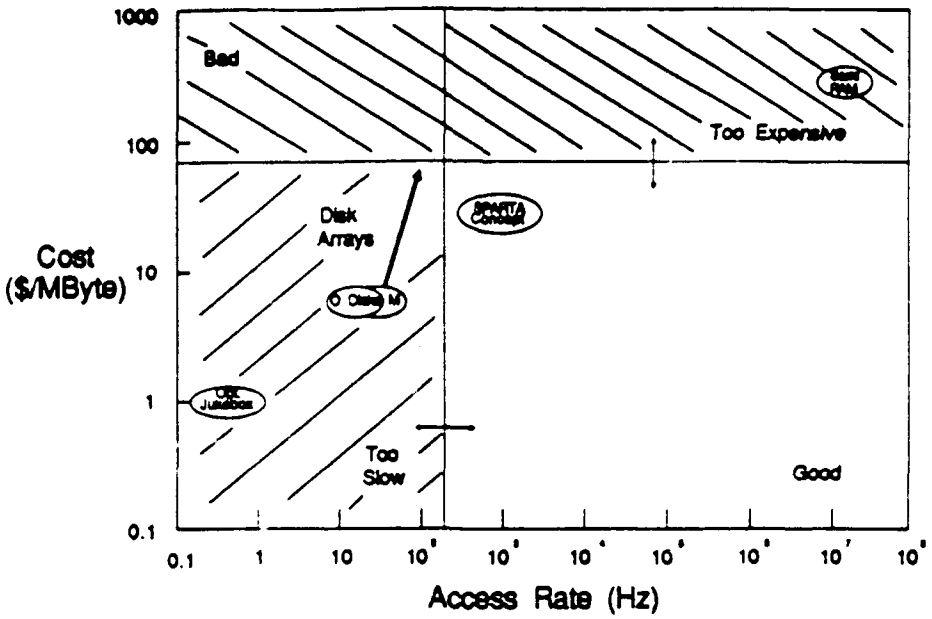

Figure 3. Cost/megabyte and access time for mass storage devices.

4 Conclusion

In conclusion, no niche appears to be absolutely safe. If a competing technology is cheap enough and close to the niche requirements, it can be arrayed to achieve niche performance. Thus cost/megabyte is the criterion which should be included in any rationale or evaluation of mass storage technology R&D. The cost/megabyte goal can be estimated based on the competition. Ultimately, with cost/megabyte on our side, the worm turns and arrays of optical mass storage devices may be used to surpass electronic mass storage.

APPENDIX A The Effect of Access Time on Effective Data Rate

An approximate idea of some of the requirements for future computer memory systems can be estimated based on the stated goals of the Teraops program. These requirements include a data transfer rate of 1 Gbyte/sec and a memory capacity of at least 10^{12} bytes. This appendix discusses how the effective data rate depends on the access time and the page size. The access time and page size requirements for computer memory are, however, very architecture-dependent.

A cache memory is a small, fast memory, used in most architectures as a place to store recently used data. The data are marked with the time of most recent use. Whenever there is a "fault" – that is, the requested data cannot be found in cache – the "oldest" data in the cache is replaced by the just-requested data. Cache memories are characterized by a total capacity and a page size (the minimum amount of data transferred from cache at one time.)

A cache memory very close to the computer should probably have a small page size. For example, the SUN workstation architecture has an internal cache of 64 Kbytes and a "page" size of 1 word. For virtual memory, the cache is further from the computer and has larger page sizes. For example, virtual memory pate size is 512 or 1024 bytes in the SUN architecture. In large systems, a hierarchy of cache memories may be used. The delay time to access any device can be hidden by suitable choice of the architecture of the system.

Memory characteristics of current and projected memory devices are shown in Figure 4. The axes - page size and effective data rate - have been chosen to show the operating range of memory concepts considered for cache or main memory in a way independent of the choice of architecture. The page size P is the amount of data transferred during any given access to the memory. The effective data rate R_e is a function of the page size and combines the effects of the access time τ_a and the data transfer rate R. R_e in megabits/second is given by

$$R_e = \frac{8P \times 10^3}{\tau_a + 8P/(R \times 10^3)}$$

where P is given in kilobytes, τ_a in seconds, and R in megabits/second.

The two horizontal dotted lines in Figure 4 indicate the current data transfer rate of Ethernet, 10 megabits/second, and the projected requirements of teraops computers, 1 gigabit/second. The dotted lines sloping up to the right indicate the total amount of memory which can be read in the indicated times of 10 msec, 1 sec, and 100 seconds.

The solid lines indicate the operating curves of several different memory devices which have been used for mass storage or cache memory. The curve for a typical personal computer floppy disk with 40 msec access time, a data transfer rate of 40 kbits/sec, and a total capacity of 720 Kbytes is shown near the lower left. The operating curve terminates at 720 Kbytes, since no page can be larger than the total diskette capacity. Clearly the design of this device to operate with a page size of 512 bits was chosen to hide the effect of the slow device access. High-end devices shown here include the IBIS 2812 magnetic disk system[10] with an access time of 20 msec and a transfer rate of 100 Mbits/sec and a single RCA optical disk [11], with an access time of 300 msecs and a transfer rate of 100 Mbits/s. Both systems have a total capacity of 20 Gbytes. The RCA optical jukebox achieves a much greater total capacity of 2.5 Terabytes, at the same data transfer rate of 100 Mbits/second but has a very slow average access time of 6 seconds [12].

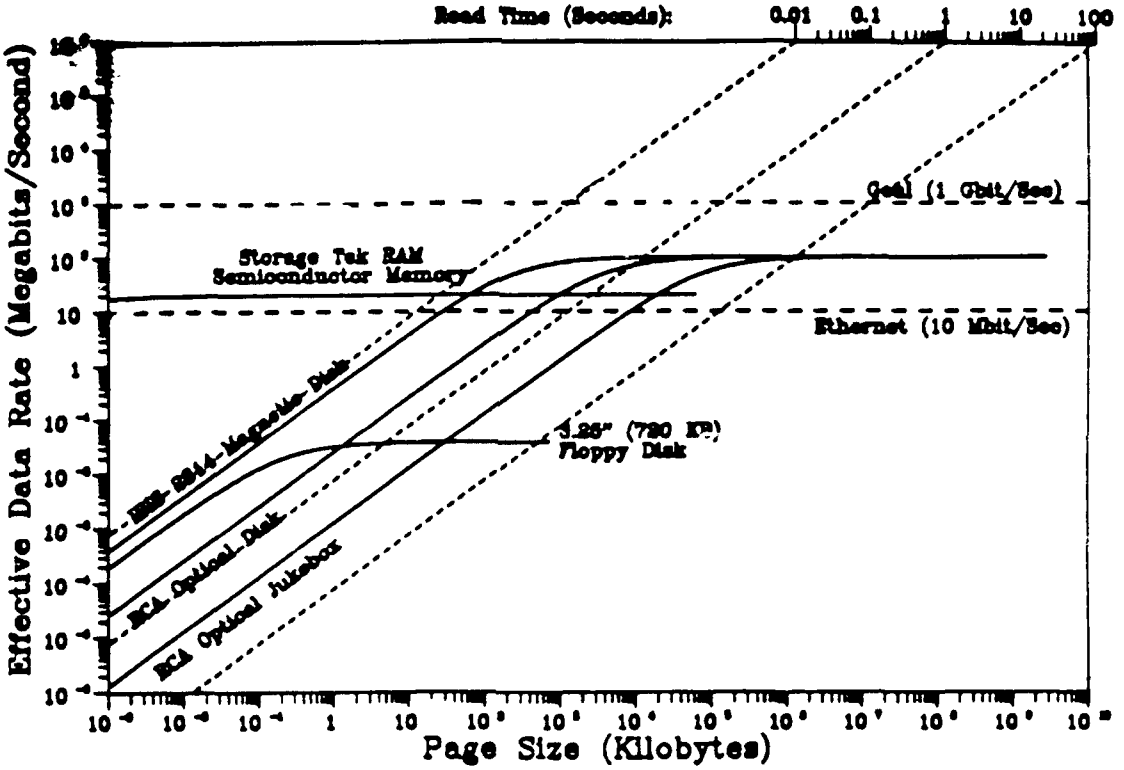

Figure 4. Operating characteristics of cache and main memory devices.

Each of these concepts leaves a gap in operating capability in the upper left corner of the chart, which obviously requires very large page sizes to hide the effect of access time. This limits these devices to use as a main memory or a cache memory some distance from the computer. The Storage Tek RAM is a semiconductor memory with an access time of 50 nanoseconds, a data transfer rate of 20 Mbits/second, and a total capacity of 60 Mbytes[9]. This device fills in the region of high data rates and small page sizes not covered by the large capacity devices discussed above.

1. J. McHugo, Boston Technologies, private communication.
2. K. Wallgren, "Supercomputing and Storage," SPIE Proc. **695** (1986) 334.
3. J. Neff, E. I. DuPont, private communication.
4. J. Goodhue and T. Downey, Bolt, Beranek, and Newman, private communication.
5. S. Brand, *The Media Lab*, Viking Press, New York (1987).
6. G. Davenport, MIT Media Lab, private communication.
7. D. Simpson, "RAIDs vs. SLEDs," System Integration, (1989) 70-82.
8. C. Stanfill, Thinking Machines, Inc., private communication.
9. Storage Technology Corp., 2270 South 88th St., Louisville, CO 80028-4358, Specification ED009-4, 07/87.
10. 1988 Disk Trend Report, Rigid Disk Drives, DISK/TREND, Inc., 1925 Landings Drive,

Mountain View, CA 94043, RSPEC-47.

11. M. L. Levene, "Applications for a high capacity, high data rate optical disk buffer," SPIE O-E LASE '88, January 15, 1988, Los Angeles, CA.
12. G. J. Ammon, "Archival optical disc data storage," Opt. Engineer. 20 (1981) 394.

4D Holographic Optical Memory

Philip D. Henshaw
Steven A. Lis
SPARTA, Inc.
24 Hartwell Avenue
Lexington, MA 02173
(617) 863-1060

INTRODUCTION

This white paper describes a multidimensional holographic memory concept which overcomes one of the primary past objections to holographic memory, the limited capacity caused by the range of spatial frequencies which can be written by the narrow cone of writing and data beams. The greatly increased capacity provides a cost per on-line megabyte which beats all existing and most proposed rapid access memory concepts. This capacity can be achieved using existing materials and optical subsystems.

First, the concept will be presented. This holographic memory relies on the unique properties of a class of materials collectively known as spectral hole burning (SHB) materials. The device will make use of a standard volume hologram recording configuration plus the additional reference beam control provided by a frequency agile laser. The additional recording dimension provided by laser frequency results in a four-dimensional memory with greatly increased capacity. The ultimate limits on capacity may be imposed by the molecular density of the recording centers and fundamental noise considerations. Capacities of 10^{12} bits and greater appear possible.

The requirements for the SHB materials will also be discussed. We will show that currently-available materials are able to meet the requirements for a high-capacity memory.

A significant factor in the possible commercial success of any memory concept is the cost per online megabyte. Because of the enormous capacity of the 4D memory concept, the expense of the optical components can be much lower than either existing electronic memory or mass storage devices, and much lower than projected 3D memory costs/megabyte.

CONCEPT

Figure 1 shows the basic means by which SHB materials provide an additional dimension. The inhomogeneous absorption spectrum is made up of a large number of homogeneously broadened absorption lines. At low temperatures, the absorbing centers within a single homogeneously broadened linewidth can be addressed independently of any other population of recording centers. This allows data to be recorded at one wavelength which cannot be seen by any other wavelength. The additional recording dimension provided by laser frequency results in a four-dimensional memory with greatly increased capacity.

One of the major factors which has kept optical holographic memory from having commercial impact is the limited capacity. If a holographic memory device cannot provide more capacity than can be achieved with a board of semiconductor RAM chips, then the switch to this new type of memory will not be made. For 3D holographic memory, this capacity limit is imposed by the diffraction-limited resolution of the cone of rays used for the reference and data beams. The net effect of this limited cone is to make only partial use of the spatial frequency response

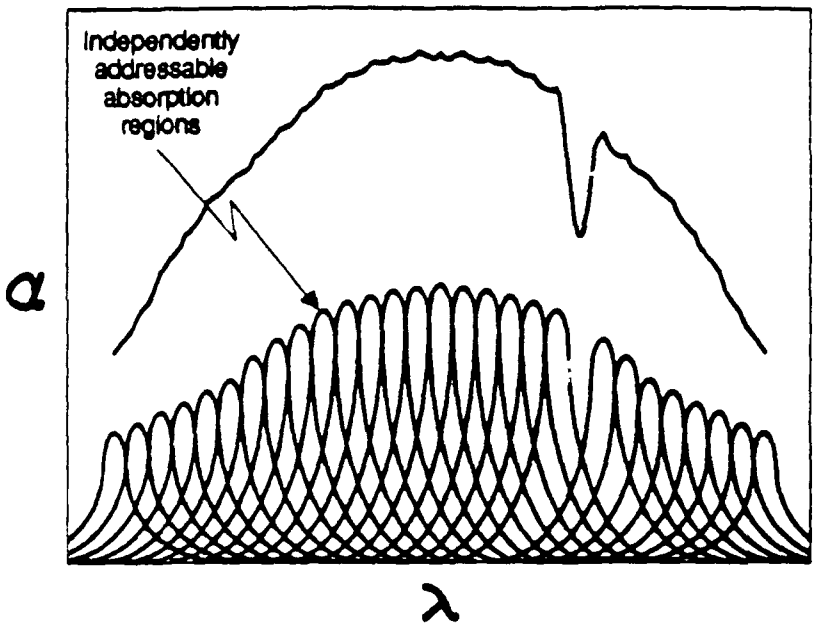

Figure 1. Spectral hole burning materials provide an additional dimension for holographic data storage which can be addressed using frequency agile lasers.

of the medium. The fringes recorded in the volume holographic medium will be approximately one wavelength in size in one spatial direction but will be many wavelengths on a side in other directions. This volume can contain many more recording centers than are actually needed in the case of heavily-doped material. These recording centers can be used more fully in the case of an SHB medium by addressing them by laser frequency. The ultimate limits on capacity may be imposed by the molecular density of the recording centers and fundamental noise considerations. Capacities of 10^{12} bits and greater appear possible.

A 4D memory architecture designed to take advantage of the unique properties of SHB materials is shown in Figure 2. Table I shows the projected capabilities of this 4D holographic optical memory. This architecture includes a frequency agile laser, a beam deflector to provide conventional angle accessing, a spatial light modulator (SLM) to introduce the data beam, a volume recording medium, and a high-speed, low noise detector array. Except for the frequency agile laser, all of these components are common to both a 4D holographic memory and a 3D holographic memory. In an advanced version of the memory, electric field may provide an additional dimension by changing the frequency of absorption through the Stark effect.[1] This additional dimension can provide engineering room to access the full potential storage capacity of the memory medium.

MEMORY MATERIAL REQUIREMENTS

SHB materials can be created by embedding dyes in a polymer host and cooling the material to cryogenic temperatures. Two of the most fundamental parameters which describe any absorbing dye molecule are the absorption cross-section per molecule and the efficiency of cov-

Table I. Projected capabilities of a 4D memory architecture.

Parameter	Value
Capacity	10^{12} bits
Data Rate	10^{9} bits/second
Access Time	1 msec

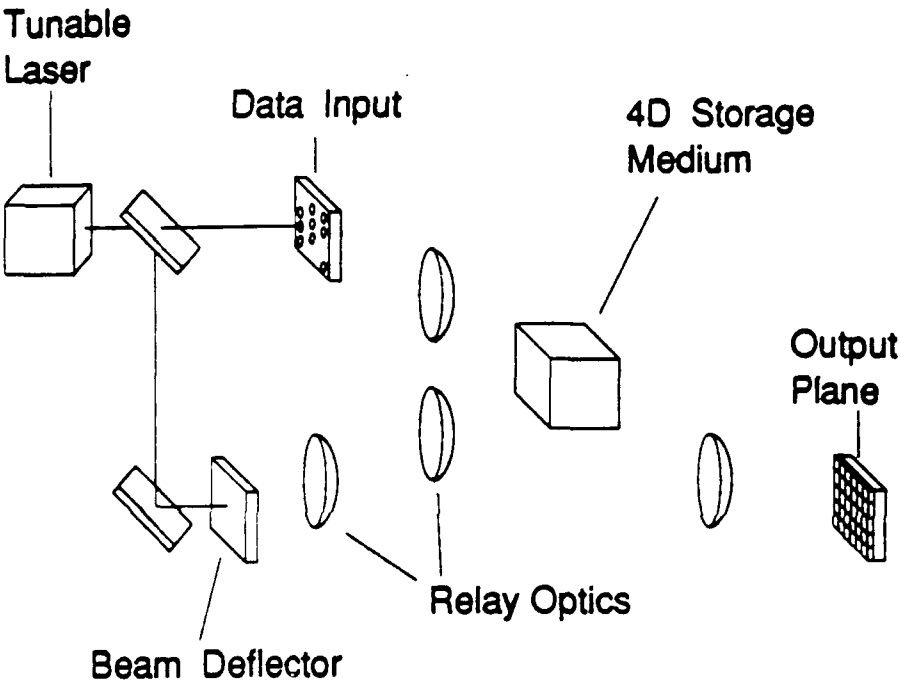

Figure 2. 4D holographic memory architecture.

ersion of an absorbed photon into a stored bit. By establishing a photon budget for writing and by considering the requirements for reliable writing and reading, a working region can be determined in which the material can successfully be used as a storage medium. The outlines of this region are shown in Figure 3 for two holographic recording techniques, one using standard absorption hologram recording techniques, and one using phase hologram recording techniques such as those invented by SPARTA.[2] (Phase holograms can be recorded near a band edge, created by burning an access channel through a heavily-doped SHB material.) The symbols on the axes indicate the location of existing dyes which have been used for spectral hole burning experiments.[3]

In contrast to the holographic storage approach, the bit-oriented storage approach leaves little or no room for repeated reading without erasure. Figure 4, shows a plot of bit-oriented materials on the same axes as the holographic materials shown in Figure 3. In this case, existing materials do not have the required values of η and σ needed for a memory device.[4]

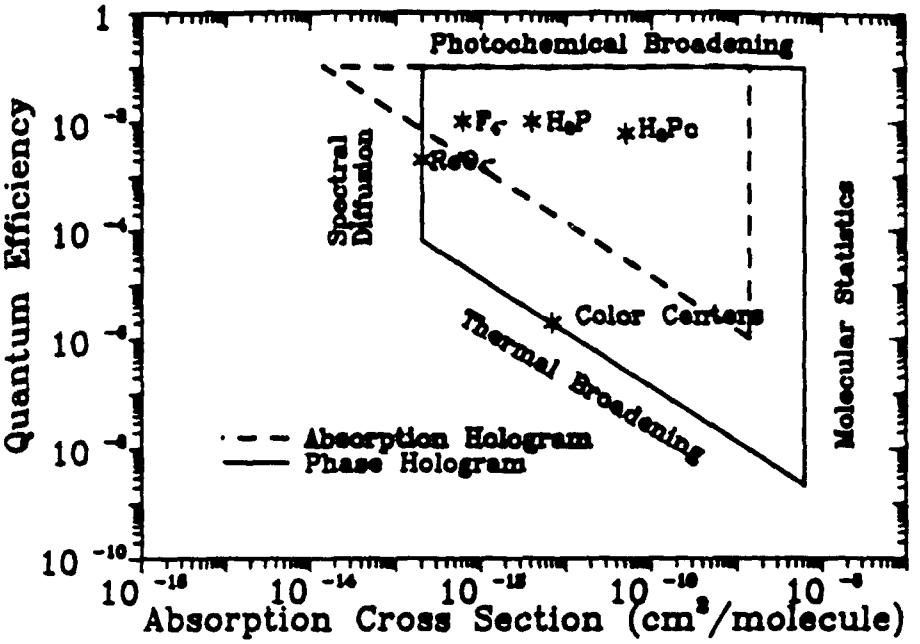

Figure 3. Spectral hole burning material parameter requirements for holographic memory.

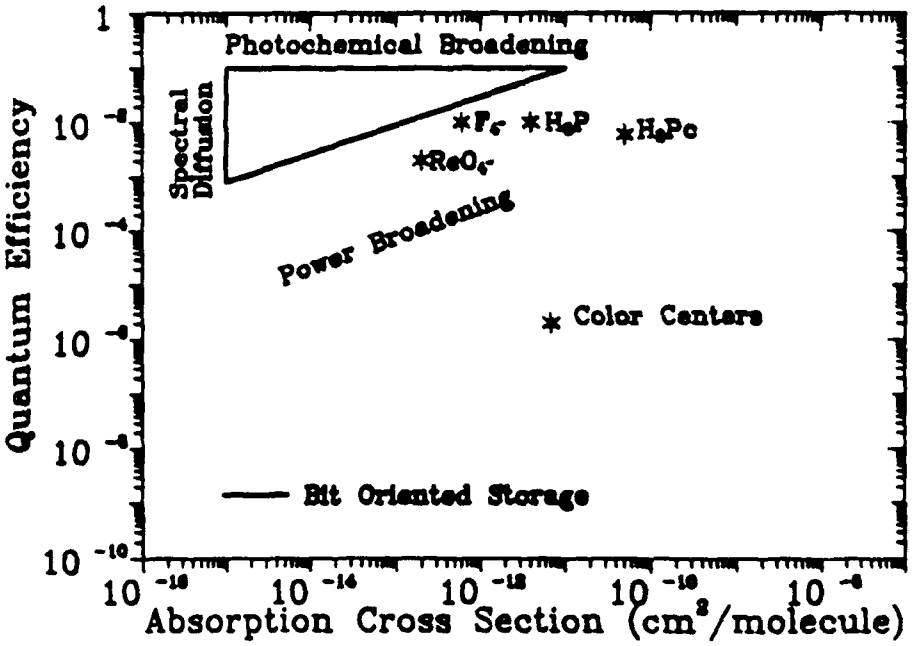

Figure 4. Bit-oriented material storage requirements.

COST PER MEGABYTE

In a related white paper, SPARTA has discussed the important role played by cost/megabyte.[5] If the cost per megabyte for a memory concept is very low, then important system characteristics such as rapid access and reliability of storage can be achieved by trading capacity for the required characteristics. Although the cost per megabyte of the storage system is driven up by this tradeoff, a low initial cost per megabyte leaves room for tradeoffs such as this to be performed.

Table II shows estimated costs per on-line megabyte for two possible memory concepts, a 3D holographic memory and a 4D holographic memory. This chart makes the key point that the enormous capacity of the 4D memory lowers the cost per megabyte to a value which is much lower than either 3D holographic memory concepts or other existing memory devices, such as magnetic or optical disk and semiconductor RAM chips.

Table II. Current and projected estimated cost/megabyte for 3D and 4D holographic memory.

Component	3D Holographic Memory Component Costs		4D Holographic Memory Component Costs	
	Current	Projected	Current	Projected
Laser	$50	$10	$30,000	$3000
SLM	$5000	$100	$5000	$100
Deflector	$1000	$0	$1000	$100
Optics	$1000	$100	$1000	$100
Detector	$1000	$100	$1000	$100
Electronics	$1000	$100	$1000	$100
Cryostat	-	-	$50,000	$5000
Total Cost	$9000	$410	$89,000	$8500
Capacity	10^9 bits		10^{12} bits	
Cost/Mbyte	$72	$3.30	$0.71	$0.07

Several key assumptions went into determining the estimated subsystem costs shown in Table II. First, we assumed that the spatial light modulator, the optics, the electronics, and the detector arrays required for the 3D and 4D holographic memories are identical. Second, we assumed that the cost of the laser for the 4D memory will be much higher in the near term, based on the requirement for rapid access to 1000 or more narrow lines. In the far term, we have assumed that the use of tunable laser diodes will lower the cost of this laser considerably. Finally, we assumed that the cost of the cryostat will be $50K for a near term system, based on an estimate from Advanced Research Systems,[6] but that this cost can be reduced considerably in a projected system based on the fact that the quoted system has a factor of approximately 100 excess cooling capacity. It is important to note that the cryostat cost, which is well-known in the near-term, dominates the cost of the other subsystems, and yet the cost of the 4D memory is still two orders of magnitude lower than the 3D memory.

CONCLUSIONS AND KEY ISSUES

This white paper has described a holographic memory concept which overcomes one of the primary past objections to holographic memory, the limited capacity caused by the range

of spatial frequencies which can be written by the narrow cone of writing and data beams. Our concept makes use of the additional degrees of freedom provided by laser wavelength and electrical bias voltage to address the fundamental capacity of an SHB medium, allowing storage densities at the molecular level. This capacity can be achieved using existing materials. A demonstration system is buildable now using presently-available spectral hole burning materials and optical components; this system would have a cost per megabyte below existing magnetic or optical disk memories.

Several key experiments must be performed to verify the analytical predictions of SHB material and memory system performance. Three key experiments can be identified:

1. Writing and reading data-bearing holograms should be examined in the laboratory. The writing sensitivity and spatial/spectral resolution of SHB materials must be quantified and compared to the analysis. A concept for reading without erasing the data, not discussed in this white paper, must be tested. The signal to noise of the readout process should be measured.
2. Testing the frequency-channel approach, which would allow the writing of phase gratings and lead to even greater capacity, should be performed in the laboratory.
3. A demonstration system should be built and tested. This system will be the key to transfer of this technology into the general computing community.

APPENDIX A: SHB MATERIAL REQUIREMENTS

This appendix addresses the material requirements for implementation of a 4D holographic memory. The limits for this memory are determined by the power requirements for writing and reading data and by the number of recording centers required to achieve high signal to noise recording.

The Kogelnik formula for diffraction efficiency of a thick hologram will be the starting point for the analysis.[7] This diffraction efficiency, η_h, is given by

$$\eta_h = [\sinh^2(\Delta\alpha L/4\cos\theta) + \sin^2(\pi\Delta n L/\lambda\cos\theta)]e^{-\alpha L/\cos\theta}. \quad (1)$$

First, we will examine the case for storage of information using volume absorption holograms. For absorption holograms, when $\Delta\alpha L/4\cos\theta$ is small

$$\eta_h = (\Delta\alpha L/4\cos\theta)^2 e^{-\alpha L/\cos\theta}.$$

The fraction of recording centers "activated" is $\Delta\alpha/\alpha$. This fraction is given by the number of photons absorbed times the quantum efficiency divided by the number of recording centers seen at any one frequency, or

$$\Delta\alpha/\alpha = (\frac{P_w T_w}{h\nu})e^{-\alpha L}\eta/\rho V(B_H/B_I).$$

At any wavelength the average absorption of a spectral hole burning material is related to the molecular cross-section, the number density of absorbers, the fraction of the absorbers seen at any wavelength, and the number of holograms which have been recorded at each wavelength. This average absorption is given by $\alpha = \sigma\rho(B_H/B_I)/2\sqrt{N_h}$ and thus the change in absorption, $\Delta\alpha$ is given by

$$\Delta\alpha = (P_w/h\nu)T_w\eta\sigma e^{-\alpha L}/2V\sqrt{N_h} \quad (2)$$

and so the hologram efficiency which can be achieved is given by

$$\eta_h = [(P_w/h\nu)T_w\eta\sigma L e^{-\alpha L}/8V\sqrt{N_h}\cos\theta]^2 e^{-\alpha L/\cos\theta}$$

For $\cos\theta \approx 1/2$ the hologram efficiency is optimized when $\alpha = 1/2L$, resulting in

$$\eta_h \approx (\frac{P_w T_w}{h\nu})^2 \frac{\eta^2\sigma^2 L^2}{16e^2V^2\sqrt{N_h}}.$$

The writing power P_w is limited by the rate at which heat can be removed from the spectral hole burning medium. The hologram efficiency will be pushed to the maximum achievable given the number of holograms, N_h, recorded at any one frequency. This maximum efficiency is $0.037/N_h^2$. The writing frame rate, T_w, is determined by the requirements for writing rate, R, and the number of pixels per frame, N_p. Therefore, in a memory system, the lower limit on the $\eta\sigma$ product will be given by

$$\eta\sigma = 4eV\sqrt{N_h\eta_h}/(P_w T_w/h\nu)L. \quad (3)$$

The $\eta\sigma$ product is essentially the sensitivity of the spectral hole burning medium. As η and σ increase from this lower bound, moving up and to the right in Figure 3, the writing power can become smaller and smaller for a given frame rate and hologram efficiency.

The right hand boundary of the required region in parameter space can be found by considering the allowed number of recording centers in the hologram volume. Using the optimum relation from before, $L = 1/2\alpha$, the expression $\alpha = \sigma\rho(B_H/B_I)/2\sqrt{N_h}$, and a requirement on the number of recording centers given a memory capacity C, we can determine the allowable upper limit on the absorption cross-section per molecule, σ. Since each recording center is binary and can only be used once to record a specific grating pattern, the number of recording centers must be equal to the capacity of the memory times a signal to noise factor which grows as the square of the signal to noise, thus $\rho V > \mathrm{SNR}^2 C$. Combining these two relationships, the upper limit on the molecular absorption can be found to be

$$\sigma < (B_I/B_H)\frac{V\sqrt{N_h}}{\mathrm{SNR}^2 CL}. \quad (4)$$

The relationships expressed by equations 1, 2, and 3 can be used to bound the region in the $\eta\sigma$ plane which can be used for volume hologram memory. The system to be used as an example has the parameters shown in Table III.

Table III. 4D Holographic Memory System Parameters

Data Rate	33 Mbits/sec
Frame Size	10^6 pixels
Frame Time	30 msec
Total Capacity	10^{12}
Dimensions	1 cm × 1 cm × 1 cm
Writing Power	3 mW
Holograms/wavelength	30
Independent Wavelengths	10^5
SNR	20

The lower bound on the $\eta\sigma$ product is found by using equation (3). In addition, we will assume that the diffraction efficiency is the maximum possible using 30 data arrays per laser wavelength, or $0.037/30^2 = 4 \times 10^{-5}$. In this case the lower bound on the $\eta\sigma$ product is

$$\eta\sigma > \frac{4 \times 2.7 \times (1\ \mathrm{cm}^3) \times (30 \times 4 \times 10^{-5})^{0.5}}{(0.03 \times 3 \times 10^{-3}/3.3 \times 10^{-19}) \times 1\ \mathrm{cm}}$$

$$\eta\sigma > 1.4 \times 10^{-15}\ \mathrm{cm}^2$$

The upper bound on molecular cross-section is found using equation (4) to be

$$\sigma < 10^5 \frac{1\ \text{cm}^3 \times 5.5}{400 \times 10^{12} \times 1\ \text{cm}}, \text{or}$$
$$\sigma < 1.4 \times 10^{-9}\ \text{cm}^2.$$

For refractive index holograms, and small values of $(\pi \Delta n L/\lambda \cos\theta)$, Kogelnik's formula for diffraction can be rewritten as

$$\eta_h = (\pi \Delta n L/\lambda \cos\theta)^2 e^{-\alpha L/\cos\theta}.$$

An important parameter is the refractive index ratio $R_{ri} = \frac{\Delta n}{\Delta k}$. This parameter is the ratio of the refractive index modulation relative to the modulation of the imaginary part of the index (related to the absorption) near a band edge. Using $\alpha = 4\pi k/\lambda$ and $\cos\theta = 1/2$, we have

$$\eta_h \approx (\frac{R_r i \Delta \alpha L}{2})^2 e^{-2\alpha L}.$$

Choosing α, as above, to be $1/2L$ we get

$$\eta_h \approx \frac{\Delta \alpha^2 R_r i^2 L^2}{4e}.$$

Using the equation for $\Delta\alpha$ from above and rearranging terms we can find the lower limit on $\eta\sigma$ for an phase grating recorded in an SHB material

$$\eta\sigma = \frac{2eV\sqrt{\eta_h}}{(P_w T_w/h\nu) R_{ri} L}.$$

The optimum absorption (in the channels) is given by $\rho\sigma L(B_I/B_H) = 1/2$ as before. The density throughout 50% of the spectral range is a factor of 100 times greater, however, and thus $50\rho V > \text{SNR}^2 C$. combining these two relations

$$\sigma < \frac{25(B_I/B_H)V}{LC\text{SNR}^2}.$$

The numerical values for the refractive index case are then given by

$$\eta\sigma > 1.3 \times 10^{-17}, \text{and}$$
$$\sigma < 6.3 \times 10^{-9}.$$

Table IV. List of Variables

η_h - hologram efficiency

$\Delta\alpha$ - absorption change (cm^{-1})

L - memory medium length (cm)

θ -angle between reference and data beams

α - average absorption (cm^{-1})

σ - molecular cross-section (cm^2)

ρ - recording center number density (cm^{-3})

(B_H/B_I) - ratio of homogeneous to inhomogeneous linewidth

P_w - writing power (W)

T_w - writing time (sec)

η - quantum efficiency of recording

V - volume of memory medium (1 cm^3)

$h\nu$ - reading and writing energy/photon

SNR - signal to noise

N_p - number of pixels

R - data rate (bits/sec)

N_h - number of holograms at a single laser frequency

REFERENCES

1. U. P. Wild, S. E. Bucher, and F. A. Burkhalter, "Hole burning, Stark effect, and data storage," Appl. Opt. 24 1526 (1985).
2. SPARTA patent disclosure, January 1990.
3. W. E. Moerner and M. D. Levenson, "Can single-photon processes provide useful materials for frequency-domain optical storage?," J. Opt. Soc. Am. B2 (1985) 915.
4. W. E. Moerner, ed., *Persistent Spectral Hole-Burning: Science and Applications*, Springer-Verlag, New York (1988).
5. P. D. Henshaw and R. F. Dillon, "Product Goals for (Optical) Mass Storage," SPARTA, Inc.
6. Heliplex HS-4 System, APD Cryogenics, Inc., 1919 Vultee Street, Allentown, PA 18103.
7. H. Kogelnik, "Coupled Wave Theory for Thick Hologram Gratings," Bell Syst. Tech. J. 48 (1969) 2909.

Ferroelectric Liquid Crystal Spatial Light Modulators

K. E. Arnett, L. K. Cotter
M. A. Handschy, M. R. Meadows
M. J. O'Callaghan, L. A. Pagano-Stauffer

Displaytech, Incorporated
Boulder, Colorado

T. J. Drabik

School of Electrical Engineering
Georgia Institute of Technology

G. Moddel

Department of Electrical and Computer Engineering
University of Colorado, Boulder

Sponsored by:
DARPA, RADC, SDIO/ONR, NSWC, AFWL

Switchable Waveplate Device

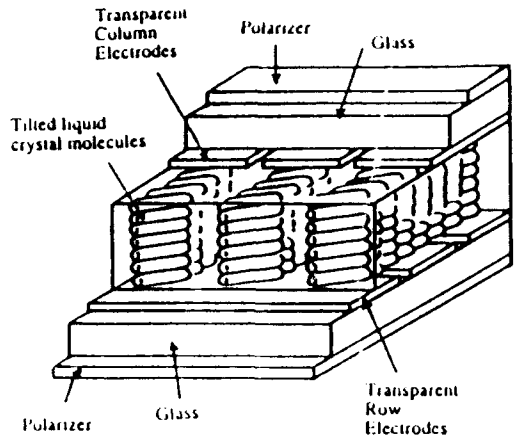

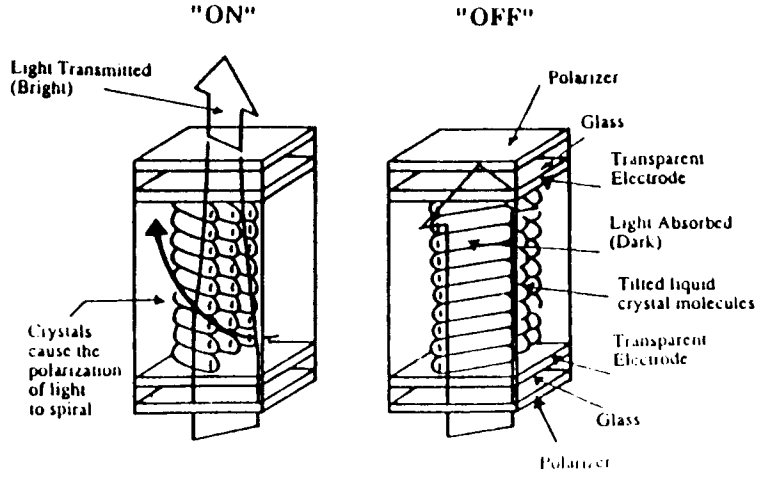

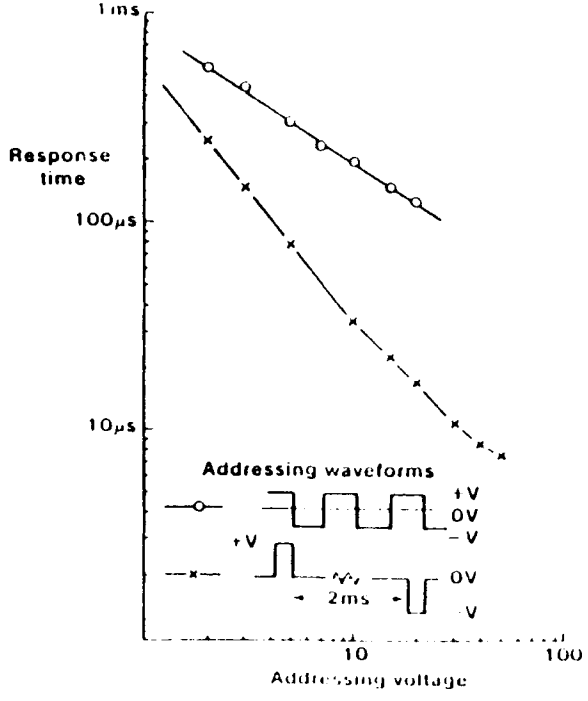

Response times for SCE6 (BDH).

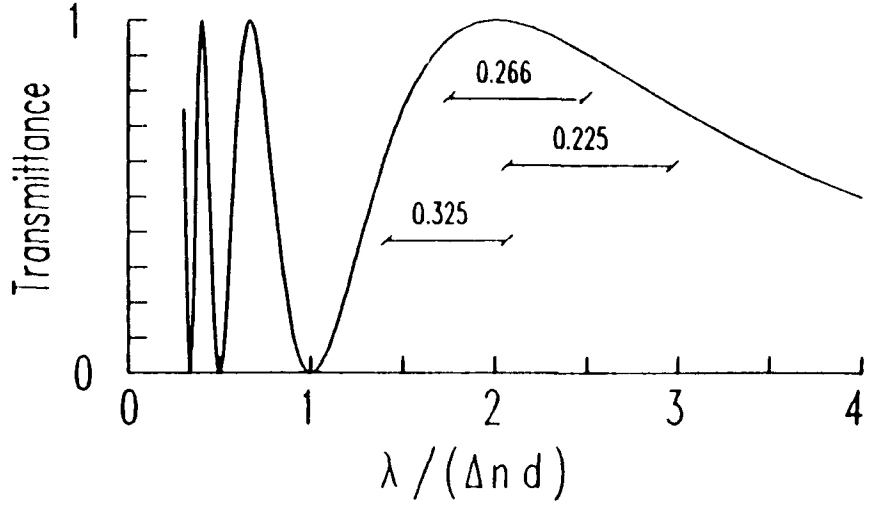

[from N. Collings, W. A. Crossland, P. J. Ayliffe, D. G. Vass, and I. Underwood, "Evolutionary development of advanced liquid crystal spatial light modulators," Appl. Opt. 28, 4740 (1989).]

Total Internal Reflection Device

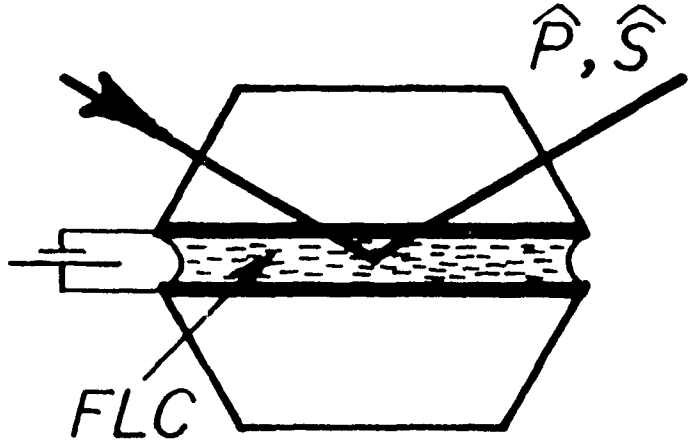

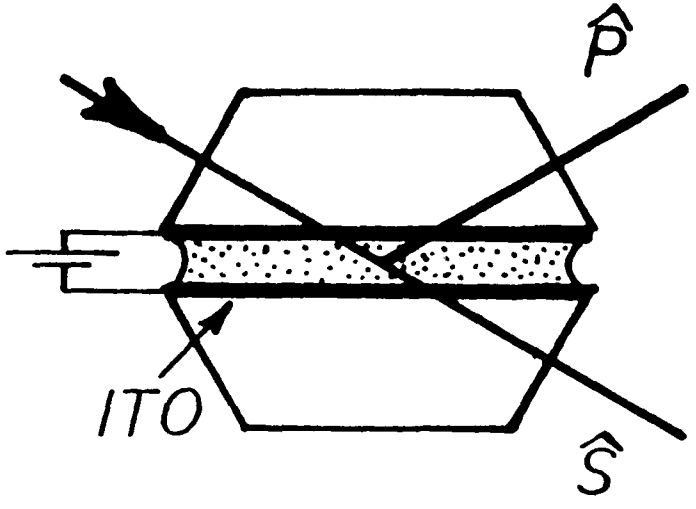

$\lambda(nm)$	T_{on}	$10^5 \cdot \frac{T_{off}}{T_{on}}$
450	0.61	1.1
550	0.76	1.9
650	0.87	2.1
750	0.82	2.2
850	0.90	2.0
950	0.83	1.2
1050	0.89	1.1
1150	0.87	1.6
1250	0.89	1.1
1350	0.85	1.4
1450	0.86	1.1
1550	0.77	2.2

Direct Drive Addressing

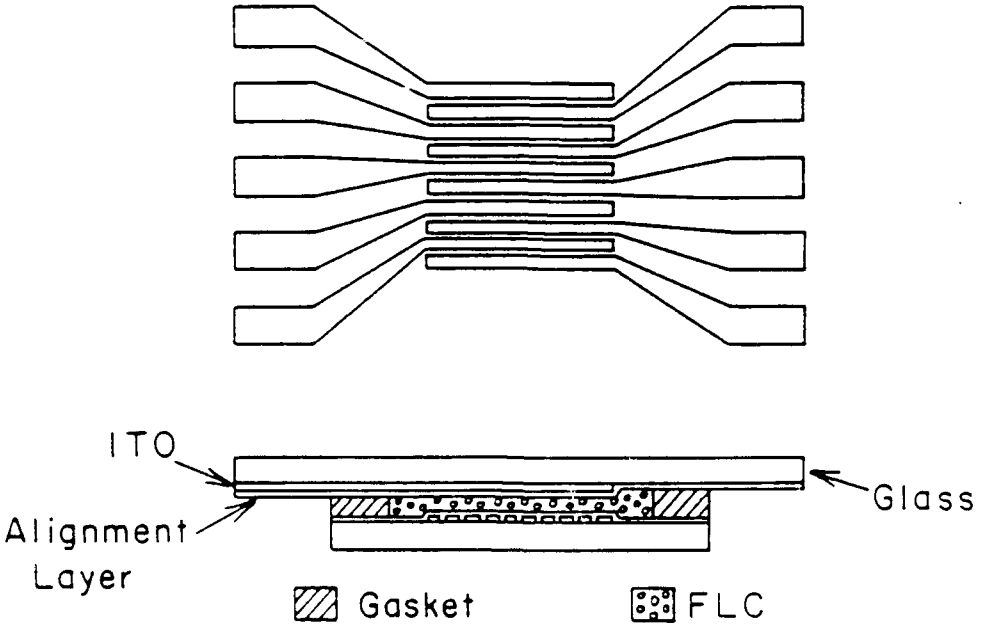

frame time	$\sim 2\tau_{FLC}$
contrast (X'ed pols.)	300:1
contrast (TIR)	10^5:1
minimum pixel size	$\sim 10\ \mu$m
feasible array size	1×1000

Matrix Addressing

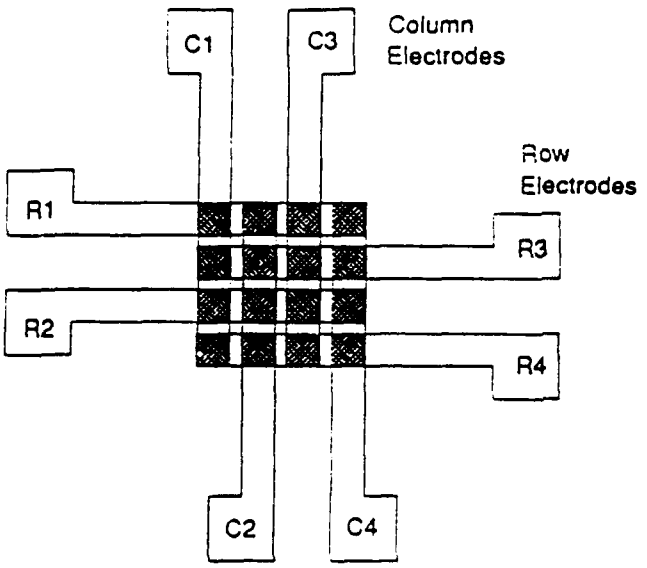

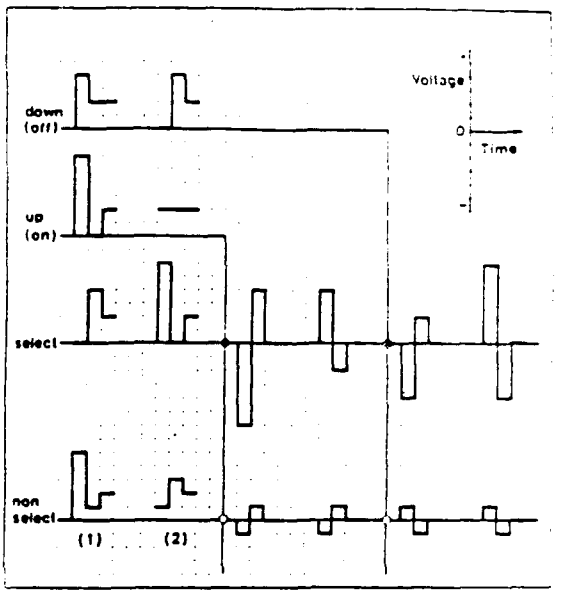

[from Jürgen Wahl, "Electronic addressing of FLC devices," Ferroelectrics **85**, 207 (1988).]

frame time	$> 2N\tau_{FLC}$
contrast	10–100:1
minimum pixel size	$\sim 10\ \mu$m
feasible array size	1000×1000

Photosensor Addressing

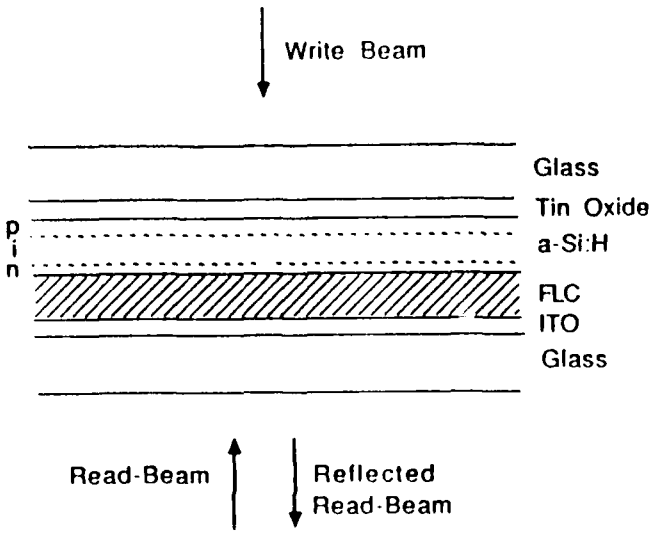

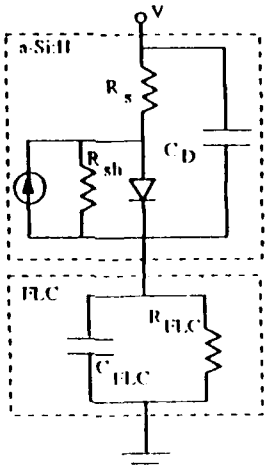

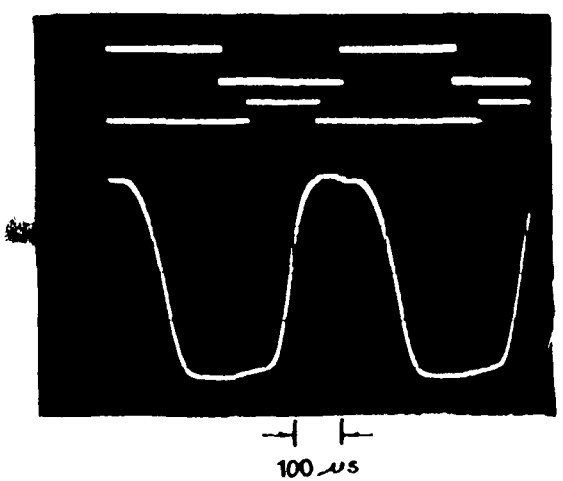

frame time	$\sim 2\tau_{FLC}$
contrast	>100:1
resolution	~ 100 lp/mm
feasible SLM SIZE	50 mm dia.

Active Backplane Addressing

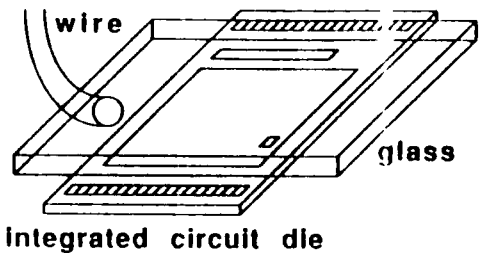

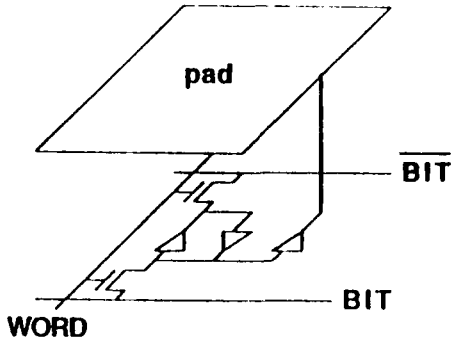

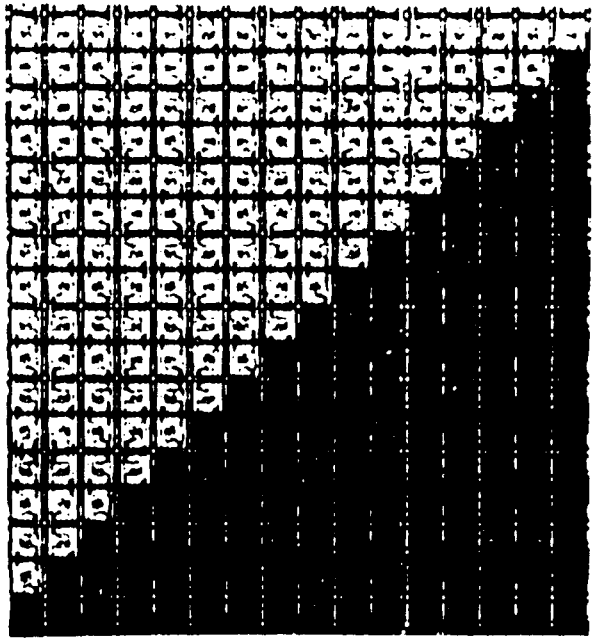

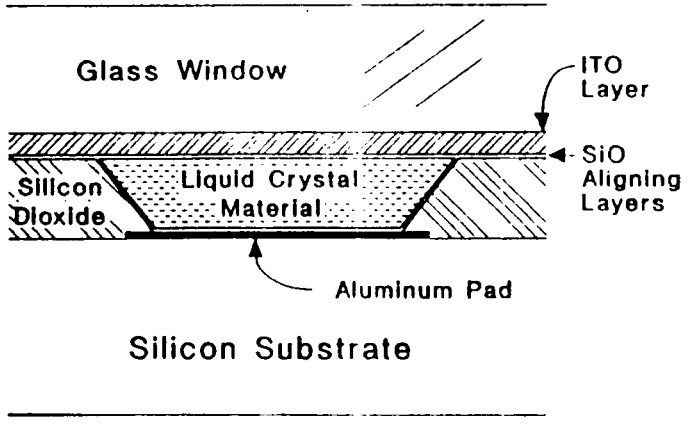

frame time	$\sim 2\tau_{FLC}$
contrast	$\sim$ 100:1
minimum pixel size	$\sim 10\ \mu$m
feasible array size	1024×1024

PHYSICAL CHARACTERIZATION OF OPTICAL STORAGE MATERIAL

Chai-Pei Kuo
Physical Optics Corporation
Torrance, California 90501

The search for proper materials for all-optical data storage has become a critical issue in development of a practical system that would provide a solution in terms of high capacity and high accessing speed operation.

In order to characterize the material to determine whether it is a candidate for optical information storage four properties must be understood.

They are: the material's light/matter interaction response
the material's ability to retain information
the material's power requirements for light/matter interaction
and the material's response speed.

Each property will be discussed separately below.

In light/matter interaction, an optical material must respond to changes on intensity, polarization, or wavelength of the illuminating light. An appropriate optical material need not respond to all three factors, but should respond to at least two of them. Research is currently being conducted on materials responding to both intensity and wavelength. Good examples include materials exhibiting two-photon absorption phenomena and materials using the spatial hole burning effect. Both kinds of material rely on third order nonlinear optical mechanisms. Because of inherent low third order coefficients, interaction with high power sources is a requirement.

So far, practical application of materials which need response to intensity of illuminating light has been limited. This leads to the conclusion that materials which are sensitive to polarization and wavelength are better choices for optical memory storage.

In analogy to magnetic storage, optical memory material should have the capability to maintain the information. The capability to allow information to be quickly erased is also an important feature required for a dynamic optical storage medium. Up to the present, no well publicized reports of such a material exist. In this paper, we describe a candidate material that could fulfil the above requirements.

As mentioned earlier, the material's response to light should necessitate writing/recording to be done at a low power level. At the same time, the material's sensitivity must be high enough to facilitate reading. For a static material, such as dicromated gelatin (DCG), Δn (index modulation) can reach 0.1. Information stored in this material can not be erased. Dynamic photo-refractive

materials on the other hand, can respond to low light intensity but also have low Δn. This seriously impairs their storage capacity.

The previously described materials have response speeds varying from nanoseconds to milliseconds. The judicious choice will naturally be those materials that respond in the nanosecond range. However, materials that fall into this region are those that use the third order nonlinearity. In this paper, we report on a material that potentially has response speed of several nanoseconds.

The promising optical storage material alluded to above is made of a composite polymer. It can be formed into a thin film relatively easily and it is extremely sensitive to a broadband wavelength, from 500 to 530 nanometers. Its sensitivity depends on the state of polarization change of blue-green light. Its index modulation has been measured to be as high as 0.01 at a recording power of 1 mW. We have used this material to record optical information. Persistence was tested two weeks after recording and the information was retained within 10%. Optical information can be recorded and addressed by two methods: holographic and direct birefringent induction.

Physical Optics Corporation, Torrance, California, U.S.A.

POC's Optical Storage Material Technology

No	Feature	Current Achievements
1	Modes	Write/Read/Erase
2	Number of Cycles without Fatique	> 1 million
3	Additional Capability	Overwrite, Holographic Non-holographic
4	Current Response Time	Microsecond to Millisencond
5	Potential Response Time	Nanosecond to Picosecond
6	Sensitivity	10 mWatt/mm^2
7	Writing/Reading Wavelengths	Visible/IR
8	Storage Life	3-6 Months
9	Potential Storage Life	20 to 30 Yr
10	Coating Size	1 mm^2 to 1 meter^2
11	Substrate	Glass, Plastic etc.
12	Laser Damage Threshold	High
13	Temperature Stability	100° for Several Hours
14	Cost	Low

Physical Optics Corporation, Torrance, California, U.S.A.

INITIAL MEMORY MEDIA STUDIES

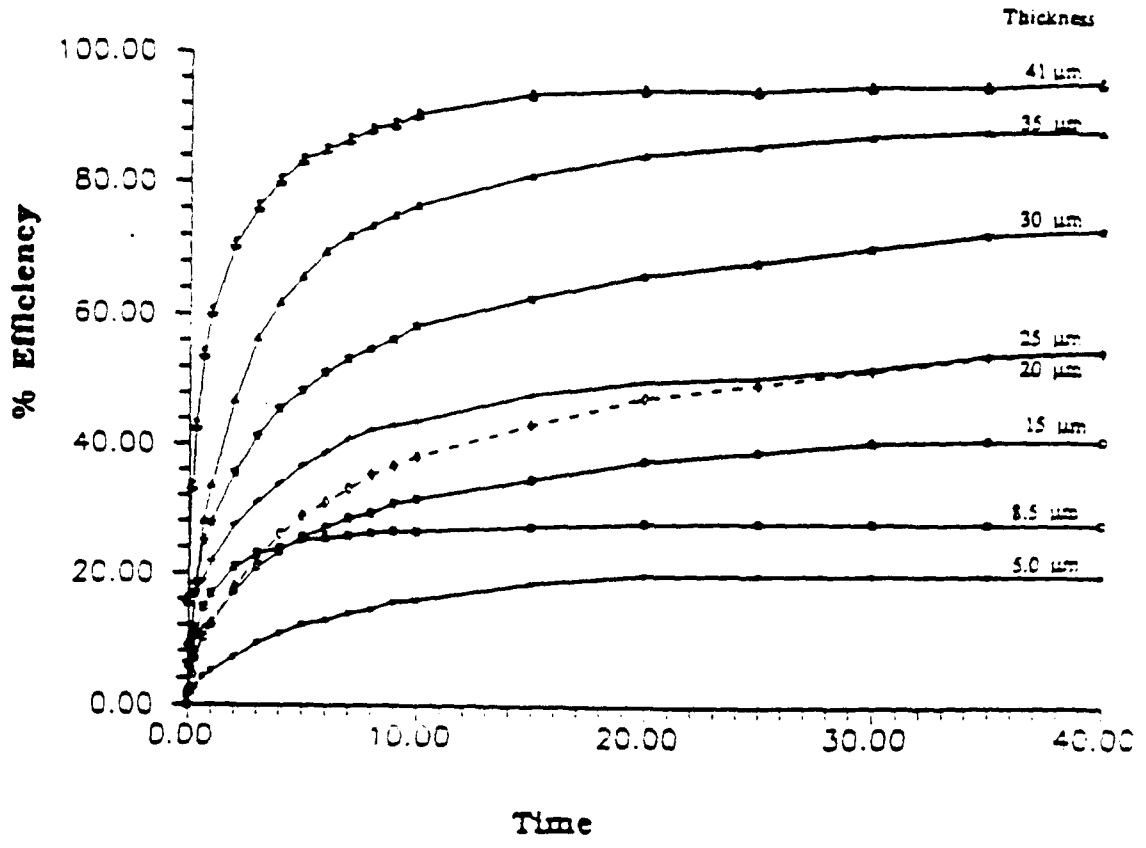

Physical Optics Corporation, Torrance, California, U.S.A.

Schematic of Optical Disk

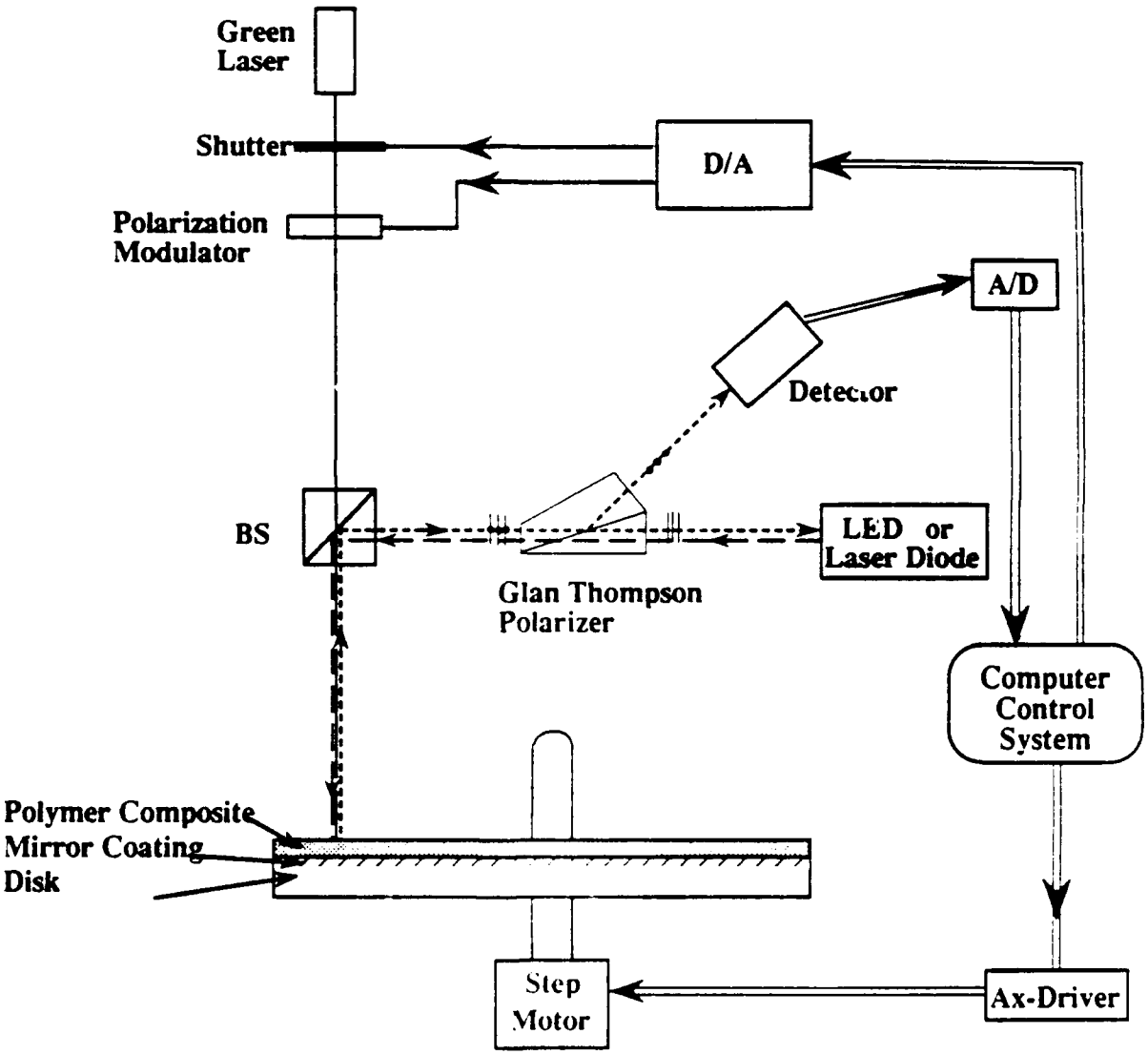

* **Dashed Line: Reading Beam**

Solid Single-Line: Recording Beam

Solid Double-Line: Control Cabel

ASCII

A = 41 ⟶ 0100 0001

P-10-3

Physical Optics Corporation, Torrance, California, U.S.A.

Recording /Reading Scheme in 3-DOMS System for Achieving High Storage Capacity

1. **Fourier Transform Holography**

   10^4 bits /mm^2 — One Page of Information (One Hologram)

2. **Bragg Angular Multiplexing**

   500 Pages at the Same Location

3. **Polarization Multiplexing**

   4 x 500 = 2000 Pages at the Same location

Total Packing Density:

$$\rho = 2000 \times 10^4 \text{ bits / mm}^2$$

$$= 2 \times 10^9 \text{ bits / cm}^2$$

Physical Optics Corporation, Torrance, California, U.S.A.

Real Time Holographic Recording/Playback Set Up

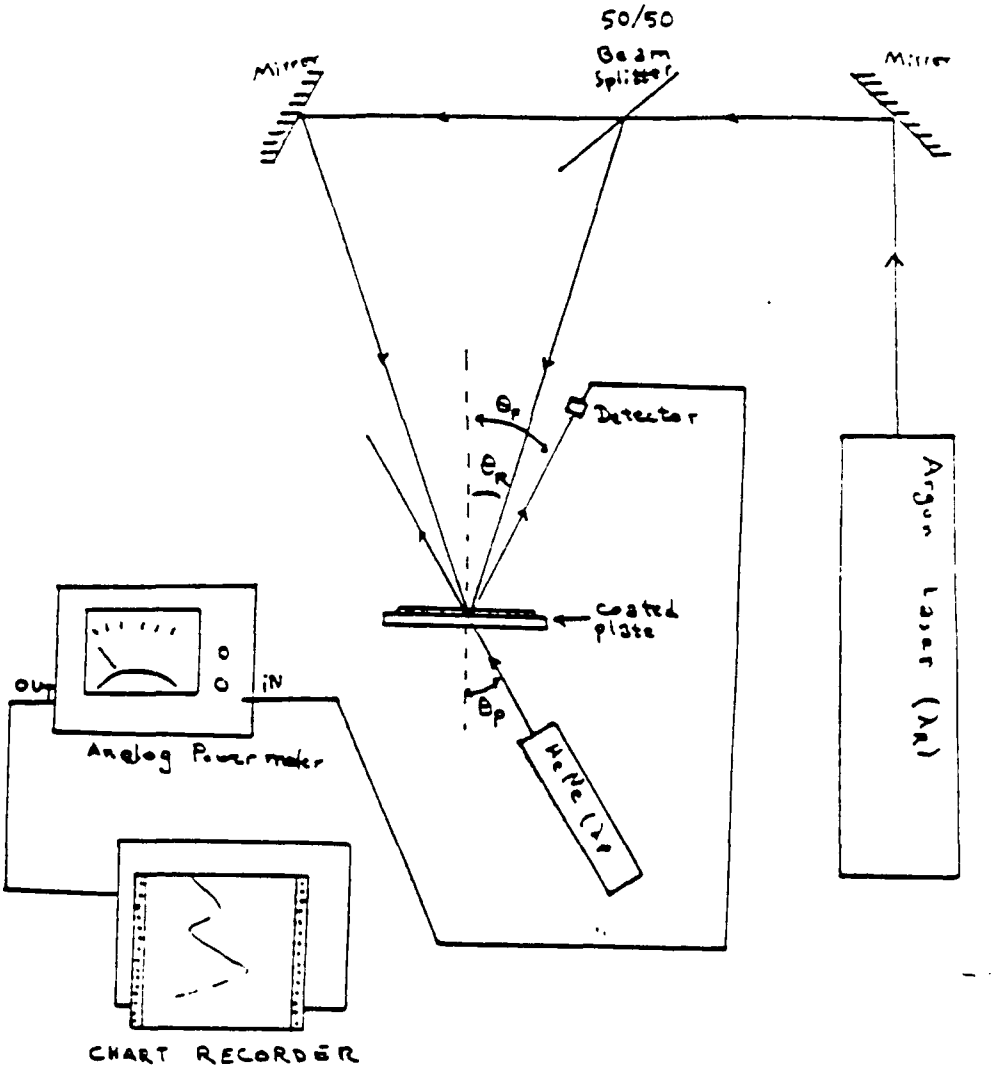

Recommendations for Studies on 3-D Storage

Prepared by: Prof. L. Hesselink

The members of the Physics group were:

L. Hesselink (chair), T. Mossberg, P. Rintzepis, R. Kachru, C. Warde, P. Henshaw and A. Craig.

The group effort was centered around a discussion of the physical attributes associated with various approaches to volume data storage, including photorefractives, polymers, stimulated echo optical memories, 2-photon storage devices and magneto-optic approaches. These systems are compared on the basis of the following criteria:

1. Read-write erasure energy per pixel
2. *Erasure mechanism*
3. Write, read and erasure time constants
4. Power requirements
5. Memory persistence time
6. Temperature dependence/requirement
7. Wavelength regime
8. Resolution: pixels/cm^2, pixels/cm^3
9. Read contrast and extinction level, or phase change
10. Coherence requirements
11. Page (holographic) or bit oriented

The results are summarized in Table 1.

As a result of the discussions in the group the following recommendations for research in this area are made:

1. Coordinate research on architectures and materials; a closely coupled study is needed to significantly advance the state of understanding related to volume data storage.

2. Since the estimated storage time in most volumetric recording media, with the exception of magneto-optic recording, is far shorter than required for archival storage, new computing approaches are needed to take advantage of the high capacity or low latency.

3. Long term materials research is needed to have an impact on new volumetric data storage systems. A sustained effort in this area will have payoff in other signal processing applications too.

4. Combine research on optical data storage, interconnects and processing to leverage efforts in different areas.

5. Apply a systems viewpoint to the study of optical and electronic components for data storage. Architecture, materials and devices need to be considered as a whole to optimize each component of a data storage and processing system. Modelling should play an integral role in this effort.

6. Identify needs for volume optical data storage devices and direct research efforts towards eliminating systems bottlenecks.

	A	B	C	D	E
1	UNCORRECTED, UNEDITED DATA				
2					
3	Criteria	Photorefractives	2-photon	stim echo	polymers
4					
5	1. Sensitivity	.5-10 nJ/micron^2	1 nJ/0.5 mm^2	10^7 photons/bit	
6	2. Erasure mech	light			switch pol dir
7	3. W,R,E time const	nsec - sec	10^-13	10^11bits/sec	1 microsec
8	4. Power reqs	mw -microw/cm^2	Gwatt/cm^2	eta=20%	>20 mW sat
9	5. Mem persist time	days to months	20 min T=75F	weeks	2 weeks room T
10	6. Temp dep/req	< Tcrit		4-30K	>115C
11	7. Wavelength	UV - IR	300nm-1.8 micron	450-880 nm	500-530 nm
12	8. Res: pix/cm^2; pix/cm^3	10^13/cm^3	10^13 bits/cm^3	20x20 microns	
13	9. Read contrast	>30db	10 db		dep on pol
14	10. Coh req	y		none	none
15	11. Page or bit?	10^6 bits.pg	page	bit	bit
16	12. Reads per write	10^7 @30db		1000	?

LIST OF ATTENDEES/CONTRIBUTORS

Professor Bruce Berra
Electrical & Computer Engineering
111 Link Hall
Syracuse University
Syracuse, NY
Phone: (315)443-4445
FAX: (315)443-4655

Dr. Di Chen
[redacted]
Phone: (719)599-0093

Dr. Alan E. Craig
AFOSR/NE
Building 410
Bolling AFB, DC 20332-6448
Phone: (202)767-4931

Dr. Uzi Efron
Hughes Research Lab.
MS 169
3011 Malibu Canyon Road
Malibu, CA 90265
Phone: (213)317-5214
FAX: (213)317-5484

Professor Sadik Esener
Dept. of Electrical & Computer Engineering
9500 Gilman
University of California, San Diego
La Jolla, CA 92093-0407
Phone: (619)534-2732
FAX: (619)534-1225

Professor Shaya Fainman
Dept. of Electrical & Computer Engineering
9500 Gilman
University of California, San Diego
La Jolla, CA 92093-0407
Phone: (619)534-8909
FAX: (619)534-1225

Dr. Lee Giles
NEC Research Institute
4 Independence Way
Princeton, NJ 08540
Phone: (609)520-1532

Dr. Mark Handschy
Display Tech
2200 Central Ave.
Boulder, CO 80301
Phone: (303)449-8933

Dr. Haim Haskal
Sparta
24 Hartwell Ave.
Lexington, MA 02173
FAX: (617)861-7934
Phone: (617)863-1060

Dr. P. Henshaw
Sparta
24 Hartwell Ave.
Lexington, MA 02173

Professor B. Hesselink
R-359B Durand Building
Stanford University
Stanford, CA 94305-4035
Phone: (415)723-4850
FAX: (415)723-3931

Dr. Vincent P. Heuring
University of Colorado Boulder
Department of Elect. & Computer Eng.
Campus Box 425
Boulder, CO 80309-0425
Phone: (303)492-8751
Fax: (303)492-2758

Dr. R. Hoyt
IBM
Almaden Research Center
Dept. K-65
650 Harry Road
San Jose, CA 95120
Phone: (408)927-2118

Dr. Albert Jamberdino
RADC/IRAP
Grifiss AFB, NY 13441-5700
Phone: (315)330-4581

Professor B. K. Jenkins
Signal & Image Processing Inst.
University of Southern California
Los Angeles, CA 90089-0272

Victor Jipson
IBM
Almaden Research Center
Department K01/802
650 Harry Road
San Jose, CA 95120-6099
Phone (408)927-2010

Dr. R. Kachru
Molecular Physics Laboratory
SRI International
333 Ravenswood Ave.
Menlo Park, CA 94025

Prof. Ray Kostuk
Optical Sciences Center
University of Arizona
Tucson, Arizona 85721
Phone: (602)621-6172

Chai-Pei Kuo
Physical Optics Corp.
20600 Gramercy Place
Suite 101
Torrance, CA 90501

Dr. Shing-Hong Lin
Physical Optics Corp.
20600 Gramercy Place
Suite 101
Torrance, CA 90501

Mr. William Miceli
Phone: (617)451-4484

Dr. Perides Mitkas
Phone: (315)471-1476
Fax: (315)443-4655

Professor Tom Mossberg
Department of Physics
University of Oregon
Eugene, OR 97403
Phone (503)346-4751

Dr. Miles J. Murdocca
Member of Technical Staff
AT&T Bell Laboratories
Room 4G-538
Crawfords Corner Road
Holmdel, NJ 07733

Professor D. Psaltis
Electrical Engineering Dept. 116/81
California Inst. of Technology
Pasadena, CA 91125

Dr. Steve Redfield
M.C.C.
3500 W. Balcones Center Dr.
Austin, TX 78759
Phone: (512)338-3408

Professor Peter Rentzepis
Chemistry Department
UC Irving
Irvine, CA 92717
Phone: (714)856-5934

Professor Armand Tanguay, Jr.
523 Seaver Science Center
University of Southern California
University Park MC-0483
Los Angeles, CA 90089
Phone: (213)743-6152

Dr. Jay Waas
Semetex Corp.
3450 Fujita Street
Torrance, CA 90505

Professor Cardinal Warde
Dept. of Electrical Engineering
& Computer Science, Rm. 13-3065
MIT
Cambridge, MA 02139
Phone: (617)253-6858

Dr. Bill Wolf
DuPont Co.
Experimental Station Bldg. E357
Wilmington, DE 19898
Phone: (302)695-7953